Reconstitution of Connexin-43 in Artificial Membranes

Dissertation

for the award of the degree

Doctor rerum naturalium

of the Georg-August Universität

within the doctoral program

Physics of Biological and Complex Systems

of the Georg-August University School of Science (GAUSS)

Submitted by

Yeimar Evelyn Portillo Castellano

Born in Caracas

Göttingen, 2022

Reconstitution of Connexin-43 in Artificial Membranes

Dissertation

for the award of the degree

Doctor rerum naturalium

of the Georg-August Universität

within the doctoral program

Physics of Biological and Complex Systems

of the Georg-August University School of Science (GAUSS)

Submitted by

Yeimar Evelyn Portillo Castellano

Born in Caracas

Göttingen, 2022

Members of the Thesis Advisory Committee

Prof. Dr. Claudia Steinem
Institute for Organic and Biomolecular Chemistry. Georg-August University
Max Planck Institute for Dynamic and Self-organization

Prof. Dr. Michael Meinecke
Biochemistry Center (BZH). Heidelberg University

Prof. Dr. Sebastian Kruss
Physical Chemistry II. University of Bochum

Members of the examination board

First referee: Prof. Dr. Claudia Steinem
Institute for Organic and Biomolecular Chemistry. Georg-August University
Max-Planck Institute for Dynamic and Self-organization

Second referee: Prof. Dr. Michael Meinecke
Biochemistry Center (BZH). Heidelberg University
Prof. Dr. Sebastian Kruss
Physical Chemistry II. University of Bochum

Prof. Dr. Burkhard Geil
Institute for Physical Chemistry. Georg-August University

Prof. Dr. Timo Betz
Third Institute of Physics. Georg-August University

Prof. Dr. Bert de Groot
Max Planck Institute for Biophysical Chemistry

Date of oral examination: 2nd of March 2022

Declaration

I, Yeimar Evelyn Portillo Castellano, hereby certify that my doctoral thesis entitled “Reconstitution of Connexin-43 in Artificial Membranes” has been written independently and with no other sources or aids than those quoted.

Göttingen, 2022

_____

Yeimar Portillo

Dedicated to my lovely mother

“Sé grènn diri ka plein sac diri”

-Martinican proverb-

Table of content

Abstract

Synthetic biology aims to engineer complex biological functions in an artificial way. A variety of molecular tools and techniques allow mimicking of processes of living systems in a synthetic way. In that context, the production of compartments with a minimal and sufficient number of components to sustain life has proven relevant in recent years [1]. Cell-free systems (CFS) are powerful platforms for the expression of proteins. In combination with membrane mimic structures, CFS can be used to synthetically reproduce processes like metabolism, transport of molecules, and communication between compartments. Connexin 43 is a transmembrane protein involved in direct cell-to-cell communication pathways in many cell types. In this project, a CFS was used to reconstitute Cx43 in artificial membranes as a first step in the direction of mimicking intercellular communication. Functional plasmids compatible with CFS were produced to express EGFP-Cx43, which allowed monitoring samples *via* fluorescence. *In vitro* protein expression took place in the presence of vesicles of L-α-PC: DOTAP: TxR in a cotranslational manner. The presence of Cx43 in vesicles was evaluated by Western Blot and fluorescence spectroscopy, reporting that ~ 50-80 % of the protein variants inserted into the vesicles. The incorporation of EGFP-Cx43 into vesicles was affected by the presence of EGFP as it made them less hydrophobic than the WT Cx43. Additionally, the incorporation of EGFP-Cx43 into GUVs and its analysis by CLSM was successful. The model system presented in this work could be further optimized and used to establish communication pathways between artificial minimal cells.

1. Introduction

1.1 Synthetic Biology

Synthetic biology is a discipline that engineers complex biological functions in an artificial manner to understand biological phenomena [2,3]. The goal of synthetic biology is to extend or modify the behavior of organisms to perform new tasks. These modifications range from genetically engineering organisms to replicating the synthesis of chemical processes [4]. The design for the modification of a feature in an organism is built in layers from the bottom to the top. The bottom layer is constituted by DNA, RNA, proteins, and metabolites (*e.g.,* lipids, amino acids, nucleotides, etc.). The next layer comprises biochemical reactions that regulate the flow of information. At the top layer, diverse biological devices are used to assemble complex pathways that function as integrated circuits [3]. From synthetic biology, the concept of "minimal cells" arises to unravel the complexity of the organization and function of living cells. Minimal cells are defined as cellular compartments having a minimal and sufficient number of components to sustain life [5]. The construction of minimal cells can be approached in two ways, in a top-down or bottom-up fashion. In top-down approaches, a bacterial target genome is reduced to a minimal gene set *in vivo*, while bottom-up approaches rely on the production and combination of molecules *in vitro* to assemble artificial minimal cells. It is important to notice that the product of both top-down and bottom-up approaches leads to the construction of artificial cells (or semi-synthetic cells) since they do not exist in nature [1].

At the molecular level, life could be understood by the cooperativity between three essential components: i) the DNA information, ii) the compartment, and iii) the metabolism. To build an artificial cell *de novo*, a unique compartment with a structure and organization similar to one of a bacteria is required. Concerning the metabolism component, ATP and GTP could be used as energy sources to carry out processes in the cell. Compartmentalization could be achieved by using phospholipid bilayers as they assemble in cell-sized vesicles in aqueous solutions. On the other hand, DNA information could be used to express proteins using transcription and translation machinery extracted from an organism to mimic a particular feature of a living cell [6].

The last process is known as cell-free technology and it has been used as a protein expression platform with high demand in recent years, especially in the field of synthetic biology to build artificial minimal cells [1,7–9].

1.2 The cell-free expression technology

Cell-free systems consist of molecular machinery extracted from cells to carry out transcription and translation processes for protein expression [7]. This technology offers an open reaction environment that allows the addition or removal of substrates to program or modify the protein of interest [7,8]. These systems can be understood as programmable liquids since they have removed many of the complexities from protein expression in cell-based approaches and bring opportunities for the rational design and manipulation of biological systems [8].

Protein synthesis with cell-free systems makes use of the biological catalysts for translation, protein folding, and energy generation from prokaryotic or eukaryotic cells [7]. The most popular systems are based on *Escherichia coli (E. coli)*, wheat germ, and rabbit reticulocytes. The choice of the system should be determined by the origin and biochemical nature of the protein of interest and the specifics of the applications. In general, systems based on *E. coli* provide higher yields and homogenous samples suitable for structural studies. In contrast, eukaryotic-based systems are reported to be less productive but efficient in providing a platform for functional studies, especially in the case of proteins that need posttranslational modifications to function [10]. Cell-free platforms can be obtained as crude extracts generated by clarifying the whole-cell lysate *via* centrifugation to remove genomic DNA, insoluble biological molecules, and non-lysed cells. In comparison, cell-free platforms can also be obtained as purified elements to carry out protein synthesis from the bottom up [7]. The latter is known as Protein synthesis Using Recombinant Elements (PURE) which was pioneered by Shimizu and colleagues [11]. The PURE system is composed of 10 translation factors, T7 RNA polymerase, pyrophosphatase, 20 aminoacyl-tRNA synthetases, creatine kinase, myokinase, and nucleoside-diphosphate kinase. All these proteins factors are overexpressed and purified in His-tagged from without loss of activity. Ribosomes are obtained from sucrose density gradient centrifugation, and the system is reconstituted in buffer with all components [12]. The general composition of the PURE system proposed by Shimizu and colleagues[11] can be found in Table 1-1, though, modifications to it

have been made for commercialization [13]. This system eliminates the possibility of degradation of template nucleic acids and protein products, and also achieves the efficient incorporation of unnatural amino acids at specific protein sites [14].

Table 1-1. Composition of the PURE system [13].

Buffer mix (x2)	***c* (mM)**		***c* (mM)**	**Enzyme mix (x10)**	***c* (μg/mL)**		***c* (μg/mL)**
L-Alanine	0.6	L-Threonine	0.6	Ala RS	688	Tyr RS	6
L-Arginine	0.6	L-Tryptophan	0.6	Arg RS	20	Val RS	8
L-Asparagine	0.6	L-Tyrosine	0.6	Asn RS	220	MTF	200
L-Aspartic acid	0.6	L-Valine	0.6	Asp RS	80	IF1	100
L-Cysteine	0.6	HEPES-KOH (pH 7.6)	100	Cys RS	12	IF 2	400
L-Glutamine	0.6	Potassium glutamate	200	Gln RS	38	IF 3	100
L-Glutamic acid	0.6	$Mg(OAc)_2$	26	Glu RS	126	EF-G	500
L-Glycine	0.6	Spermidine	4	Gly RS	96	EF-Tu	1000
L-Histidine	0.6	DTT	2	His RS	8	EF-Ts	500
L-Isoleucine	0.6	Creatine phosphate	40	Ile RS	395	RF1	100
L-Leucine	0.6	ATP	6	Leu RS	40	RF2	100
L-Lysine	0.6	GTP	6	Lys RS	64	RF3	100
L-Methionine	0.6	CTP	2	Met RS	21	RRF	100
L-Phenylalanine	0.6	UTP	2	Phe RS	165	MK	30
L-Proline	0.6	FD[a]	20 μg/mL	Pro RS	102	CK	40
L-Serine	0.6	tRNA mix	112 OD_{260}/mL	Ser RS	19	NDK	11
Ribosome (x20)	***c* (μM)**			Thr	63	PPiase	10
70S ribosome	20 μM			Trp RS	11	T7 RNA polymerase	100

c, concentration. [a] 10-Formyl-5,6,7,8-tetrahydrofolic acid. RS, tRNA synthetase. MTF, methyltetrahydrofolate. IF1, initiation factor 1. EF-G, elongation factor G. EF-Tu, elongation factor Tu. EF-Ts, elongation factor Ts. RF1, Release factor 1. RRF, ribosome recycling factor. MK, myokinase. CK, creatine kinase. NDK, nucleoside-diphosphate kinase. PPiase, peptidylprolyl-isomerase.

1.2.1 Expression of membrane proteins using the PURE cell-free system

The automation and optimization of cell-free platforms for the *in vitro* synthesis of proteins has found a variety of applications suitable for functional and structural proteomics [8,10]. A variety of features make membrane proteins one of the most problematic targets in expression studies. Their hydrophobic nature often promotes unfolding and aggregation[15]. Purification of proteins in native membranes and further reincorporation into an artificial membrane normally involves the usage of detergents and continues to be a crucial step to the study of the structure and function of these molecules [16]. To circumvent that, cell-free systems represent an alternative for the expression of these hydrophobic proteins. The open nature of the system allows the addition of accessory reagents (such as lipids), folding catalysts, or a variety of amphiphilic molecules that can assess protein insertion and proper folding into artificial membranes [10]. In cell-free systems, membrane proteins have been expressed as precipitates followed by successful solubilization in presence of detergents [15,17]. Other reported additives are bicelles (assemblies of phospholipids and detergents), amphipols (amphiphilic polymers), nanodiscs, vesicles derived from biological membranes (*e.g.,* microsomes), and liposomes [2,17-19]. The illustration in Figure 1-1 summarizes the insertion of membrane proteins in presence of microsomes, liposomes, or micelles in the cell-free reaction as hydrophobic mimetic structures in an aqueous solution. The presence of a hydrophobic environment stabilizes the newly-synthesized protein and prevents its aggregation.

Choosing the right additive for cell-free expression depends on the nature of the target protein and the downstream applications. Liposomes are spherical membrane vesicles formed from synthetic or biological lipid extracts that in combination with cell-free systems provide a hydrophobic environment for the direct insertion and folding of the protein [17]. Several reports have described the successful expression of membrane proteins in presence of liposomes. Some of these proteins include the apo cytochrome b5 [20], aquaporin Z [21], bacteriorhodopsin [22], ATP synthase [13,23], ADP/ATP carrier [24], Cx43 [25–27]. The work of Long and colleagues, showed that the presence of cardiolipin in the liposomes added to the cell-free reaction increased both the rate of translation and the efficiency of integration of the ADP/ATP carrier [24]. This example shows that the presence of specific lipids could be essential for the target protein to properly assemble and be functional. Thus, lipids can act as co-factors for the proteins as well as have a chaperone-like effect over the expression of proteins [17].

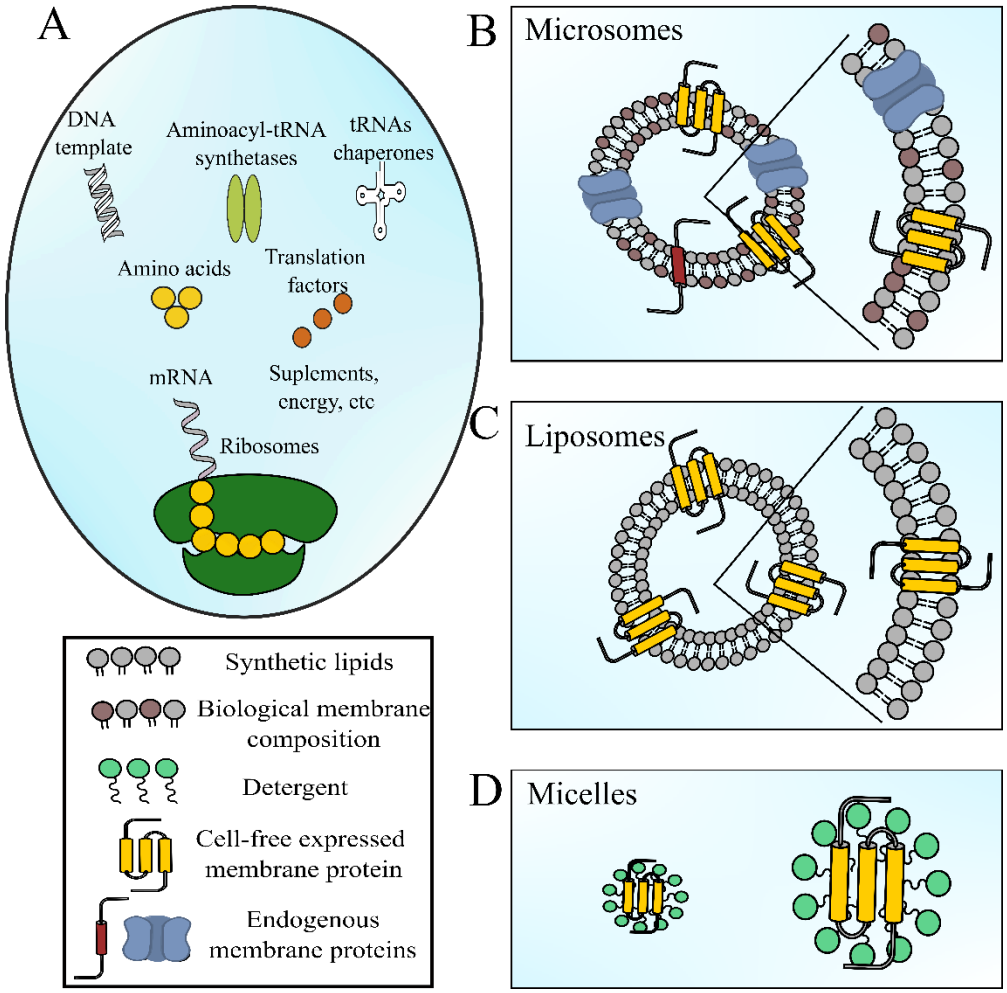

Figure 1-1. Expression of membrane proteins using a cell-free system in presence of membrane mimics. A) purified components necessary to express proteins in vitro. Stabilization of membrane proteins by proving a hydrophobic environment in which they can insert and properly fold: B) microsomes (vesicles derived from native biological membranes), C) liposomes, D) micelles. Adapted from [17].

The functional behavior of a process in a cell depends not only on its components but also on their connection to other processes and the context in which those cells operate. Communication between different cell types requires multiple communication channels and interconnection between them [3]. Therefore, establishing communication pathways in an artificial manner seems important in the context of building minimal cells.

1.3 Intercellular communication through gap junctions

1.3.1 Gap junctions and connexin 43

Gap junctions represent a ubiquitous component of all multicellular vertebrate organisms and serve important functions in direct intercellular communication between most cell types. Gap junctions play a dynamic role in developmental regulation and signal transduction pathways using classic signaling molecules such as cAMP and other nucleotides, calcium ions, inositol triphosphate, as well as providing direct pathways for metabolites that mediate cell homeostasis, and ions that propagate electrical signals in the heart and nervous systems [28]. In more detail, Gap junctions are specialized regions of the plasma membrane in which protein oligomers are in contact between adjacent cells. Thus, forming pores for direct intercellular communication that allow the exchange of small molecules up to 1 kDa [29].

Gap junction channels are formed by head-to-head docking of hexameric assemblies (connexons) from two different cells. They can be constituted from one (homomeric) or different proteins (heteromeric) from a multigene family of homologous proteins called connexins. Six connexin units assemble to form a connexon (or hemichannel) which locates in the lipid bilayer of a cell and allows transport of molecules[30]. Connexins have four transmembrane segments forming α-helices. The N and C termini, as well as the loop connecting the second and third transmembrane helices, are located on the cytoplasmic side of the cell. The extracellular side of the membrane contains two loops that connect the first transmembrane helix to the second, and the third to the fourth transmembrane α-helix (see structure of the protein in Figure 1-2). A total of 21 different connexins have been identified in the human genome [31], and comparisons of the amino acid sequences of those connexins have shown that the four transmembrane domains and the two extracellular loops are the most conserved domains, while the most variable sequences are found in the cytoplasmic central loop and the C-terminal domain [28].

Connexin 43 (Cx43) is ubiquitously distributed in the human body and the most studied protein from the connexin family. It was initially described as a protein required for direct cell-to-cell communication, but it has been demonstrated that it can also mediate communication between non-opposed cells, through tunneling nanotubes and extracellular vesicles, therefore playing a role in paracrine communication. Intercellular communication mediated by Cx43 can be

modulated by posttranslational modifications that include phosphorylation, acetylation, nitrosylation, sumoylation, and ubiquitylation [31] as well as intracellular pH changes [32]. Given these features, Cx43 has also been chosen as a candidate to mimic intercellular communication in a synthetic way by several authors [25–27,33,34].

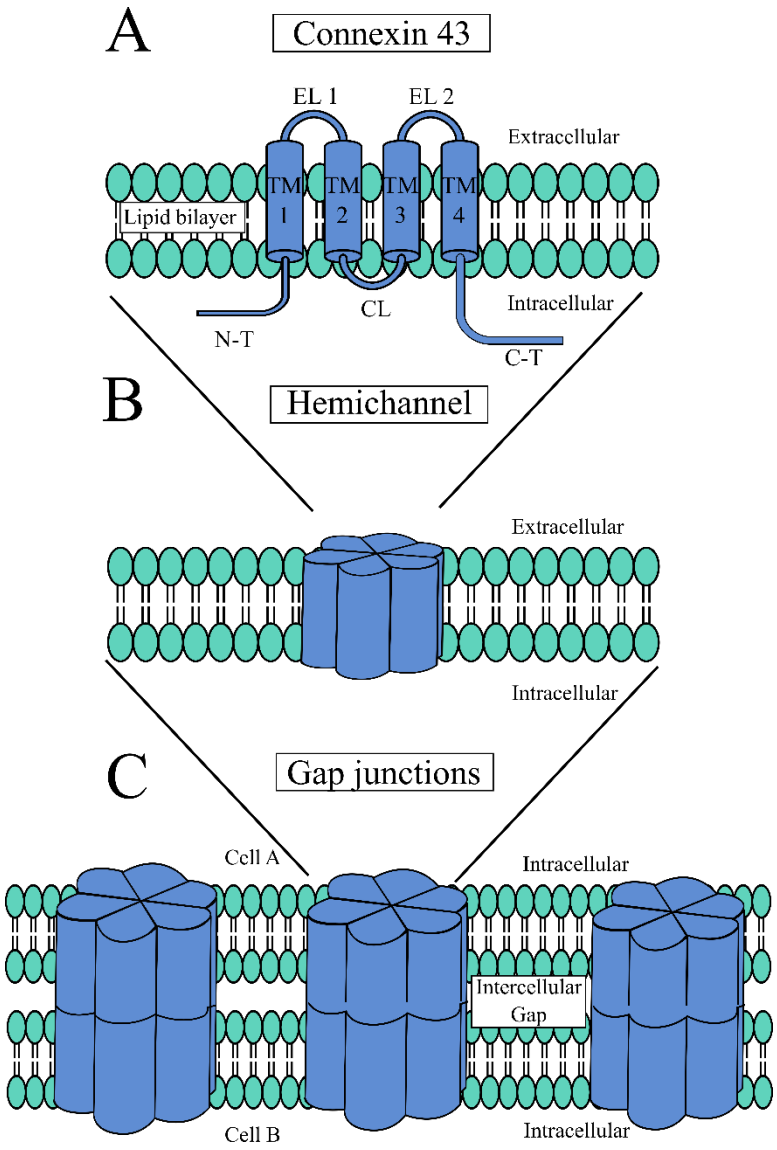

Figure 1-2. A) Structure of Cx43 embedded in a lipid bilayer. Cx43 is constituted by four transmembrane domains (TM 1-4), two extracellular loops (EL 1-2), a cytoplasmic loop (CL), and an N- & C terminal domain (N-T & C-T). B) Six connexin subunits assemble to form a hemichannel which can transport small molecules across the lipid bilayer. C) Hemichannels from two different cells can interact to form a direct pathway that connects the cytoplasm of both cells, known as the Gap junction channel.

1.3.1.1 Expression of Cx43 using cell-free systems

Cell-free systems have been used to express and directly insert Cx43 into membranes of dog pancreatic microsomes [33,34] or liposomes [26,27] using a reticulocyte lysate, or the PURE cell-free system in presence of liposomes [25,35]. These studies have shown that Cx43 integrates in the bilayer membranes in a cotranslational manner, and the amount of inserted protein increases with increasing the concentration of the vesicles in the cell-free reaction [25,33]. Using protease protection assays, have demonstrated that Cx43 inserts into microsomes or liposomes in an inside-out configuration, exposing the C and N termini to the extracellular side of the membrane [25,34] as it happens in the membranes of the rough endoplasmic reticulum in natural systems [36]. The functionality of Cx43 contained in those membranes has been tested by electrophysiological determinations [34], dye- and peptide transfer assays [27], as well as quenching assays [25]. Dye-transfer assays have shown that is possible to connect Cx43 proteoliposomes with U2OS [27] and U87 [26] cultured cells expressing Cx43, reporting a success of ~61 ± 33 % and 58 %, respectively. Cx43 directly inserted into exosome-mimetic membranes has been used as carriers to deliver small interfering RNA (siRNA) into cultured cells through the gap junction system [26]. In that sense, the delivery efficiency of siRNA molecules to U87 MG and A549 cells through Cx43 inserted in exosome-mimetic membranes was ~50 % and ~30 %, respectively [26]. These results are evidence of the potential of Cx43 proteoliposomes as minimal cells to deliver molecules of interest to living cells and opens the way to further applications.

2. Scope of Thesis

Cell-free systems can be understood as programmable liquids, which typically contain enzymes necessary for the transcription and translation processes independent from a cell [8]. Their open nature provides a platform to build minimal cells and mimic processes of living cells in an synthetic manner [1,37]. The functional behavior of a process in a cell depends on its components as well as on their connection to other processes and the context in which those cells operate [3]. In vertebrates, gap junctions are cluster of intercellular channels that allow direct diffusion of ions and small molecules between adjacent cells [30]. These intercellular channels are constituted by of six connexin molecules, forming a hemichannel that locates on the membrane of each adjacent cell. From the connexin family, connexin 43 (Cx43) is the most studied protein [38] and given its ability to establish direct communication pathways between two cellular compartments, it will be the protein model for this project.

Using a bottom-up approach, the cell-free technology will be used to reconstitute Cx43 in artificial membranes to potentially mimic cell-to-cell communication through the gap junction system. In more detail, functional plasmids compatible with the cell-free machinery will be produced to explore three main elements throughout the project: i) the direct incorporation of Cx43 into vesicles, ii) the characterization of Cx43 proteoliposomes, and iii) the incorporation of Cx43 into vesicles of different sizes. For the incorporation of Cx43 into artificial membranes, the cell-free reaction will be tested in the presence of vesicles of different lipid composition and concentration. The expression and insertion of Cx43 into membranes will be evaluated by Western Blot and fluorescence spectroscopy or microscopy. To characterize the proteoliposomes, protease assay will be conducted to determine the orientation and possible configuration the Cx43 adopts when incorporated into membranes. Additionally, functional assays will be carried out by the planar bilayer method to evaluate the single-channel behavior of Cx43 when express using the model system proposed in this project. Finally, the incorporation of Cx43 into vesicles of different size will be evaluated by fluorescence spectroscopy. Similarly, the insertion of Cx43 into the membrane of GUVs and its distribution will be analyzed by confocal laser scanning microscopy since these compartments could be to direct visualize connection between these artificial cells through the gap junction system.

3. Materials and Methods

3.1 Materials

3.1.1 Buffers

To develop this project, different buffers were used depending on the experiments and their purpose. The name and composition of each buffer are listed in Table 3-1. All buffers were diluted in ultrapure water and filtered (pore size Ø 0,2 nm). For buffers C and D, the osmolarity of the solution was measured with the Osmomat 030 (*Gonotech GmbH, Berlin, Germany*).

Table 3-1. Buffers and their composition according to the type of assay they were used for.

Buffer	Composition	Purpose of use
A.1	30 mM Tris pH 7.4	Synthesis of Cx43 in aqueous solution.
A.2	30 mM Tris pH 8.0	Protein digestion assays with TEV.
B	10 mM HEPES pH 7.4 100 mM KCl	Synthesis of proteo-Cx43 for Western Blot assays. Functional attempts at the Orbit 16
C	80 mM HEPES pH 7.4 40 mM KCl 40 mM glucose 0.05% NaN_3 211 mOsm	Fluorescence spectroscopy and microscopy; assays with SUVs, LUVs, and GUVs.
D	Sucrose at 211 mOsm	inner solution to prepare GUVs by electroformation.
E	10 mM HEPES pH 7.4 500 mM KCl 10% glycerol	Functional attempts with Cx43 at the Orbit 16.

3.1.2 Lipids and Fluorophores probes

In this work, artificial membranes systems were prepared to mimic the properties of biological membranes. These lipid model systems were composed of a matrix lipid containing a phosphocholine head group, in combination with a fluorescent probe, and in some cases, mixed with positively or negatively charged lipids. The matrix lipid was a major part of all lipid compositions. When small and large unilamellar vesicles were prepared, L-α-phosphatidylcholine from soybean (L-α-PC; *M*= 776 g/mol) was mainly used as matrix lipid, while 1-palmitoyl-2-oleoyl-sn-glycero-3-phosphocholine (POPC; *M*= 760,07 g/mol) was

used when preparing giant unilamellar vesicles. Additionally, 1,2-dioleoyl-sn-glycero-3-phosphocholine (DOPC; *M*= 786.11 g/mol) and 1,2-diphytanoyl-sn-glycero-3-phosphocholine (DPhPC; M: 846.25 g/mol) were also used as matrix lipids for comparison purposes (see structures in Figure 3-1).

The matrix lipids were often mixed with 1,2-dioleoyloxy-3-trimethylammonium-propane (DOTAP; *M*= 698,54 g/mol) as a positively charged lipid or with 1-palmitoyl-2-oleoyl-sn-glycero-3-phospho-(1´-rac-glycerol) (POPG; *M*= 770.98 g/mol) as a negatively charged lipid. On the other hand, DPhPC membranes were mixed with cholesterol (*M*= 386.65 g/mol) to give fluidity to the membrane system. To localize the samples and get insights about the model system and methods employed, the fluorophore probes 1,2-dihexadecanoyl-sn-glycero-3-phosphoetanolamine (*M*= 743.93 g/mol) or Texas Red™-DHPE (TxR) was added to the lipid mixtures (see structures in Figure 3-2).

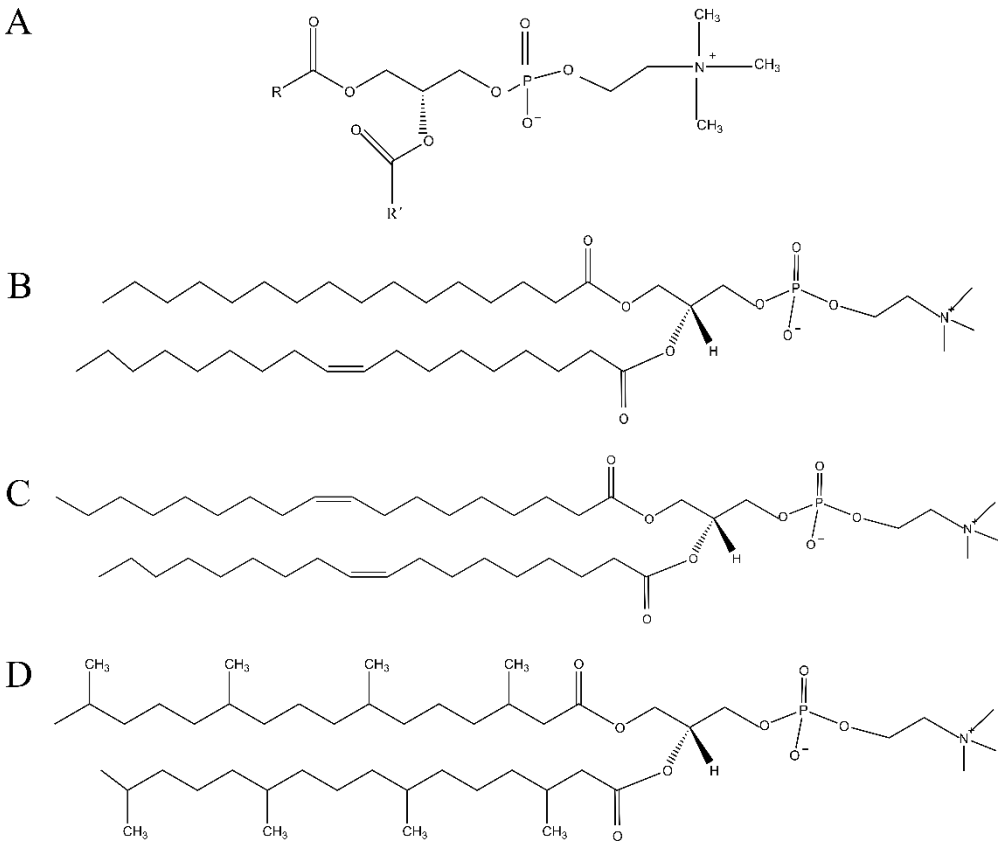

Figure 3-1. Structures of matrix lipids: A) L-α-PC, B) POPC, C) DOPC, D) DPhPC.

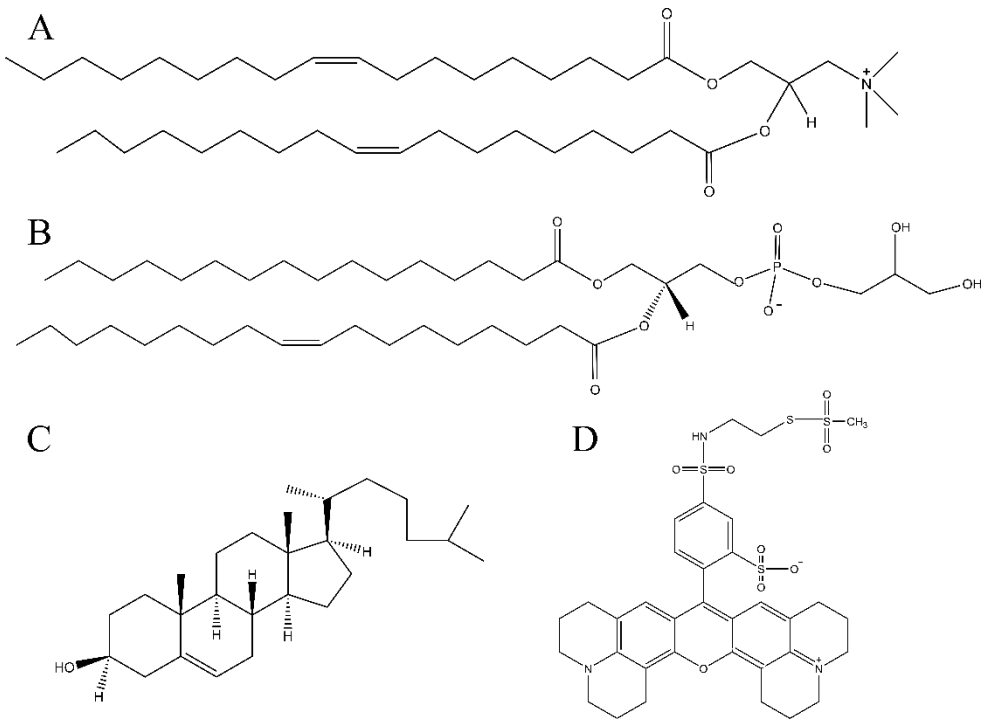

Figure 3-2. Structures of lipids: A) DOTAP, B) POPG, C) cholesterol, D) Texas Red™-DHPE.

3.1.3 DNA vectors

For this project, three plasmids based on the pET28a (+) vector were used, all three containing the mammalian Cx43 gene (from *Mus musculus*). The plasmid containing the wild type (WT) form of the gene, WT Cx43 plasmid, was synthesized by *Biomatik* (see structure in Figure 3-3). As it is characteristic of pET28a (+) vectors, the plasmid comprises a kanamycin resistance sequence, the lac operon, a ribosome binding site (RBS), and a T7 promoter and terminator sequences. Additionally, it contains the sequence of the gene coding for the Cx43 protein (GJA1), a 6x-Histidine (His6) tag located at the C-terminal domain, and two necessary protective bases for the stable insertion of the gene into the vector.

The second cloning vector, pET-LIC, was a gift from Scott Gradia (vector #29663. *Addgene, Massachusetts, USA*), and served as a template for the customization of N-EGFP Cx43 plasmid via Ligation Independent Cloning (LIC) (see section 3.2.1.1). This vector, also based on the pET system, has a TEV-cleavable His6 fusion tag on the N-terminus, an enhanced Green Fluorescent Protein (EGFP) as a reporter gene, a SspI restriction site (of particular interest for the LIC cloning approach), and a second His6 at the C-terminus.

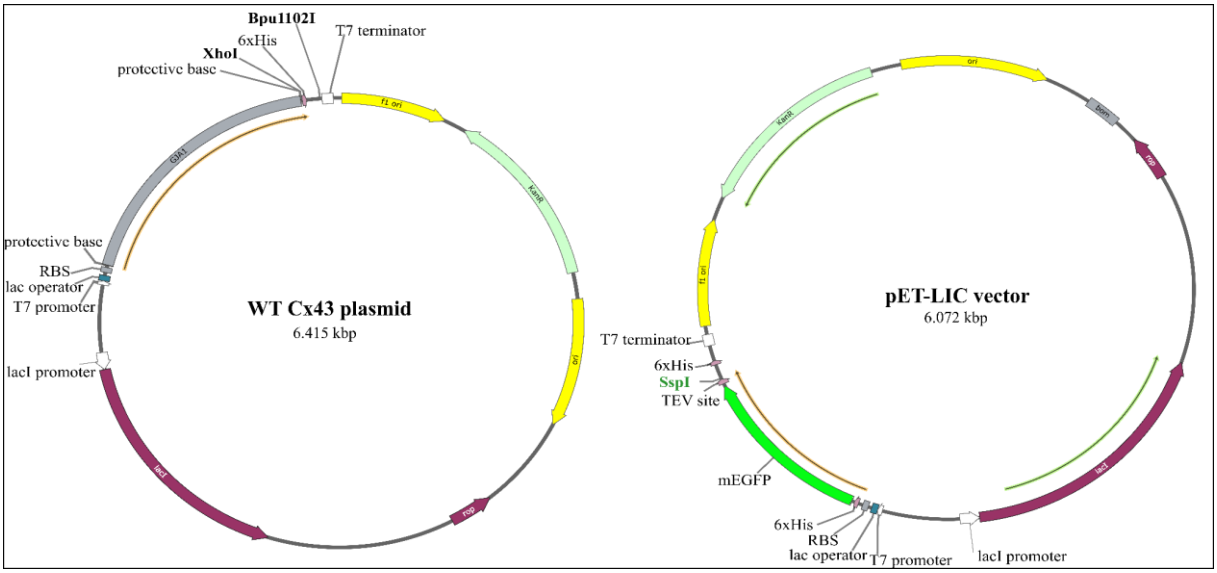

Figure 3-3. WT Cx43 plasmid and pET-LIC vector used to produce the N-EGFP Cx43 plasmid by ligation independent cloning or the C-EGFP plasmid by Gibson assembly. Both vectors are based on the pET28a(+) system and contain a kanamycin resistance sequence (Kan R), a lactose operon sequence (lac operator), a ribosomes binding site (RBS), a T7 promoter and terminator sequence, Histags (His 6), and restriction sites for vector cleavage assays by restriction endonucleases, e.g., SspI site in the pET-LIC vector.

3.2 Preparative Methods

3.2.1 Cloning methods

Molecular cloning represents a set of experiments procedures used to generate a population of organisms containing the same recombinant DNA molecule. These procedures are now standard in science, and they include DNA isolation, restriction enzyme assays, polymerase chain reaction (PCR), molecular cloning, and genome editing [39]. The classical cloning approach uses the vast repertoire of restriction enzymes commercially available to digest a DNA vector at the Multiple Cloning Site (MCS) and insert the DNA of interest using different ligation approaches [40]. On the other hand, the DNA of interest or insert can be obtained by the polymerase chain reaction (PCR), which amplifies target sequences from a DNA template. The basic premise of PCR relies on thermal cycling, a process in which the DNA-containing solution is heated and cooled repeatedly to (i) melt the DNA, (ii) anneal short DNA fragments (or small oligonucleotides called primers) to the complementary target DNA, and (iii) enzymatically replicate the primer-bound sequences using thermophilic DNA polymerases such

the Taq polymerase. Later on, the product can be used for analytical detection, sizing, cloning, or sequencing [41].

3.2.1.1 Ligation Independent Cloning

Ligation independent cloning (LIC) is a method that utilizes exonuclease activity to expose complementary single-stranded DNA (ssDNA) sequences that can be specifically annealed. The annealing process occurs within the host organism, instead of *in vitro*, following the transformation of the annealed molecules within the host [42]. This cloning method does not involve restriction enzymes or DNA ligase, instead. Instead, single-stranded and complementary tails are created at the ends of the PCR product and the linear plasmid vector allowing non-covalent associations between the two molecules [43]. In this project, the LIC method was used to obtain the N-EGFP Cx43 plasmid containing the sequence coding for Cx43 protein, an EGFP at the N-terminus followed by a TEV cleavage site. A scheme of the procedure is shown in Figure 3-4Figure 3-4.

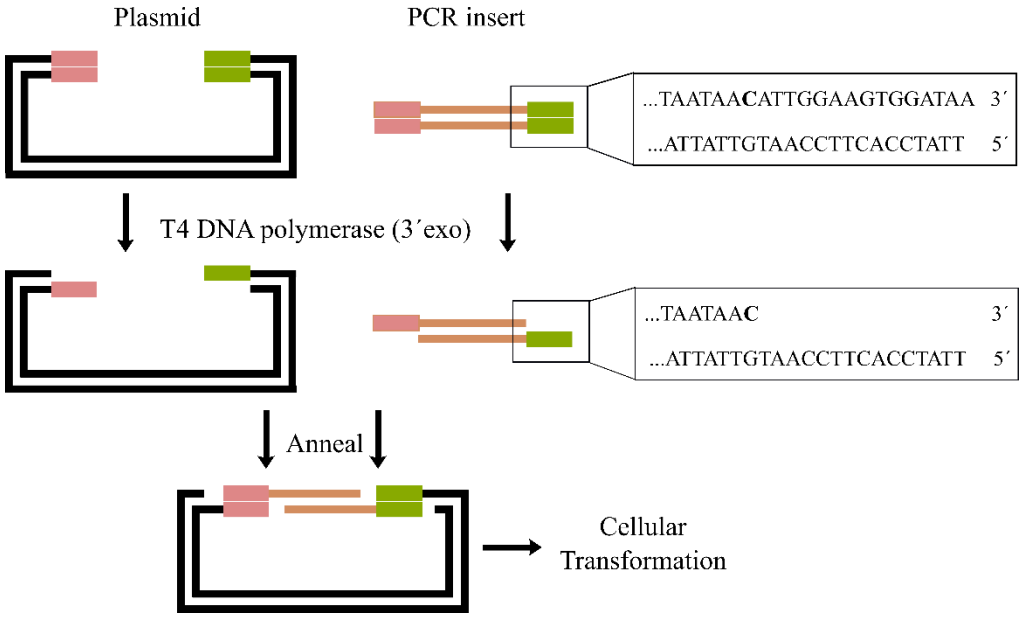

Figure 3-4. Ligation independent cloning procedure. Both vector and DNA insert are treated with an exonuclease to expose complementary single-stranded DNA sequences. Both DNA sequences can anneal for a certain incubation time, and the mixture is directly added to a bacterial host for cellular transformation.

The WT-Cx43 plasmid served as a template to amplify the Cx43 sequence by PCR (see reaction mixture on Table 3-2) using the thermocycler conditions seen in Table 3-3**Error! Reference source not found.** (see primer sequences in the Appendix section 8.1). The PCR product was run in a 1 % agarose gel, purified by gel extraction, and mixed as shown in Table 3-4 to prepare the PCR product to undergo the LIC reaction. This reaction mixture was incubated on a thermocycler first at 22°C for 30 min, and then at 75 °C for 20 min.

Table 3-2. Reactions mixture for amplification of Cx43 sequence for LIC reaction by PCR.

Component	Volumes (µL)
Water	31
5x Phusion GC buffer	10
10 mM dNTPs	1
Forward (LIC) primer	2.5
Reverse (LIC) primer	2.5
Template DNA (C_f = 10 ng)	1
DMSO	1.5
Phusion Polymerase	0.5
Total volume	50

Table 3-3.Thermocycler conditions for the amplification of Cx43 by graded PCR.

Step	Temperature (°C)	Time (s)
Initial denaturation	98	60
Denaturation I	98	20
Annealing I	64	30
Elongation I	72	50
Repeat x10	--	--
Denaturation II	98	20
Annealing II	72	30
Elongation II	72	50
Repeat x20	--	--
Final elongation	72	300

Table 3-4. The reaction mixture for LIC- PCR product.

Component	Volumes (µL)
Purified PCR product (C_i= 50-150 ng)	10
dCTP (C_i= 25 mM)	2
X5 T4 DNA polymerase buffer	4
DTT (C_i= 100 mM)	1
T4 DNA polymerase	0,4
Water	2.6
Total volume	20

On the other hand, 500 ng of the pET-LIC vector were digested with SspI (incubation at 37 °C for 2 h; see Table 3-5), run on an agarose gel, purified by gel extraction, and prepared for LIC reaction. The mixture to prepare the linear vector for LIC is shown in Table 3-6 and was incubated on a thermocycler at 22 °C for 30 min, and then at 75 °C for 20 min. Once both products had gone through the LIC reaction (the linear product and vector), they were mixed as shown in Table 3-7, incubated at RT for 10 min for the annealing step, and then transformed into chemically competent *E. coli* DH5α cells. Upon transformation, cells predictably repair the nicks and gaps in the chimeric DNA and propagate the desired plasmid product.

Table 3-5. The reaction mixture of the digestion assay for the LIC vector template using SspI.

Component	Volumes (µL)
Water	13.25
X10 Buffer G	2
DNA template (C_f= 50 ng)	3.75
SspI	1
Total volume	20

Table 3-6. The reaction mixture of the linearized vector for LIC reaction.

Component	Volumes (µL)
Linearized purified vector	10
dGTP (C_i= 25 mM)	2
X5 T4 DNA polymerase buffer	4
DTT (C_i= 100 mM)	1
T4 DNA polymerase	0.4
Water	2.6
Total volume	20

Table 3-7. LIC reaction. The mixture of LIC-PCR product and LIC-linearized vector.

Component	Volumes (µL)
LIC-PCR product	2
LIC-linearized vector	2
Water	6
Total volume	10

3.2.1.2 Gibson Assembly

The Gibson assembly is an *in vitro* recombination system characterized by its capacity to assemble and repair overlapping DNA molecules in a single isothermal step. These overlapping DNA molecules are joined by using three enzymes: i) an exonuclease, which chews back the ends of the fragments and exposes complementary single-stranded DNA (ssDNA) overhangs on each molecule that specifically anneals; ii) a polymerase, which fills the gaps in the annealed products; and iii) a ligase, which covalently seals the resulting nicks (see Figure 3-5). These methods have been proven helpful in cloning multiple inserts into a vector without relying on the availability of restriction sites and for rapidly constructing large DNA molecules, *e.g.,* plasmids [42]. The Gibson assembly was utilized in this project to customize the C-EGFP Cx43 plasmid containing the sequence coding for Cx43 and EGFP at the C-terminus. For the procedure, the GeneArt™ Gibson Assembly HiFi kit by Invitrogen™ (*Fisher Scientific GmbH, Schwerte, Germany*) was used according to the manufacturer's instructions. This kit requires that each DNA fragment shares 20-40 bp terminal homology with the adjacent fragment [44]. Therefore, primers for PCR amplification should be up to 65 bp in length, thus containing 20-40 bp as the requisite homology sequence for the Gibson Assembly at the 5′end and 18-25 bp specific to the DNA of interest. For this work, a PCR was carried out to amplify the EGFP sequence from the pET- LIC vector and insert it into the WT-Cx43 vector which served as the template. The reaction mixture and thermocycler conditions for the PCR can be found in Table 3-8 and Table 3-9, respectively. The sequence of the primers used can be found in Table 8-2 in section 8.1 of the Appendix.

Table 3-8. The reaction mixture for the PCR cloning of the EGFP sequence from the WT-Cx43 vector.

Component	Volumes (µL)
Water	31
5x Phusion GC buffer	10
10 mM dNTPs	1
Forward (Gibson) primer	2.5
Reverse (Gibson) primer	2.5
Template DNA (C_f=10 ng)	1
DMSO	1.5
Phusion Polymerase	0.5
Total volume	50

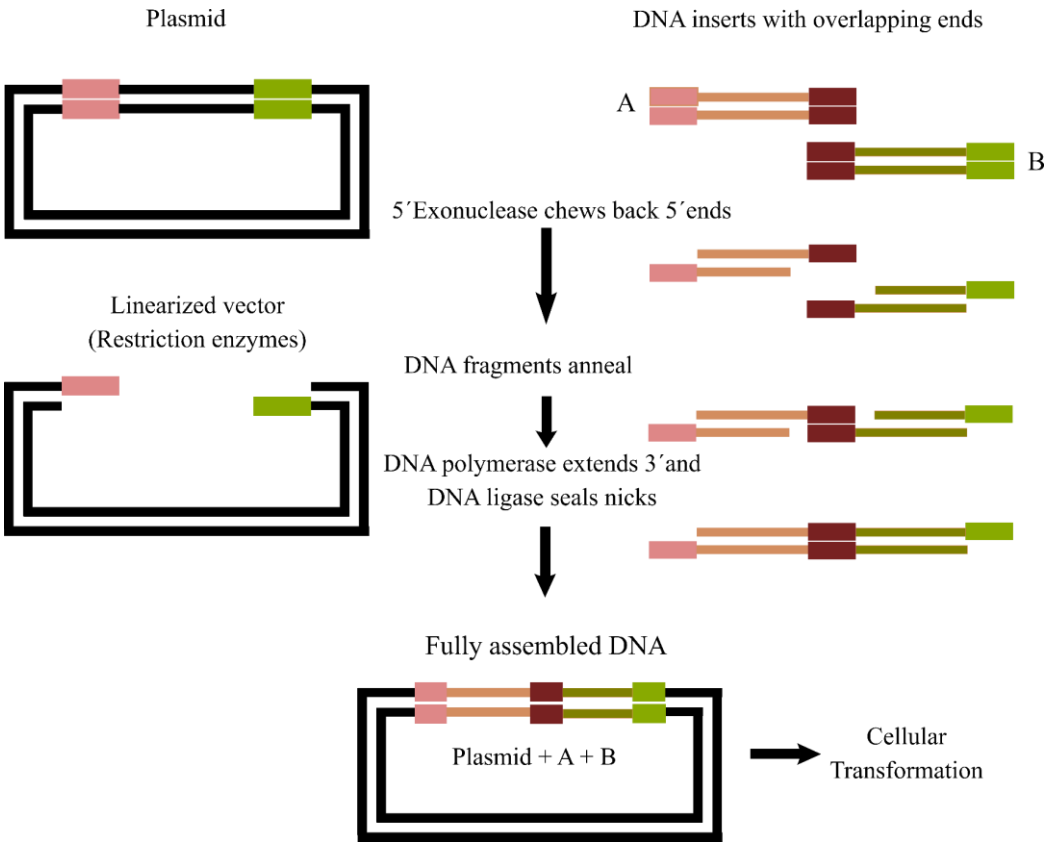

Figure 3-5. The Gibson Assembly procedure. Multiple DNA sequences can be assembled into one DNA vector. Both, the linear vector, and the DNA inserts with overlapping ends are treated with an exonuclease that exposes single-stranded complementary ends. The DNA inserts and vector are given a certain time for the annealing step. Next, a DNA polymerase fills the gaps from the annealed product and a DNA ligase seals the nicks. Afterward, the fully assembled DNA plasmid is added to a bacterial host for cellular transformation.

Table 3-9. Thermocycler conditions for the PCR cloning of EGFP sequence from WT-Cx43 vector.

Step	Temperature (°C)	Time (s)
Initial denaturation	98	60
Denaturation I	98	20
Annealing I	80	30
Elongation I	72	50
Repeat x5	--	--
Denaturation II	98	20
Annealing II	76	30
Elongation II	72	50
Repeat x5	--	--
Denaturation III	98	20
Annealing III	72	30
Elongation III	72	50
Repeat x 20	--	--
Final elongation	72	300

On the other hand, the WT-Cx43 vector served as a template to insert the EGFP sequence at the C-terminus domain to obtain the C-EGFP Cx43 plasmid. For that purpose, double digestion in a single tube was performed using the restriction enzymes XhoI and Bpu1102I by mixing the components as shown in Table 3-10 and incubated at 37 °C for 2 h. The digested product was run in 1 % agarose gel and purified by gel extraction using a QIAquick® gel extraction kit (*QIAGEN Sciences, Maryland, USA*).

Table 3-10. The reaction mixture for single and double enzymatic digestion of DNA template vector for the Gibson Assembly of C-EGFP Cx43 plasmid.

Components	Sample 1 (µL) Vector + XhoI + Bpu1102I	Sample 2 (µL) Vector + XhoI	Sample 3 (µL) Vector + Bpu1102I
Water	7.2	11.2	11.2
X10 Buffer G	2	2	2
DNA template	2.8	2.8	2.8
XhoI	4	4	--
Bpu1102I	4	--	4
Total volume	20	20	20

Finally, for the Gibson Assembly reaction the GeneArt™ Gibson Assembly HiFi Master mix was combined with the DNA insert and vector in equimolar ratios (see Table 3-11). This mixture was incubated at 50 °C for 15 min for both the product of interest and the control reaction. Following the incubation step, the reaction mixture was immediately used for transformation into *E. coli* DH5α cells.

Table 3-11. Reaction mixture to obtain C-EGFP Cx43 plasmid via Gibson Assembly.

Component	Sample reaction (µL)	Control reaction (µL)
Recommended DNA molar ratio/ *Positive control mix	Vector: Insert = 1:1 (X)	10*
GeneArt™ Gibson Assembly HiFi Master mix	10	10
Water	(10-X)	--
Total volume	20	20

3.2.2 Bacterial Transformation

The plasmids used in this work were cloned into *E. coli* DH5α cells prior to the isolation and purification steps. The bacterial transformation was achieved by adding an aliquot of the plasmid solution (3 µL from a 500 ng/µL stock) into an aliquot of the competent cells DH5α (50 µL) and incubating for 30 min on ice. Subsequently, the cells were subjected to 42 °C for 45 s to induce the uptake of exogenous DNA via heat shock. After, the cells were incubated for 5 min on ice, and 250 µL of S.O.C media (*Fisher Scientific GmbH, Schwerte, Germany*) were added and incubated at 37 °C for at least 1 h (see composition in Table 3-12). After that, the cells were spread onto LB-agar plates (see composition in Table 3-13) supplemented with 50 ng/µL of kanamycin to ensure selective growth of the transformed cells and incubated at 37 °C overnight.

Table 3-12. Composition of S.O.C media for cell growth [45].

Component	Concentration
Trypton	2.0 % (*w/v*)
Yeast extract	0.5 % (*w/v*)
NaCl	10 mM
KCl	2.5 mM
$MgCl_2$	10 mM
$MgSO_4$	10 mM
Glucose	20 mM

*Table 3-13. Composition of the LB-media and LB-agar plates used for plasmid cloning. *Agar-agar was only added to the preparation if LB-agar plates were prepared.*

Component	Concentration (*w/v*)
Trypton	1.0 %
Yeast extract	0.5 %
NaCl	1.0 %
Agar-agar*	1.5 % *
pH 7.4	

3.2.3 Plasmid Isolation

After cloning the plasmid into the *E. coli* cells, isolation and purification of the plasmid were essential to check the fidelity of the recombinant DNA sequence and to provide a stock for protein expression. For this purpose, the NucleoBond® Xtra Midi EF-kit *(Macherey-Nagel, Düren, Germany)* was used according to the recommendations of the manufacturer. The buffer solutions mentioned in this section were provided by the isolation kit which included no information regarding buffer compositions.

Following cellular transformation, a single colony was taken from the LB-agar plate into 100 mL of LB media and incubated at 37 °C and 250 rpm overnight. This cell suspension was centrifuged (4500 rpm, 4 °C, 20 min) and the resulting pellet was resuspended by pipetting 8 mL RES + RNase A buffer. This step was followed by the addition of 8 mL LYS-EF buffer and 5 min incubation at RT which led to cell lysis and the formation of an insoluble network composed of protein-SDS complexes and high MW RNA molecules [46]. In the meantime, the silica-based anion exchange resin column provided by the kit was equilibrated by adding 15 mL of EQU-EF buffer. The cell lysate was neutralized by adding 8 mL of NEU-EF buffer, mixed by panning the tube, and incubated for 5 min on ice. Next, the suspension was centrifuged (4500 rpm, 4 °C, 10 min) to separate the lysate from the cell's debris, and it was directly applied to the equilibrated column. Subsequently, the column was rinsed with 5 mL of FIL-EF buffer, 35 mL of ENDO-EF buffer, and 15 mL of WASH-EF buffer to remove the protein complexes and impurities from the column. Lastly, the plasmid was eluted with 5 mL of ELU-EF buffer and purified by isopropanol-ethanol precipitation. The eluted fraction was well-mixed with 3,5 mL of isopropanol, centrifuged (15000 g, 20 °C, 45 min), washed with endotoxin-free

ethanol, and centrifuged again (15000 g, 20 °C, 5 min). After removing the solvent from the sample, the plasmid pellet was dissolved in 20-30 µL of ultrapure water, the concentration was checked via UV-Vis spectrometry, aliquots of 500 mg/µL were prepared and stored at -20 °C until further use.

3.2.3.1 Plasmid sequencing

Directly after purification, all plasmids were sequenced to check the fidelity of their sequences to ensure that no errors (or possible mutations) could prevent protein expression. The sequencing reactions were carried by the company *Microsynth SeqLab GmbH* (Göttingen, Germany). The plasmids were sent in a concentration of 18 ng/µL, premixed with the primers listed in Table 8-1 and Table 8-2 (see section 8.1 in the Appendix), and analyzed by Sanger sequencing to evaluate the integrity of the sequences coding for Cx43 and EGFP.

3.2.4 Preparation of unilamellar vesicles

3.2.4.1 Preparation of lipid films

The lipid mixtures used to prepare liposomes varied according to the aim of the experiments. In general, they consisted of L-α-PC, POPC, POPG, DPhPC, DOPC, and cholesterol, which were normally mixed with Texas Red™-DHPE as a fluorophore probe to trace the sample along with the preparations either visually or by fluorescence spectroscopy or microscopy.

The preparation of the lipid films started by cleaning the tubes with 400 µL of chloroform to wash away any possible organic dirt. Next, the tubes were filled with certain volumes of the desired lipid from a stock solution to reach the desired molar ratio and combination. Subsequently, the chloroform was evaporated by applying a nitrogen flow and under incubation at 30 °C for ~15 min. The residual solvent was removed by incubating the lipid films under vacuum for 2 h. The lipid films used to prepare small and large unilamellar vesicles had a total mass of 5 mg, while the lipid films used to prepare giant vesicles had a total mass of 0.5 mg. The films were sealed with Parafilm®, protected from light, and stored at 4° C for up to 3 weeks.

3.2.4.2 Preparation of small and large unilamellar vesicles

The preparation of both small (SUVs) and large unilamellar vesicles (LUVs), started by hydrating the lipid films with 250 µL of buffer B (see Table 3-1) and letting them sit at RT for 30 min. Subsequently, the tubes were vortexed three times for ~30 s with a five-minute interval, resulting in the formation of multilamellar vesicles (MLVs). To obtain SUVs, the vesicle suspension was treated in an ultrasonic bath [47] for 30 min at RT with 60 % power. On the other hand, LUVs were obtained by extruding the vesicle suspension through a polycarbonate membrane of 100 nm pores 31 times [48].

3.2.4.3 Preparation of giant unilamellar vesicles

Giant unilamellar vesicles (GUVs) were prepared by two methods: i) electroformation [49,50], ii) the natural swelling/hydration method [51]. For the electroformation approach, the desired lipid composition was dissolved in chloroform to reach a concentration of ~0.5 mg/mL that was directly added onto indium tin oxide (ITO) covered slides. The ITO slides were placed under vacuum for at least 1 h to remove the chloroform and obtain a lipid film. Subsequently, the ITO slides were assembled into a chamber by using a silicon ring and sealed with the help of Teflon spacers and a copper strip located on one side of each ITO slide for electrical connection. Afterward, a sucrose solution (211 mOsmol/kg) was filled into the chamber, the voltage generator was connected and a sinusoidal voltage of 5 Vpp (peak-to-peak) at a frequency of 500 Hz was applied overnight, resulting in the formation of GUVs [49,50]. After the collection of the vesicles, a phosphate test of the samples was carried out prior to assembling a reaction mixture with the cell-free expression kit. To prepare GUVS following the natural swelling approach, a lipid film of 0.5 mg/mL was hydrated with a solution containing the components from a cell-free expression system and incubated at 37 °C for 3 h for promote the expression of the protein of interest. Under these conditions, the production of GUVs and the expression of the protein would take place in a simultaneous manner [27].

3.2.5 Determination of lipid concentration in vesicles: The Phosphate test

To standardize all reactions in which vesicles were used (regardless of their size), the lipid content in the vesicles had to be determined prior to the protein expression step. The phosphate test is based on the Molybdenum Blue procedure [52,53] which consist of digesting and oxidizing the sample of interest with an oxidizing agent, leading to the formation of a phosphomolybdic acid which is exposed to a reducing agent (in this case ascorbic acid), resulting in the formation of the molybdenum blue complex which can be evaluated *via* absorption spectroscopy [54–56], allowing the calculation of phosphate concentration *via* the Lambert-Beer relation.

The procedure started by combining 20 µL of the vesicles suspension with 200 µL of 70 % perchloric acid ($HClO_4$) in a glass tube and incinerating the content at 220 °C for 1 h to digest the sample and obtain inorganic phosphate. The phosphate in the sample was bound in a phosphomolybdate complex by the addition of a solution containing NH_4MoO_4 and $HClO_4$ (700 µL reagent A, see Table 3-14). Following, ascorbic acid (700 µL reagent B, see Table 3-14) was added as a reducing agent, thus leading to the formation of blue staining after the incubation of the samples in a water bath at 80 °C for 5-10 min.

Table 3-14. Compositions of reagents A and B for the determination of lipid content in the vesicle's samples.

	Composition	**Concentration (*w/v*) (%)**
Reagent A	NH_4MoO_4	0.45
	$HClO_4$	12.6
Reagent B	Ascorbic acid	1.7

For the preparation of the calibration curve, a stock solution of NaH_2PO_4 (c= 0.089 g/L) was diluted with ultrapure water up to 100 µL and prepared in duplicates following the scheme shown in Table 3-15 and incinerated at 220 °C for 1 h. After this step, the standards were mixed with reagents A and B in the same manner as for the samples and incubated in a water bath at 80 °C for 5-10 min. After the formation of the blue complex, the absorption (A_{820}) of all samples and standard solutions were measured at 820 nm using a Jasco V-650 UV-Vis spectrometer (*Jasco Corp., Tokyo, Japan*). The standard with no phosphate served as a blank when measuring the absorption of the vesicle samples. The A_{820} values of the standards were

plotted against the phosphate content to generate the calibration curve, following a linear trend, to which a linear fitting model was applied. By finding the relation between the linear equation from the calibration curve and extrapolating the A_{820} values from the samples, the amount of phosphate in the samples could be determined.

Table 3-15. Phosphate standard solution for the preparation of the calibration curve.

Amount NaH_2PO_4 (µg)	**0**	**0.25**	**0.50**	**1.0**	**1.5**	**2.0**
Volume NaH_2PO_4 (µL)	0	12.5	25	50	75	100
Water (µL)	100	87.5	75	50	25	0

3.2.6 Protein synthesis: Cell-free expression

Gene expression is fundamental in all cellular processes. The genetic information contained in the DNA molecule is transcribed into RNA, which is subsequently translated into a protein; this is the so-called central dogma of biology [57]. Cell-free protein synthesis is an *in vitro* approach than only requires the addition of a DNA template (circular or linear) or mRNA to the reaction mixture and incubation for several hours to obtain the protein of interest. Shimizu and colleagues [11,12] constructed a highly purified synthesis system from *E. coli* components, the so-called PURE system (Protein Synthesis Using Recombinant Elements). This system contains a His-tagged version of all protein factors (check detailed composition in Table 1-1 in section 1.2) that facilitates separation of their purification and the expression of the protein [12]. In this work, the PURExpress® *In Vitro* protein synthesis kit (*New England Biolabs, Frankfurt am Main, Germany*) is used. This kit consists of two solutions (A and B) containing all necessary components to synthesize the protein of interest. Due to the reconstitution methods of its recombinant proteins factors, this system has minimal contaminating exonucleases, RNases, and proteases. Therefore, the template DNA is not exposed to digestion and the protein of interest is free of posttranslational modifications [58].

Experimental approach:

For the expression of Cx43, all three plasmids described in sections 3.1.2 and 3.2 were used as DNA templates to carry out the protein synthesis reaction. The WT Cx43 plasmid was used for establishing and optimizing the CFE method with the PURExpress® *In Vitro* protein synthesis kit in the research group, while the C- & N-EGFP Cx43 plasmids were used to localize the

protein in the vesicle's membrane and characterization of the proteoliposomes. Following instructions from the manufacturer, solutions A, and B from the kit were added to a reaction tube together with an RNase inhibitor (C_f= 1 unit/µL), the DNA template (C_f= 40 ng), and the vesicles prepared as described in section 3.2.4 (see the composition of the reaction mixture in Table 3-16). Concerning the concentration of the lipid in the vesicles, several concentrations were tested (0.5; 1.5; 3; 5.5 mg/mL) when adding LUVs to the reaction. When adding SUVs, the standard concentration of lipids used was 3 mg/mL, while when adding GUVs the concentration was 30 µg/mL. Following, the reaction was mixed by pipetting up and down and incubated at 37 °C for 3 h. It is worth mentioning that the total volume of the reaction ranged from 25-30 µL to avoid a drop in the synthesis productivity by the kit [58].Those changes depended on the concentration of the prepared vesicle suspension and the concentration aimed to have in the reaction mixture.

Table 3-16. Composition of the reaction mixture for the cell-free expression of Cx43 using the PURExpress® In Vitro Synthesis kit.

Component	Volume (µL)
Solution A	10
Solution B	7.5
RNase Inhibitor (C_f= 1 unit/µL)	0.5
DNA template (C_f= 40 ng)	2
Liposomes*	X
Buffer	Y
Total volume	25- (X+ Y)

3.2.7 Density gradient centrifugation

Density gradient centrifugation (DGC) is a method for the separation of molecules or cell particles into zones by centrifugation. The method consists of adding the molecules of interest to a gradient media in which they are soluble and the application of a centrifugal force, allowing for the separations of the molecules according to their buoyant density [59,60]. In this work, HistoDenz™ (*Sigma-Aldrich, Taufkirchen, Germany*) was used as a density gradient medium to separate samples after CFE to obtain enriched fractions containing the previously formed proteoliposomes. To achieve that, the sample directly after protein expression was diluted with buffer B to reach a volume of 40µL, which was directly mixed with 40 µL of an 80 % (*w/v*) HistoDenz™ solution and transferred to an ultracentrifugation tube to form the first layer of

density gradient medium. On top of it, 40µL of a 30 % (*w/v*) HistoDenz™ solution and 20 µL of buffer were overlayed. Following, the samples were centrifuged at 50.000 rpm at 4 °C for 1.5 h (*Centricon T-1065, rotor: TST 60.4, Kontron Instruments, Osterode am Harz, Germany*) leading to the separation of the molecules according to their density. Thus, the vesicles were located at the top layer, followed by the proteoliposomes in the top-middle, and finally denser particles like non-inserted Cx43 and proteins from the PURExpress® kit were located at the bottom layers (see Figure 3-6). Subsequently, 7 fractions of 20 µL each were gradually collected and further analyzed by UV-Vis spectroscopy, fluorescence spectroscopy, or by Western Blot.

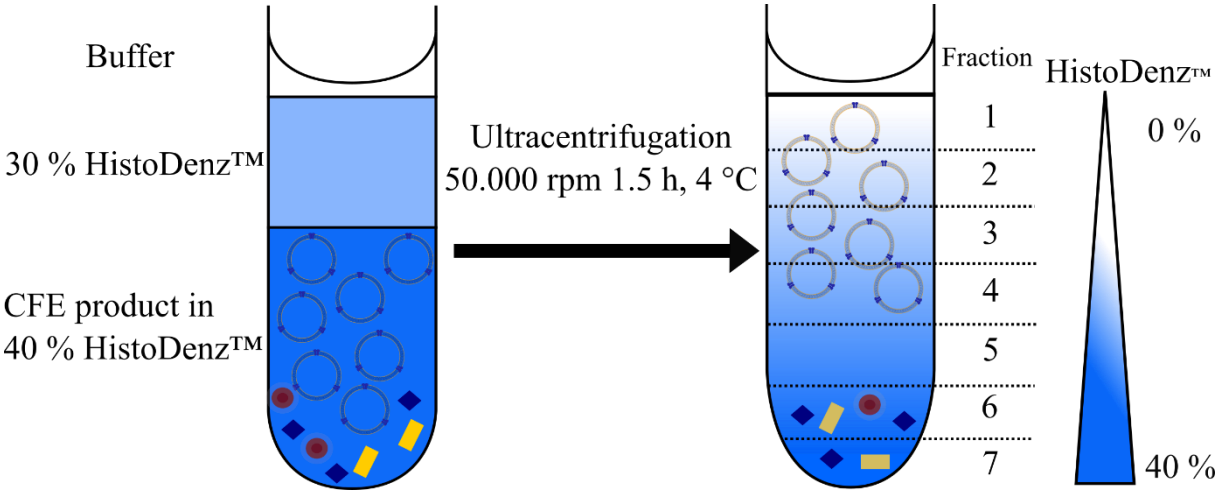

Figure 3-6. Schematic illustration of the procedure for density gradient centrifugation for the purification step to separate Cx43-proteoliposomes from the components from the CFE reaction mixture (depicted as yellow rectangles and red circles) or aggregated, non-inserted Cx43 (blue squares). Ultracentrifugation was carried in a HistoDenz™ gradient and seven fractions were collected.

3.2.8 Sodium Dodecyl Sulfate-Polyacrylamide gel electrophoresis

Sodium Dodecyl Sulfate-Polyacrylamide gel electrophoresis (SDS-PAGE) is a method that separates protein by molecular weight. The detergent SDS denatures secondary and non-disulfide-linked tertiary structures of the proteins, thus making them linear, and coating them with a negative charge to allow their separation through electrophoresis according to their molecular weight [61]. The Laemmli SDS-PAGE is a system of discontinuous gel based on glycine-Tris buffer appropriate for resolving large proteins (between ~20 and beyond 100 kDa). The acrylamide gels are characterized by the total percentage of acrylamide and the cross-linker

bisacrylamide relative to the total concentration [62,63]. This system is composed of an *upper stacking gel* and a *lower resolving* gel. The *stacking gel* has a lower percentage of polyacrylamide allowing proteins to move quickly and stack in a tight band while *resolving gel* has a higher percentage of acrylamide, where separation of proteins occurs [64].

In this work, the Laemmli SDS-PAGE was used to resolve the Cx43 protein variants with an approximate molecular weight ranging from 43-78 kDa. For this, polyacrylamide gels were prepared by using a Mini-PROTEAN® Tetra cell (*Bio-Rad Laboratories Inc., Hercules, USA*). To cast the gels, glass panels were cleaned with ethanol 70 % (v/v) prior to adding the acrylamide solution. The resolving gel (15 %, see the composition of buffer in Table 3-17) was added to the glass chamber and covered with isopropanol p.a. during polymerization. Afterward, isopropanol was removed and the stacking gel solution (5 %, see the composition in Table 3-17) was added on top followed by the insertion of a comb that serves to create the lane pockets to apply the samples. Polymerization of the gels was initialized by ammonium peroxydisulfate (APS, 10 % (*w/v*)) and catalyzed by N, N, N′, N′-tetramethyl ethylenediamine (TEMED), and for both gels (stacking and resolving), polymerization was led for ~30 min. After polymerization gels were either used directly for electrophoresis or stored for later use at 4 °C for up to 2 weeks. The gels were mounted in the electrophoretic chamber, the combs were removed and the Laemmli buffer (see composition in Table 3-18) was added. Meanwhile, the samples were mixed with loading buffer (see composition in Table 3-18) and incubated at 80 °C for 5 min. Samples obtained directly after CFE were mixed with 2X loading buffer while samples recovered from the density gradient centrifugation were mixed with 6X loading buffer. Following, the samples were loaded into the gel pockets alongside a protein marker (PageRuler Plus Prestained Protein Ladder; *Thermo Fisher Scientific*, Waltham, USA) for size comparison. A constant voltage was applied (120 V for 30 min followed by 160 V for 1 h), migration of the bands was visible due to the bromophenol blue present in the loading buffer. After the bromophenol blue front reached the end of the gel, electrophoresis was stopped, and the gel was removed from the glass cassette. Gels were washed with ultrapure water, heated in a microwave (800W, 45 s), and either stained with Coomassie brilliant blue or used for Western Blot. In the case of staining, a solution of Coomassie brilliant blue (see composition in Table 3-18) was added to the gels and incubated for at least 1 h under shaking conditions. Afterward, gels were washed with water prior to imaging with the Azure 3000 system (*Azure Biosystems, Dublin, USA*).

Table 3-17. Composition (per gel) of stacking and resolving gels for SDS-PAGE.

	Components
Resolving gel 15 %	1.15 mL ultrapure water
	2.5 mL Rotiphorese® Gel 30 (30 % acrylamide, 0.8 % bisacrylamide)
	1.3 mL of 1.5 M Tris pH 8.8
	50 µL of 10 % (*w/v*) sodium dodecyl sulfate (SDS)
	25 µL ammonium persulfate (APS)
	2.5 µL tetramethyl ethylenediamine (TEMED)
Stacking gel 5 %	2.04 mL ultrapure water
	510 µL Rotiphorese® Gel 30
	375 µL 1 M Tris pH 6.8
	30 µL 10 % (*w/v*) SDS
	15 µL APS
	1.5 µL TEMED

Table 3-18. Composition of the solutions used for the Laemmli SDS-PAGE procedure.

Solution	Components
Laemmli buffer	25 mM Tris pH 8.3
	192 mM Glycine
	0.1 % (*w/v*) SDS
Loading buffer	175 mM Tris/HCl
	100 mM DTT
	15 % (*w/v*) SDS
	0.02 % (*w/v*) bromophenol blue
Coomassie staining solution	80 mg/mL Coomassie Blue G-250
	In 3 mL of concentrated HCl

3.2.9 Western Blot

Western blotting or immunoblotting is a routinely used method to qualitatively identify proteins from complex biological samples. The separation of proteins is attained by gel electrophoresis (SDS-PAGE) based on their molecular weight; this is followed by the subsequent transfer and immobilization of the proteins to membrane support, and the selective detection using an antibody-mediated reporter system [65,66]. Proteins separated by gel electrophoresis are transferred and immobilized to a nitrocellulose or polyvinylidene fluoride (PVDF) membrane. These membranes are washed, blocked, and incubated with specific antibodies that only bind to the protein of interest, allowing the specific detection of the protein of interest. Following

the addition of the primary antibody, proteins can be detected by two approaches: i) Radioactive or by ii) Enzyme-linked reagents. In the first case, iodinated (^{125}I) staphylococcal protein A or streptococcal protein G binds to the primary antibody and is then visualized by autoradiography. On the other hand, the enzyme-linked approach involves the detection of the protein by using enzyme-coupled secondary antibodies that can be detected by chemiluminescence, normally involving a horseradish peroxidase (or alkaline phosphatase) coupled antibodies [67]. In this work, Western Blot was used as a qualitative method to identify the synthesized protein by means of cell-free expression.

Experimental approach:

The Western blot procedure started by separating the protein samples by SDS-PAGE as described in 3.2.9 except that staining the gel after electrophoresis did not take place. Instead, it was incubated in blotting buffer (for composition see Table 3-19) for 30 min together with two gel sized Whatman papers and one nitrocellulose membrane (*Bio-Rad Laboratories Inc., Hercules, USA).* Afterward, the proteins were transferred from the gel to the nitrocellulose membrane by electroblotting in a semi-dry approach. For this, the gel-membrane sandwich was placed between two Whatman papers previously soaked in blotting buffer (see Figure 3-7) and located in the Trans-Blot® device (*Bio-Rad Laboratories Inc., Hercules, USA*) for protein transfer by applying 180 mA, 15 V per gel for 45 min. The success of the transfer was visualized by incubating the nitrocellulose membrane in a Ponceau S solution for 2 min (see composition in Table 3-19). Following this, the membrane was washed with 0,1 M NaOH and ultrapure water and incubated with 5 % (*w/v*) milk solution in TBT buffer (see composition in Table 3-19) for 1 h at RT to prevent unspecific binding which could lead to interference or artifacts. Subsequently, the primary antibody was dissolved in milk-TBT solution in a ratio of 1:200, added to the membrane, and incubated for 1 h at RT (see the list of used antibodies in Table 3-20). After incubation with the primary antibody, the membrane was washed three times for 10 min with TBT buffer (10 mL) to remove the excess of unbound antibody. Next, the membrane was incubated with the secondary antibody diluted in milk-TBT buffer in a ratio of 1:1000 for 1 h at RT. The unbound secondary antibody was washed away by rinsing the membrane three times with TBT buffer (10 mL, 20 min incubation). In all cases, the Goat anti-mouse Ig (HRP) (*BD Pharmigen, San Diego, USA*) was used. Then, the membrane was incubated for 2 min in a 1:1 mixture of chemiluminescence solution (*Cytiva, Amersham ECL*

Prime). The HRP coupled to the secondary antibody catalyzes the oxidation of luminol in the presence of hydrogen peroxide, and the luminol which is in the excited state immediately decays in a light-emitting pathway. The resulting chemiluminescence was detected with an imaging system Azure 3000 (*Azure Biosystems, Dublin, USA*). The protein marker was in bright field mode to allow correlation of the molecular weights of the detected protein.

Table 3-19. Composition of the buffers used for Western Blot.

	Component	Concentration
Blotting Buffer	Tris	20 mM
	Glycine	150 mM
	SDS	0.05 % (*w/v*)
	Methanol	20 % (*w/v*)
TBT buffer	Tris	10 mM
	NaCl	150 mM
	Tween 20	0.2 % (*w/v*)
Ponceau S	Ponceau S	0.1 % (*w/v*)
	Acetic acid	5% (*w/v*)

Table 3-20. List of primary and secondary antibodies used for detecting Cx43 via Western Blot.

Protein to detect	**1st antibody-antigen**	**Epitope**	**Dilution factor used**	**Manufacturer**
N- & C-EGFP Cx43	Monoclonal mouse IgG_{2b} anti-GFP antibody	Amino acids 167-182 of GFP	1:200	Santa Cruz Biotechnology
WT, C- & N-EGFP Cx43	Monoclonal mouse IgG1 anti-cx43 antibody	Amino acids 241-254 of Cx43	1:200	Santa Cruz Biotechnology
Ezrin	Monoclonal mouse IgG1 anti-His antibody	Sequence of HHHH	1:1000	QIAGEN

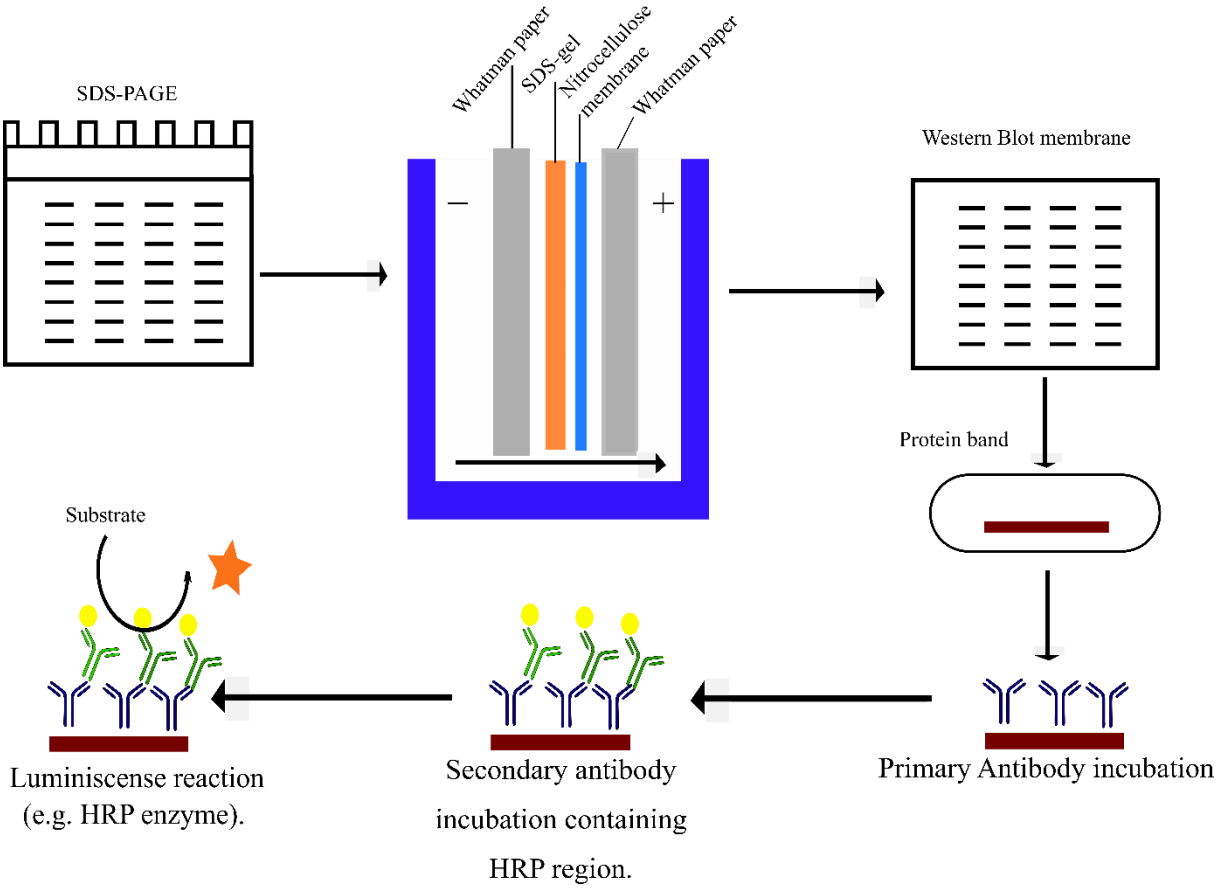

Figure 3-7. Summary of Western Blot procedure. Upon protein separation by SDS-PAGE, the gel was incubated in blotting buffer and assembled in a gel-nitrocellulose membrane sandwich. Transfer of proteins from the SDS-gel to the nitrocellulose membrane occurs while being exposed to an electric field. The nitrocellulose membrane is then blocked with milk-TBT, and after several washing steps, is incubated with the primary antibody dissolved in milk-TBT. The primary antibody specifically binds to the protein of interest. Next, the membrane is incubated with a secondary antibody in milk-TBT that recognizes a region of the primary one. Finally, the membrane is incubated with solutions containing luminol and hydrogen peroxide that catalyzes the oxidation of luminol, followed by the emission of light.

3.3 Biophysical Methods

3.3.1 Dynamic Light Scattering

Dynamic light scattering (DLS), also known as photon correlation spectroscopy, is a method based on the property of macromolecules dissolved in a liquid to scatter light from an incident light beam in all directions of space. The total scattered light field at a given point in space is the result of the superposition of all the wavelets scattered from the individual particles that fluctuate with time, given that macromolecules follow random movements due to Brownian motion [68]. When the movements of particles over a time range is monitored, information about the size of macromolecules can be obtained, given that large particles diffuse slowly, they will

encounter similar positions at different time points, unlike smaller particles (*e.g.,* solvent molecules) which move faster and therefore do not adopt any specific position. The motion of macromolecules due to Brownian motion depends on factors like their size, temperature, and solvent viscosity [69]. When analyzing spherical particles in a diluted dispersion, the Stokes-Einstein equation relates the translational self-diffusion coefficient with the hydrodynamic radius R of the particle:

Equation 3-1

$$D = (k_B\, T)/6\pi\, \eta\, R$$

Where k_B is the Boltzmann constant, T the absolute temperature, and η the viscosity of the suspending medium. Thus, for spherical nanoparticles, the particle hydrodynamic radius, including a solvation layer may be derived from the DLS experiments [70,71].

Regarding the DLS setup, light from a laser is focused on a sample, and the light scattered at a given scattering angle is collected by a square-law detector (photomultiplier). The output of the photomultiplier is then digitized by a photon counting system and the output is sent to an autocorrelator [71].

Experimental approach:

In this project, DLS was used to estimate and determine the size of the vesicles before and after cell-free expression. In general, after preparing the liposomes as explained in section 3.2.5, SUVs, LUVs, and GUVs were diluted 50 times with the respective buffer used for their preparation (buffer C and D, see Table 3-1) and evaluated using a Zetasizer Nano S (*Malvern Panalytical Nuremberg, Germany*). In the same manner, the size of the particles obtained after CFE was also evaluated. It is worth mentioning here, that GUVS obtained by electroformation usually display a heterogenous size distribution, therefore DLS is not an appropriate method to determine the size of GUVs. Despite that, DLS was used in a qualitative sense to evaluate if the overall size distribution of the vesicles (SUVs, LUVs, and GUVs) changed after protein expression and its insertion into the artificial membranes.

3.3.2 UV-Vis spectroscopy

Spectroscopy may be defined as the study of the quantum interaction of electromagnetic radiations with matter [72]. An electron is excited if the frequency of the incident electromagnetic radiation matches the difference in energy between two electronic states of a molecule. That energy difference depends on the electronic structure and the environment of the molecule under analysis [73], and it is usually described by the Bohr-Einstein relation shown in Equation 3-2 [74].

Equation 3-2

$$\Delta E = \frac{h \cdot v}{\lambda} = h\, c\, \bar{\upsilon}$$

where v is the frequency of the electromagnetic radiation, c is the speed of light in the vacuum, λ is the vacuum wavelength [74].

The energy of a molecule is given by its movement through space (translational), its rotatory motion (rotational), the oscillatory movement of the atoms with respect to each other (vibrational), and the distribution of its electron density (electronic energy). The corresponding energy states can be calculated by the Schrödinger equation. In the ultraviolet-visible (UV-Vis) region of the spectra, the energy levels correspond to electron density distributions (orbitals) [73]. If the frequency of radiation corresponds closely to the energy difference of the transition between two energy states, resonance excitation takes place, leading to a change in the electron density distribution, and an electronic transition from the highest occupied molecular orbital (HOMO) to the lowest unoccupied molecular orbital (LUMO). The energy required for this transition is provided by radiation. This process is known as induced absorption [74].

In the UV-Vis region, the wavelike character of the matter is more noticeable in contrast to its particle-like character (photons). In that sense, UV-Vis spectroscopy measures the attenuation of light when the light passes through or interacts with an absorbing substance [74]. The absorbance (A) of a sample is directly proportional to the distance the light travels through the sample and to the concentration of the absorbing species. This linear relationship is known as the Lambert-Beer Law (see Equation 3-33) and allows the accurate measurement of the concentration of absorbing species in the sample [74,75].

Equation 3-3

$$A(\lambda) = \varepsilon \cdot l \cdot c$$

Where $A(\lambda)$ is the measured absorbance at a defined wavelength (λ), ε is the absorption or extinction coefficient, l is the optical path length through the absorber, and c is the absorber concentration. Hence, by measuring $A(\lambda)$, c can be determined (see rearranged Equation 3-4). The Lambert-Beer law assumes that monochromatic radiation falls perpendicularly onto the sample. Since the absorption coefficient is a molecule-specific quantity, any chemical change of the molecule or interaction with the solvent, leads to false results when the Lambert-Beer law is applied [73].

Equation 3-4

$$c = \frac{A\,(\lambda)}{\varepsilon \cdot l}$$

Experimental approach:

In this project, UV-Vis spectroscopy was used to determine the concentration of lipids in the prepared vesicles before their addition to the CFE reaction. The determination of the lipid content was carried out by the phosphate test described in section 3.2.5 using a spectrophotometer Jasco V-650 (*Jasco Corp., Tokyo, Japan*). Furthermore, UV-Vis spectroscopy was also used to determine the concentration of the DNA templates obtained after plasmid isolation for all three Cx43 variants (WT Cx43, C- & N-EGFP Cx43) using a NanoDrop™ 2000c (*Thermo Fisher Scientific, Waltham, USA*). This instrument was also used to determine the absorption of Texas Red™ at 583 nm in the different fractions collected from DGC to evaluate the distribution of the vesicles among them.

3.3.3 Fluorescence

Luminescence is the emission of light from any substance and occurs from electronically excited states. This phenomenon is divided into two categories, fluorescence, and phosphorescence, which depend on the nature of the excited state. In excited singlet states, the electron in the excited orbital is paired to the second electron in the ground-state orbital, resulting in a return to the ground state either by non-radiative processes or by emission of photons, in a process known as *fluorescence*. On the other hand, phosphorescence is the emission of light from the triplet excited states, in which the electron in the excited orbital has the same spin orientation as the ground-state electron. Transition to the ground state are forbidden and the emission rates in phosphorescence are slow (in the range of milliseconds to seconds) [76,77].

Following light absorption, a fluorophore is usually excited to a higher vibrational level of either S1 or S2. Molecules in condensed phases rapidly relax to the lowest vibrational level of S1 (with some exceptions), in a process called an internal conversion. Fluorescence emission generally results from a thermally equilibrated excited state, that is, the lowest energy vibrational state of S1. Additionally, energy losses between excitation and emission are universal for fluorescent molecules in solution, this is known as the Stokes-shift, caused by the rapid decay to the lowest vibrational level of S1. In addition, fluorophores can display further Stokes-shifts due to solvent effects, excited-state reactions, complex formation, and/or energy transfer [77].

3.3.3.1 Fluorescence Spectroscopy

In fluorescence spectroscopy, samples containing fluorophores are excited by light irradiation with a specific wavelength. The resulting emission signal can be detected by a spectrofluorometer and further analyzed. Many fluorophores are sensitive to their surrounding environment, thus, the emission spectra and intensities of extrinsic probes are often used to determine the location of a probe in a sample [77].

Fluorescence spectroscopy was performed to analyze the distribution of C- & N- EGFP Cx43 in vesicles obtained after the CFE and purification step by DGC. The purpose of the experiments was to check the presence of the protein synthesized by CFE and spot the fractions in which proteoliposomes were located with higher probability. The vesicles fraction (SUVs, LUVs, or GUVs) contained Texas Red™, which made the location of the liposomes by using this method possible. All experiments were performed using a fluorescence spectrometer FluoroMax® 4 from Horiba (*Horiba Scientific, Bensheim, Germany*). The experiment started by diluting proteoliposomes (20 µL) in buffer C (580 µL) by a factor of 30 in a quartz cuvette. For all experiments, control recordings were made with a) a cuvette containing only buffer C, and b) a cuvette containing diluted vesicles taking into consideration the dilution factors of the samples evaluated. The control samples were excited at 561 nm and their spectra was recorded from 400-700 nm. When evaluating the fluorescence of Texas Red™ in the vesicles, samples were excited at 561 nm and the emission was acquired from 570-650 nm, while for the samples containing EGFP-Cx43, the excitation of molecules was performed at 489 nm and the emission signal was acquired from 495-550 nm. All determinations were carried out at 25 °C.

3.3.3.2 Confocal Laser Scanning Microscopy

Confocal laser scanning microscopy (CLSM) requires that samples of interest fluoresce. In simple terms, by filtering out the exciting light without blocking the emitted fluorescence, it is possible to see only the objects that are fluorescent [78]. In the case of CLSM, the key is to use two pinholes (apertures) to restrict the excitation and detection beams. Thus, suppressing the detection of light that is out of focus. The two pinholes are mounted in image planes (thereby the term “con”-focal) that enhance both lateral and axial resolution in contrast to conventional microscopy [79,80].

In a CLSM experiment, the laser beam is focused on the sample, the fluorescence light is emitted directly back through the sample using the optical pathway while passing through a small pinhole before reaching the photomultiplier. The smaller the pinhole, the less stray light or fluorescence from out-of-focus areas within the specimen reaches the detector. Hence, it is possible to obtain optical sections of the specimen and reconstruct its 3D structure [78].

In addition to the pinholes, it is the scanning process that differentiates CLSM from other optical instruments. To get spatial information, the sample can be either moved with respect to a stationary optical path, stage scanning, or the laser beam is scanned over the sample, laser scanning. In laser scanning, galvanometric mirrors are typically used to move the light beam in x- and y-directions. The position of the beam on the sample will change with the positions of the mirrors, but the position of the light path entering the back aperture of the objective will be stationary, thus exciting the sample at a given position depending on the angles of the two mirrors [79]. An exemplary scheme illustrating the principles of confocal microscopy can be seen in Figure 3-8.

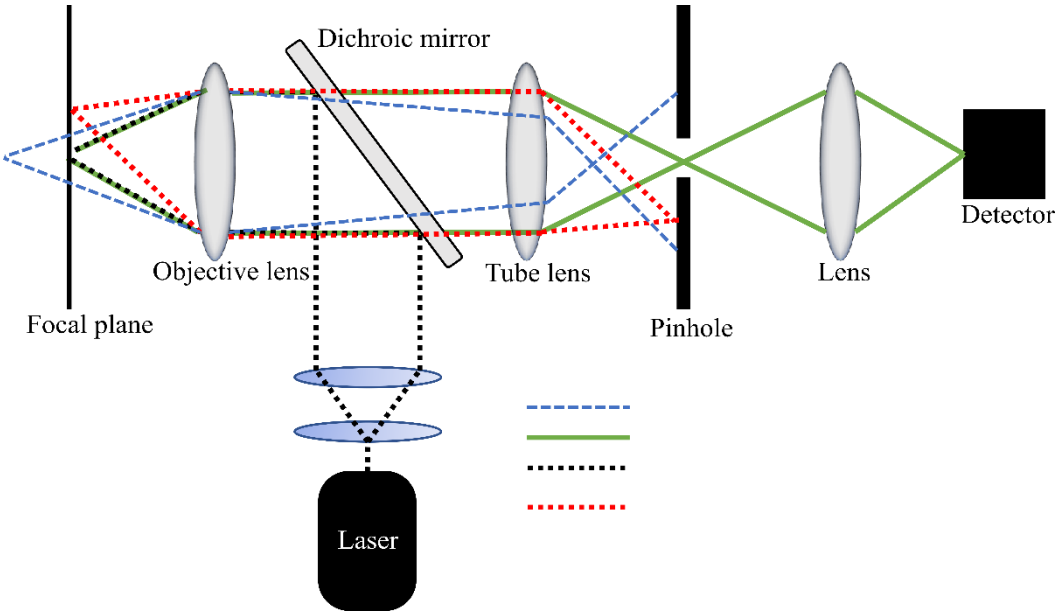

Figure 3-8. Schematic illustration of a simple confocal microscope that illustrates the function of the pinhole. The beam coming from the laser excites the sample (black dashed line), and light originating from the focal plane passes through the pinhole and reaches the detector (green solid line). The light originating from positions adjacent to the focal spot (red dashed line) or from a different focal plane will be cut out by the pinhole (blue dashed line).

Experimental approach:

In this project, CLSM was used to monitor the incorporation of Cx43 into artificial membranes. For that, the C- or N-EGFP Cx43 plasmid was added to the CFE reaction supplemented with GUVs to stabilize the protein production by direct incorporation into the liposomes. GUVs were prepared as described in section 3.2.4.3, and their integrity was checked by CLSM right after electroformation (and before the CFE step). The giant vesicles were added to the CFE reaction

to reach a concentration of 30 µg/mL, and after the protein synthesis step (3 h), the samples were added to Petri dish chambers (passivated overnight with BSA 4 mg/mL in buffer C) and let it incubate at RT for at least 1 h to allow deposition of the vesicles at the bottom of the chamber. All samples and control reactions were diluted considering the same dilution factors as for the CFE reaction. To image the lipid membranes from the GUVs, Texas Red™ was excited at 561 nm (DPPS laser 561 nm; 20 mW) and detected in the range 600-700 nm. On the other hand, to image the presence and localization of C- or N-EGFP Cx43, the sample was excited at 488 nm (Argon laser 485, 488, 514 nm; 25 mW) and detected in the range 495-580 nm. Additionally, GUVs without TxR in the membrane were also used for the CFE reactions, and micrographs were taken in bright field mode to check the integrity of the vesicles before and after the protein synthesis step. These determinations were made by using an upright microscope LSM 710 (*Carl Zeiss GmbH, Jena*) when fluorophores in the lipid membranes were present, or an upright FluoView 1200 (*Olympus, Tokyo, Japan*) when no fluorophores were present in the lipid membranes. In both cases, a water immersion objective was used (40x, refractive index: 1.33, numerical aperture: 1.0).

3.3.4 The automated Black Lipid Membrane method: Orbit 16

Voltage-clamp has been the technique of choice to study the function of ion channels [81,82]. In principle, a potential difference is applied across a lipid membrane where protein channels are inserted, resulting in fluctuations of current that represent the opening and closing events of the single-channel molecules. This can be done in a whole-cell or single-channel configuration, either by using the patch-clamp or the planar lipid bilayers technique [80-82]. In the latter case, isolated ion channels are reconstituted into planar lipid bilayer membranes that separate two aqueous compartments. This strategy allows the manipulation of the lipid and aqueous environment surrounding the protein to elucidate structure-function relationships [82]. Conventionally, planar lipid bilayers can be formed by two methods: a) The painting, or b) the monolayer method. The painting or bulk method is the classic black lipid membrane (BLM) system. For this method, a bilayer assembles spontaneously after a lipid solution, dissolved in a non-polar solvent, is spread across a small aperture in a hydrophobic partition that separates two aqueous compartments [82,85]. In this case, the lipid bilayer formed by the painting technique

incorporates hydrocarbon molecules from the organic solvent, thus affecting the thickness of the bilayer [84]. On the other hand, bilayers formed with the monolayer method are solvent-free. In this case, the lipid solution is spread to form a monolayer in an air-water interface allowing enough time for the evaporation of the solvent to occur. Then, bilayers are formed by bringing the two monolayers from the different compartments into contact through the aperture by raising the levels of the aqueous solution above the aperture by gravity flow [86,87].

The insertion of channel proteins into planar bilayers has been proven to be a challenging step, hence several methods have been developed. Soluble proteins can be directly added to the aqueous solution around the bilayer, they diffuse and incorporate into it. On the other hand, given the hydrophobic nature of membrane proteins, they are usually incorporated into vesicles as carriers that facilitate the transfer and incorporation of the protein channels to the lipid bilayer [88]. Two major approaches have been widely used to achieve this. In the first approach, the incorporation of proteins into planar lipid bilayers via monolayers at the air-water interface in equilibrium with vesicle suspensions. The monolayers located on opposite sides of the aqueous compartments, already containing the protein of interest, are risen over the aperture to form a bilayer [89,90]. The second approach consists of fusing a channel containing vesicles (proteoliposomes) with preformed planar lipid bilayers [88]. In this case, different salt gradients are set up in the two opposite compartments, creating an osmotic pressure on the proteoliposomes, the following rupture of the vesicles and allowing the incorporation of the proteins into the bilayers [84]. Depending on the nature of the protein and the environmental conditions necessary to transfer it into a planar bilayer, the lipid composition of both the vesicles or bilayers can be controlled, as well as conditions of the aqueous solution, *e.g.,* by addition of calcium ions [81,88].

Lipid bilayers formed by conventional methods are not stable enough and often require laborious work and high quantities of resources (*e.g.,* volumes of purified protein and lipid material), therefore current technologies make use of smaller devices. In this work, an automated-BLM system was used to evaluate the functionality of cell-free synthesized Cx43. The Orbit 16 (*Nanion, Munich, Germany*) is an automated-BLM platform that can be used for electrophysiological experiments. It was used together with the MECA (Micro-Electrode-Cavity Array) chip which consists of a 4 by 4 array of circular micro-cavities in a highly inert polymer. The BLM cavity can hold small volumes of electrolyte solution (in the microliter

order) and each of them contains an individually addressable Ag/AgCl micro-electrode. The Orbit 16, provides a platform to record the single-channel activity of 16 microcavities that work in an individual and simultaneous manner [91].

Experimental approach:

After production of Cx43 proteoliposomes via CFE and its subsequent purification by DGC, fractions containing the proteoliposomes were used as a delivery system to insert Cx43 into the planar bilayers to check whether the protein was active when synthesized by the mentioned method. The insertion of Cx43 into planar lipid bilayers was accomplished by charged-mediated vesicle fusion. The vesicles containing Cx43 were composed of L-α-PC: DOTAP: TxR (89.5: 10: 0.5) having a positive overall charge, which was supposed to interact with the negative charge present in the lipid bilayers to enhance the fusion of the vesicles. Thus, lipid bilayers were composed of L-α-PC: POPG (90: 10).

Table 3-21. Steps of the protocol to measure the activity of Cx43 at the Orbit 16 showing the approximate times at which each step took place.

Step	Timepoint (s)
Bilayer formation (at -40 mV)	-
Capacitance test	-
Exchange to buffer E	-
Capacitance check	-
Start recording	0
Vesicles/proteoliposomes addition	30
Exchange to buffer B	140
Change of potential to 0 mV	200
Change of potential to + 40 mV	260
Taurine addition	320
Exchange to buffer B	370

The protocol started by adding 150 µL of buffer B (see composition in Table 3-1) into the cavities of the MECA chip with the help of a syringe plunger to ensure that aqueous solution passed through the Trans side of the micro-chamber. A potential of +40 mV was applied to the system to check if the microchambers were filled with solution. Afterward, the lipid solution (final concentration of 10 mg/mL dissolved in n-decane) was spread onto the chip by using a magnetic stirrer and adding approximately a volume of 0.30 µL. To ensure the formation of bilayers in the system the capacitance was measured, and potential bilayers were destroyed by

applying a “ZAP” voltage. The bilayers were repainted by stirring, the aqueous solution in the chamber was carefully exchanged to buffer E (see composition on Table 3-1), and the capacitance was measured a second time to evaluate the quality and stability of the membranes before adding the protein fraction to the chamber.

After bilayer formation, the recording of the events started with a potential of -40 mV (see protocol procedure in Table 3-21). After 30 s, the proteoliposomes fraction was added, and the aqueous solution was exchanged to buffer B after 2 min, to prevent further fusion events from happening in the BLM chamber. Next, the potential of the system was changed to 0 and +40 mV, after 1 min in each case. When changes in the conductance or noise levels were visible in the system, a solution of Taurine was added as a blocker of Cx43 to check whether the signal came from the protein. The effect of Taurine was recorded for 1 min, and it was followed by an exchange of the aqueous solution using buffer B to check if the effect of Taurine was reversible. A schematic illustration of the experimental setup used to test the functionality of Cx43 at the Orbit 16 is shown in Figure 3-9.

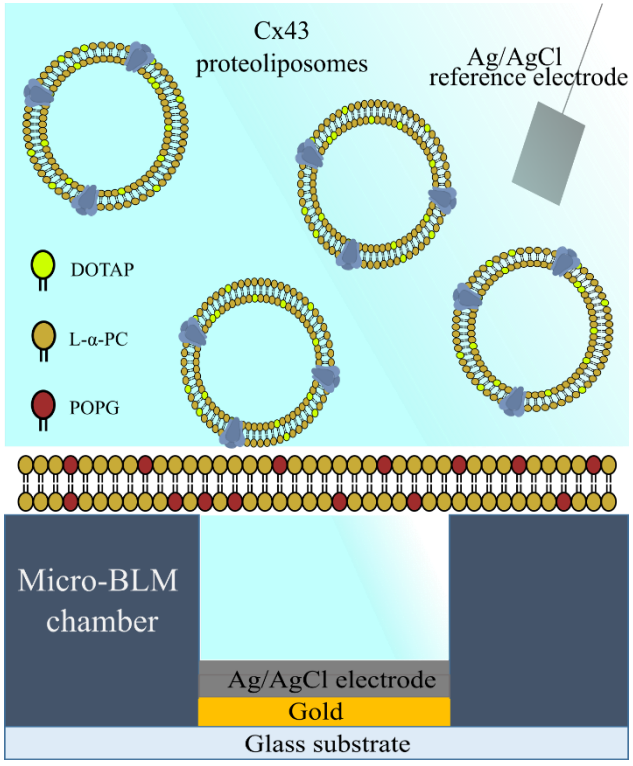

Figure 3-9. Schematic illustration showing the experimental design to test Cx43 functionality by the automated-BLM method using the Orbit 16. A planar lipid bilayer with negative charges was spread onto the micro-BLM chamber, while positively charged vesicles containing Cx43 were added to the trans compartment to enhance protein transfer by charged-mediated fusion.

3.4 Analysis

For the design and analysis of the DNA sequences, SnapGene® 6.0 (*GSL Biotech LLC, San Diego, USA)* was used. Therefore, it was possible to carry out *in silico* experiments in the software to get familiar with the cloning methods according to the material and resources available.

Concerning image processing either for SDS-PAGE or Western Blot membranes, the ImageJ software was used to adjust the brightness and contrast of the pictures shown in section 4. Moreover, the analysis of integrated protein in the vesicles for all experiments was derived from the adjusted Western Blot pictures. In summary, the signal of the membranes was inverted so the background would appear dark and the protein signal brighter. For each specific membrane, a region of interest (ROI) was created as a squared region of a defined size in one lane. The ROI fit the average signal of the protein for all consecutives lanes in the Western Blot membranes since it had to be moved laterally to record the intensity of the pixels from the lanes of interest. The signal of the background was also considered by measuring the intensity of the pixels at different points of the membrane where protein bands were absent. Following, the relative amount of protein on each lane was obtained by dividing the intensity of the pixels in that specific fraction by the total intensity of the pixels in all fractions (sum from F 1-7).

For the data obtained by fluorescence spectroscopy, the emission spectra of Texas Red™ were normalized against the minimum emission value, to ensure that all values started from a common point and to stablish comparisons. On the other hand, the emission spectra of GFP were normalized against the maximum excitation peak for GFP at 495 nm. However, these normalization approaches did not give accurate information about the relative amount of vesicles or protein present on each fraction after the purification of proteoliposomes by DGC. Therefore, the emission signal for each fraction was evaluated against the total emission from all fractions to obtain the relative values. These determinations were made at 610 nm for Texas Red™ to evaluate the presence of vesicles, or at 510 nm for GFP to evaluate the presence of protein in all fractions.

Data in the plots, tables, and text was reported as (average ± standard deviation). Along with the text, “N” represents the number of independent determinations (or samples).

The sizes of GUVs were measured on ImageJ by adding a scale bar to each micrograph and scaling the image by finding a relation between the distance in pixels against the known distance in μm. Following, GUVs were crossed transversally with a straight line, and the distance was also measured in the software for GUVs that were perfectly discernible from one another in the micrographs.

4. Results

4.1 Production of functional plasmids for cell-free expression

Cell-free protein production has been a valuable tool for understanding how mRNAs are translated into functional polypeptides and since this technique does not depend on cellular integrity, it provides a flexible platform for the expression of challenging proteins. Cell-free systems can be understood as "programmable liquids" composed of the enzymes necessary to transcribe and translate nucleic acid molecules (DNA or mRNA). This technology has been used for several applications to gain information on both, functional and structural biology [8,10,18].

The cell-free expression approach has been used to synthesize a variety of proteins [8] including Connexin 43 (Cx43) in presence of liposomes as membrane mimics [25,26,35]. In this work, Cx43 was expressed and reconstituted in artificial membranes by using a cell-free system as a way to mimic cell-to-cell communication. To achieve that goal, Cx43 was expressed, directly incorporated into vesicles of different sizes, and qualitatively characterized. This chapter is organized into four parts. The first one describes the production of functional DNA vectors, containing sequences for Cx43 and an enhanced green reporter protein (EGFP), which are important to monitor protein incorporation into the vesicles. The second part focuses on the synthesis of Cx43 by means of cell-free expression under different conditions *in vitro* and the insertion of the protein into liposomes. Following, the characterization of Cx43-proteoliposomes was performed by gathering information about the orientation of the protein and its functionality. Lastly, the insertion of Cx43 in liposomes of different sizes was monitored.

4.1.1 Functional plasmids for the expression of Cx43

The three plasmids coding for Cx43 (WT Cx43, C- & N-EGFP Cx43) used in this project are based on the pET28a(+) system. The WT Cx43 plasmid was ordered and synthesized by Biomatik, while the variants containing the EGFP tag were customized in the lab. To obtain the N-EGFP Cx43, the ligation independent cloning (LIC) approach was used whereas C-EGFP Cx43 was obtained by using the Gibson assembly method. A DNA template compatible with

the PURExpress® system requires a T7 promoter and ribosome binding site (RBS) sequences upstream the open reading frame (ORF), as well as a T7 terminator sequence downstream the termination codon [14,58]. Additionally, the WT- and N-EGFP Cx43 plasmids contain Histag (His6) sequences that were intended for the purification of Cx43 from a bacterial system. However, those results will not be shown in this project. The plasmids C- & N-EGFP Cx43 have an EGFP sequence located at the C- or N-terminal domain of Cx43 which was intended to monitor the incorporation of Cx43 into lipid membranes by fluorescence, and to compare the functional behavior of both proteins. Previously, Carnarius and colleagues demonstrated that the presence of a GFP sequence located at the C-terminal domain of Cx43 alters the conductance of Cx43 in single-channel measurements [92]. Figure 4-1 compares WT Cx43, C- & N-EGFP Cx43 plasmids showing all necessary sequences for the cell-free reaction and features relevant for this project, *e.g.,* the presence of the EGFP sequence in plasmids C- & N-EGFP Cx43.

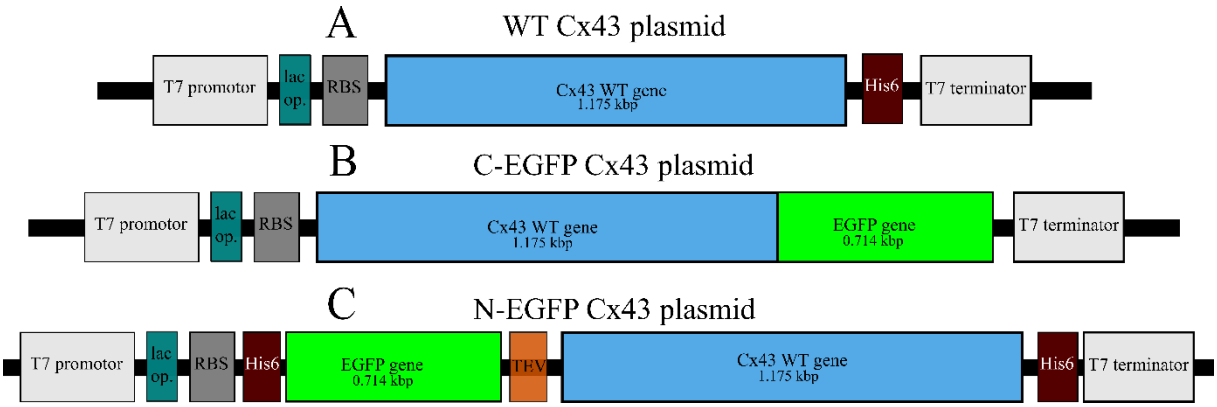

Figure 4-1. Scheme illustrating the relevant sequences contained in the functional plasmids used in this project to carry out the expression of Cx43 in vitro. A) WT Cx43. B) C-EGFP Cx43. C) N-EGFP Cx43. Lac op., lactose operon. RBS, ribosome binding site. His6, Histag sequence. TEV, Tobacco Etch Virus sequence for protease cleavage. EGFP, enhanced green fluorescent protein.

To build the plasmid constructs, both the WT Cx43 plasmid and pET-LIC vector were used as DNA templates to amplify Cx43 and EGFP sequences to obtain the desired functional plasmids containing the EGFP sequence at the C- or N-terminal domain. Figure 4-2 illustrates a scheme where the relevant sequences to synthesize N-EGFP Cx43 are depicted, as well as the product of a control PCR reaction (in Figure 4-2. A), and the product of the DNA sequences necessary to carry out the LIC reaction. For this, the Cx43 sequence was amplified from the WT Cx43 plasmid by PCR as illustrated in Figure 4-2. B. Lanes 1-2 show a DNA size between 1-1.5 kbp,

which is in accordance with the size of the Cx43 sequence provided by Biomatik (1.175 kbp). In the same figure, the product from the digestion assay using SspI to linearize the pET-LIC vector can be observed, showing a unique band with an approximate size of 6 kbp (lanes 3-4).

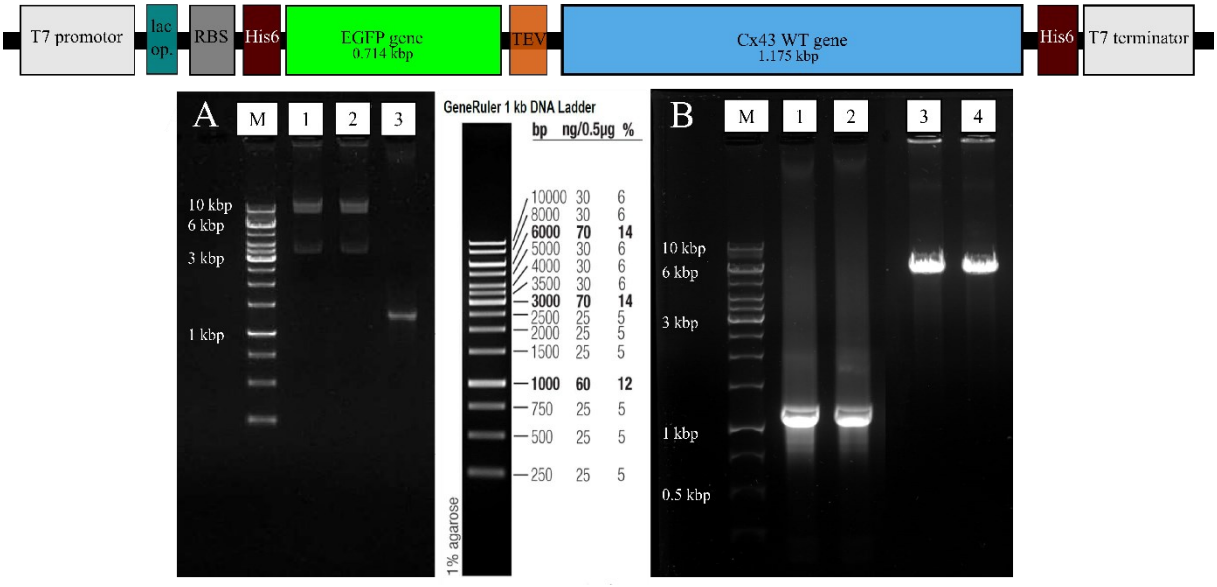

Figure 4-2. Agarose gels showing the DNA product to build the N-EGFP plasmid. A) Full circular Cx43 WT plasmid in lanes 1 and 2, and the PCR product of Lambda DNA as a control of the thermocycler conditions and PCR amplification in lane 3. B) Sequence of Cx43 amplified by PCR for LIC reaction in lanes 1-2, and product of the linearized pET-LIC vector from the restriction assay with SspI in lanes 3-4. Lane "M" corresponds to the DNA ladder sample for comparison purposes. On top, a scheme showing the relevant sequences necessary to carry out protein synthesis by cell-free systems.

To build the C-EGFP plasmid, the EGFP sequence was amplified from the pET-LIC vector and the WT Cx43 plasmid served as vector template for the Gibson assembly. Figure 4-3.A illustrates the product of EGFP sequence amplified by PCR showing DNA size of approx. 700 bp as expected. In Figure 4-3. B, the product of the double digestion assay with the enzymes XhoI and Bpu1102I is visible (lanes 2-3) which is necessary to obtain a linear vector with sticky ends. As controls, a sample of the uncut WT Cx43 vector was added to lane 1, whereas a control for a single digestion assay was performed to the WT Cx43 vector in presence of XhoI or Bpu1102I, which is visible in lanes 5 and 6, respectively. In this case, four forms of the uncut vector appeared on the agarose gel showing sizes ranging from 3-10 kbp, while the double digested vector showed an expected approx. size of 6 kbp.

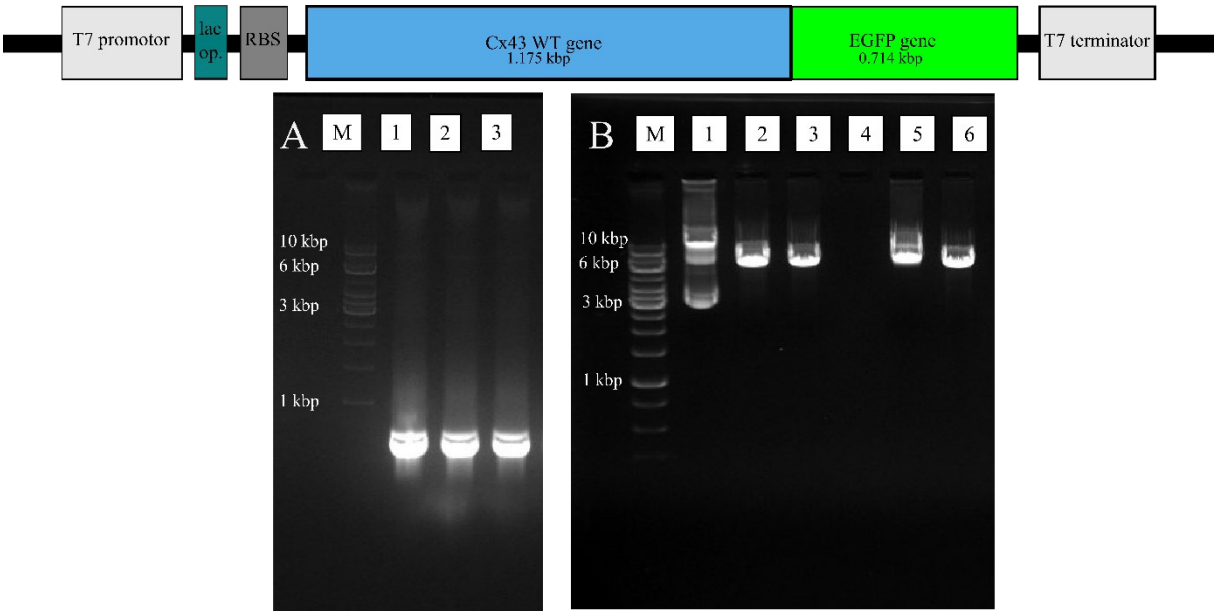

Figure 4-3. Agarose gels showing DNA product for the Gibson Assembly reaction. A) Sequence of EGFP amplified by PCR for the Gibson assembly shown in lanes 1-3. B) Product of the linearized vector with XhoI and Bpu1102I for the construction of C-EGFP plasmid. Lane 1: uncut WT Cx43 plasmid; Double digestion in lane 2-3: vector linearized with XhoI and Bpu1102I; single digestion in lane 5: vector linearized with XhoI, lane 6: vector linearized with Bpu1102I. Lane "M" corresponds to the DNA ladder sample for comparison purposes. On top, a scheme showing the relevant sequences necessary to carry out protein synthesis by cell-free systems.

4.2 Direct incorporation of Cx43 into liposomes

4.2.1 Cell-free expression of Cx43

Cell-free reactions can be supplemented with a variety of compatible solutes, that support the expression of membrane proteins stabilizing them by providing a hydrophobic environment [13-15]. This work focuses on the synthesis of Cx43 in presence of liposomes and the effects of modifying certain parameters in the reaction mixture.

After having functional plasmids for Cx43, the next step was to express the protein variants using the cell-free expression (CFE) approach. Figure 4-4 illustrates the product of the synthesized Cx43 variants and its analysis *via* SDS-PAGE and Western Blot. In Figure 4-4.A, the product of the Cx43 variants is compared to the product of a negative control sample that contains all components of the CFE reaction except for a DNA template ("No DNA"), and by which no protein synthesis should take place. As a positive control, the DHFR plasmid provided in the PURExpress® kit was used to check and control the expression parameters of the reactions. The synthesis product of the WT, C- & N-EGFP Cx43 are highlighted with a red dot

along the lanes, and as expected, differences in molecular weight between the WT protein (~43 kDa) and its variants containing the EGFP tag (~70 kDa) are also visible. As it is noticeable, the analysis of protein synthesis products *via* SDS-PAGE is challenging and can lead to misinterpretation of the data given the presence of multiple proteins in the CFE kit itself. Synthesized proteins in an SDS-PAGE appeared as enriched and darker bands from the already existing proteins in the CFE kit, which can be discernible when comparing the protein bands from the samples containing Cx43 with the negative control ("No DNA"). In consequence, Western Blot represents a highly sensitive method to analyze the production of proteins *via* CFE. Figure 4-4. B & .C illustrate the product of the three Cx43 variants analyzed *via* Western Blot with antibodies recognizing specific sequences of the Cx43 and GFP genes, respectively. Thus, representing proof of the functionality of the plasmids and the successful synthesis of the proteins.

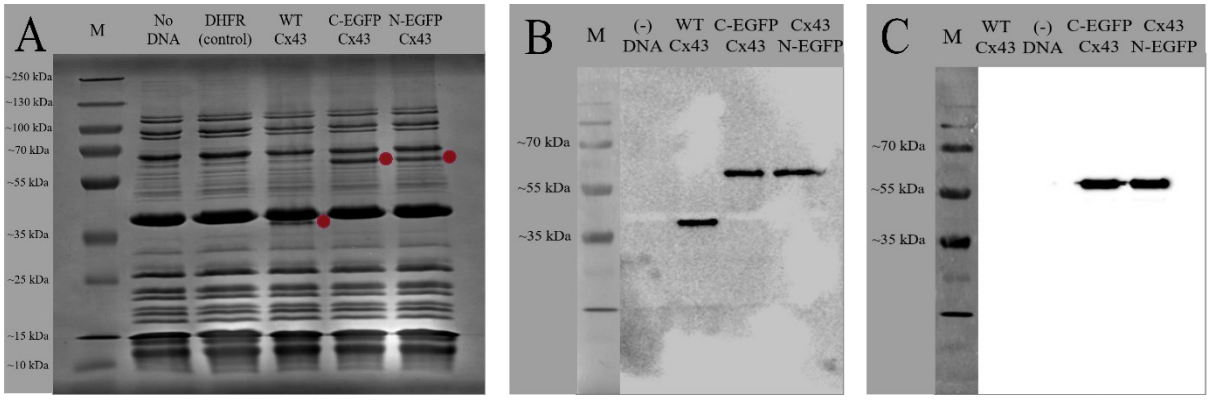

Figure 4-4. Cell-free expression of connexin 43 (Cx43) in aqueous solution (30 mM Tris). A) SDS-PAGE showing the expression product of the Cx43 variants (WT, C-EGFP, and N-EGFP), DHFR as a positive control of the reaction mixture, and a sample with all components of the reaction except the template DNA as a negative control. Western Blot shows the expression product of Cx43 variants and negative control by using in B) the Cx43 antibody and in C) the GFP antibody to check the presence of both sequences in the recombinant proteins. The red dots correspond to the expressed protein product.

After a successful expression, insertion of Cx43 into vesicles and obtaining enriched fractions of proteoliposomes for further analysis was the next step. Therefore, Cx43 was expressed in the presence of large unilamellar vesicles (LUVs of 100 nm) to achieve stabilization of the protein by providing a hydrophobic environment in which it could insert and properly fold as it is expressed [25]. Cx43 was cotranslationally expressed in presence of vesicles, and proteoliposomes were purified *via* density gradient centrifugation (DGC) by collecting seven fractions. Figure 4-5 shows the product of the seven collected fractions after DGC (F 1-7). The distribution of protein in the different fractions was analyzed *via* SDS-PAGE (Figure 4-5. A)

and Western Blot using a Histag or Cx43 antibody (Figure 4-5.B & .C, respectively). Figure 4-5.A reveals the presence of enzymes and protein factors from the PURExpress® kit in all recovered fractions, though it seems that proteins from the kit with high molecular mass (MW) locate preferentially in fractions 3-6 while proteins with lower MW locate in fractions 6-7. This outcome is confirmed by the Western Blot analysis with the Histag antibody depicted in Figure 4-5.B, showing the recognition of WT Cx43 as well as the pure elements from the kit that also contain a Histag in their sequence [11]. Furthermore, the successful expression and specific recognition of Cx43 among the fractions is visible from Figure 4-5.C when using the Cx43 antibody. Figure 4-5.C brings to the attention that even when using a specific antibody recognizing amino acids 241-254 from Cx43, bands in the upper and lower region are also recognized with an approx. size around 250 and 15 kDa. The upper bands were present in most cases when expressing Cx43 in presence of vesicles, and it could represent a hint that Cx43 adopts a hexameric structure forming the hemichannel pore in those artificial membranes. On the other hand, the PURExpress® kit is likely to contain a protein factor of lower MW that gets recognized by the Cx43 antibody as revealed by the analysis of Western Blot membranes with Ponceau S (data not shown).

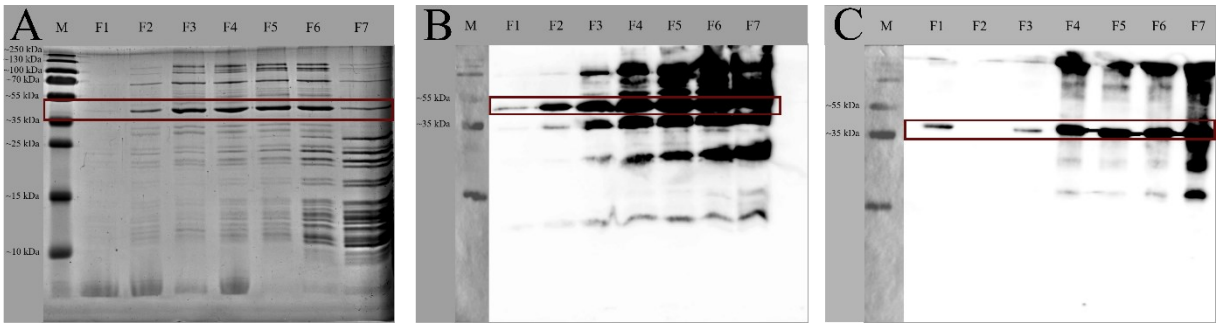

Figure 4-5. Expression of Cx43 WT in presence of LUVs in the reaction mixture. After incubation for CFE, samples were purified by DGC, recovered in 7 fractions, and analyzed by A) SDS-PAGE, and Western Blot with B) a Histag antibody, and C) the Cx43 antibody. Vesicles were composed of DOPC: TxR (99:1) with a final lipid concentration in the reaction mixture of 0.1 mg/mL in B) and C) while composed of L-α-PC: DOTAP: TxR (89.5:10:0.5) with a concentration of 3 mg/mL in the reaction mixture in A). The red box indicates the region where Cx43 locates in the SDS-PAGE and Western blot membranes.

4.2.2 Effect of different lipid compositions on the incorporation of Cx43 into vesicles

In aqueous solutions, the solubility of membrane proteins expressed by means of CFE increases upon the addition of membrane mimics, such as liposomes [17]. Depending on the nature of the protein, altering the lipid composition of vesicles present in the cell-free reaction can be advantageous. Basically, CFE systems offer the opportunity to insert translated proteins into the desired membrane of choice [93]. In this section, the impact of incorporating Cx43 into vesicles with different lipid compositions is evaluated. Figure 4-6 illustrates the effect of introducing vesicles to the CFE reaction with neutral, positive, or negative net charges. Vesicles were composed of L-α-PC as matrix lipid in combination with 0.5 % of Texas Red™-DHPE for localization purposes, and 10 % of DOTAP or POPG to form vesicles with a net positive or negative charge, respectively. All reactions were carried out independently and contained 1.5 mg/mL of the lipid of interest in the reaction mixture. For all lipid compositions, a protein band located between 35 and 55 kDa accounts for Cx43 as it is visible from Figure 4-6. A-C. When comparing the amount of protein present on each fraction after DGC for each lipid composition, it becomes clear that Cx43 locates preferentially in fractions 4-7 when supplementing the CFE reaction with neutrally or negatively charged vesicles. When having neutrally charged vesicles, ~20 % (N= 1) of the total protein was found in fractions 1-4 while ~50 % (N= 1) when negatively charged vesicles were used (see Figure 4-6. D). On the other hand, ~59 % (N= 5) of the total protein was found in fractions 1-4 (presumably containing the liposomes) when positively charged vesicles were added to the CFE reaction. For comparison, it is worth noting that the resolution of the protein bands revealed by Western Blot was variable for all tested cases.

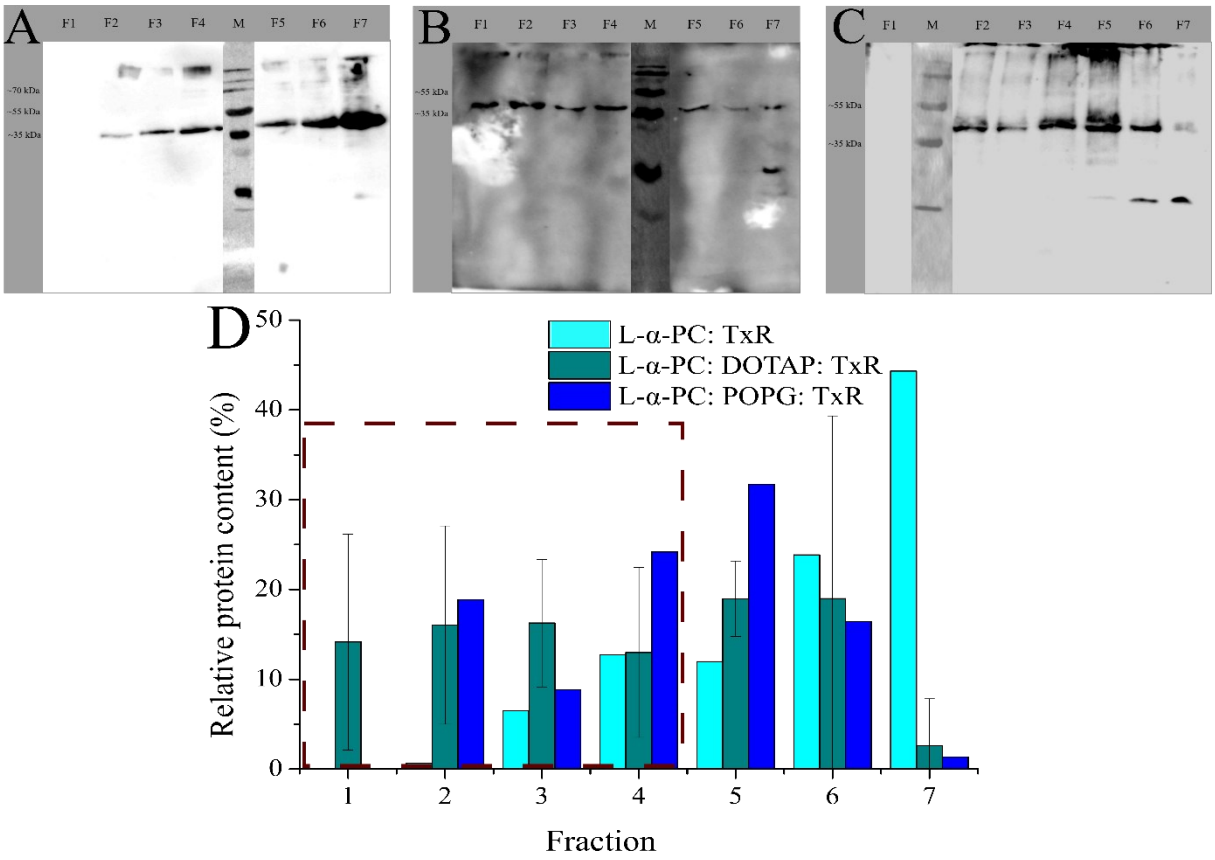

Figure 4-6. Effect of lipid composition on the incorporation of WT Cx43 in vesicles containing 1.5 mg/mL of L-α-PC as a matrix lipid. Western Blot membranes with lipid composition showing different charges. A) L-α-PC: TxR (99.5:0.5); B) L-α-PC: DOTAP: TxR (89.5:10:0.5); C) L-α-PC: POPG: TxR (89.5:10:0.5); D) comparison of the relative protein content in the different fractions collected from DGC for all three lipid compositions. The concentration of lipids in the vesicles was 1.5 mg/mL for all membranes.

Now, to compare the effect of having different matrix lipids in the vesicles, three different lipid compositions were tested with a concentration of 3 mg/mL in the reaction mixture: 1) L-α-PC: DOTAP: TxR (89.5: 10: 0.5); 2) DPhPC: Chol: TxR (89.5: 10: 0.5); 3) DOPC: TxR (99.5: 0.5). An exemplary case of the Western Blot membranes can be found in Figure 4-7. A-C. Concerning the presence of protein in fractions 1-4 after DGC, vesicles composed of DPhPC: Chol: TxR reported the highest amount with ~84 %, (N= 1) followed by the vesicles with L-α-PC: DOTAP: TxR and DOPC: TxR with ~ 76% (N= 3) and 43% (N= 1), respectively. The analysis of Western Blot membranes suggests that adding DPhPC: Chol: TxR to the CFE mixture leads to higher amounts of integrated protein in fractions 1-4, though the quality of the bands is not clearly defined. Therefore, it is worth mentioning that obtaining Western Blot

membranes for the latter two compositions represented a challenge since the membranes often showed impurities that made analysis impossible and led to the repetition of the experiments several times.

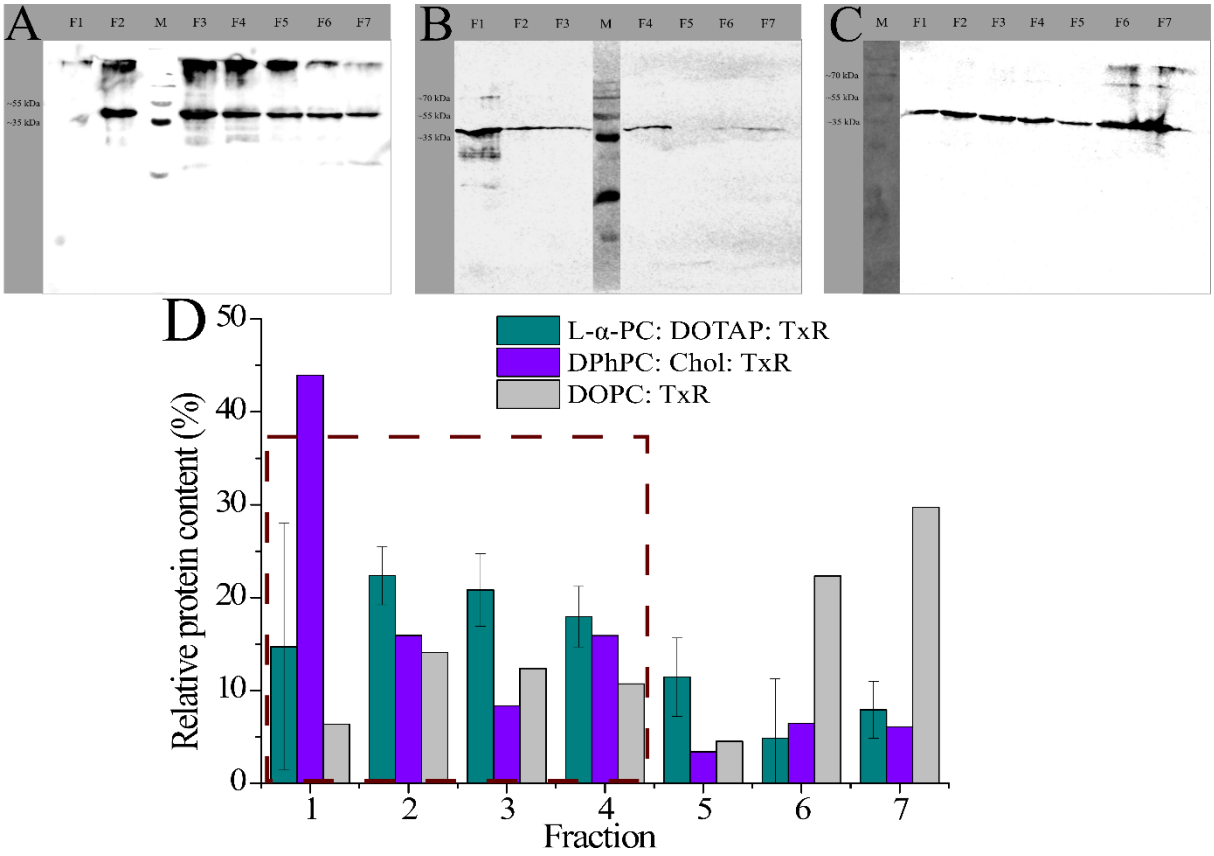

Figure 4-7. Effect of lipid composition on the incorporation of WT Cx43 in vesicles containing 3 mg/mL of lipid. Western Blot membranes with lipid compositions: A) L-α-PC: DOTAP: TxR (89.5:10:0.5); B) DPhPC: Cholesterol: TxR (89.5:10:0.5); C) DOPC: TxR (99.5:0.5); D) comparison of the relative protein content in the different fractions after DGC for all three lipid compositions. The concentration of lipids in the vesicles was 3 mg/mL for all membranes.

4.2.3 Effect of lipid concentration on the incorporation of Cx43 into vesicles

In cell-free systems, a second key factor influencing the stabilization of membrane proteins by the presence of liposomes is the concentration of the lipids provided in the reaction. It has been reported that protein insertion increases proportionally with the concentration of liposomes in the cell-free mixture [24,25,94]. To evaluate the effect of lipid concentration on the reconstitution efficiency of Cx43 into vesicles, the reaction mixture was supplemented with

L-α-PC: DOTAP: TxR (89.5: 10: 0.5) at four different concentrations: a) 0.5 mg/mL; b) 1.5 mg/mL; c) 3 mg/mL; d) 5.5 mg/mL (see Figure 4-8). The lipid content on each fraction was estimated by measuring the absorption of Texas Red™ at 583 nm after DGC for all concentrations. When supplementing the reaction mixture with 0.5 mg/mL of lipid, Texas Red™ seems to be homogenously distributed with approx. 14-15 % on each fraction (Figure 4-8. A; N= 1). In contrast, when adding 1.5 mg/mL, 3 mg/mL, or 5.5 mg/mL of lipid to the CFE reaction, the highest amount of vesicles was located within fractions 1-4, and it showed a decrease in fractions 5-7. This suggests that most vesicles in fractions 1-4 could be available for protein insertion. When supplementing the CFE reaction with 1.5 mg/mL of lipids, 73 % (N= 3) of the vesicles were available in fractions 1-4, while when adding of 3 mg/mL or 5.5 mg/mL up to 86 % (N= 11) and 88 % (N= 3) of the vesicles were found in fractions 1-4, respectively (see Figure 4-8. B-D).

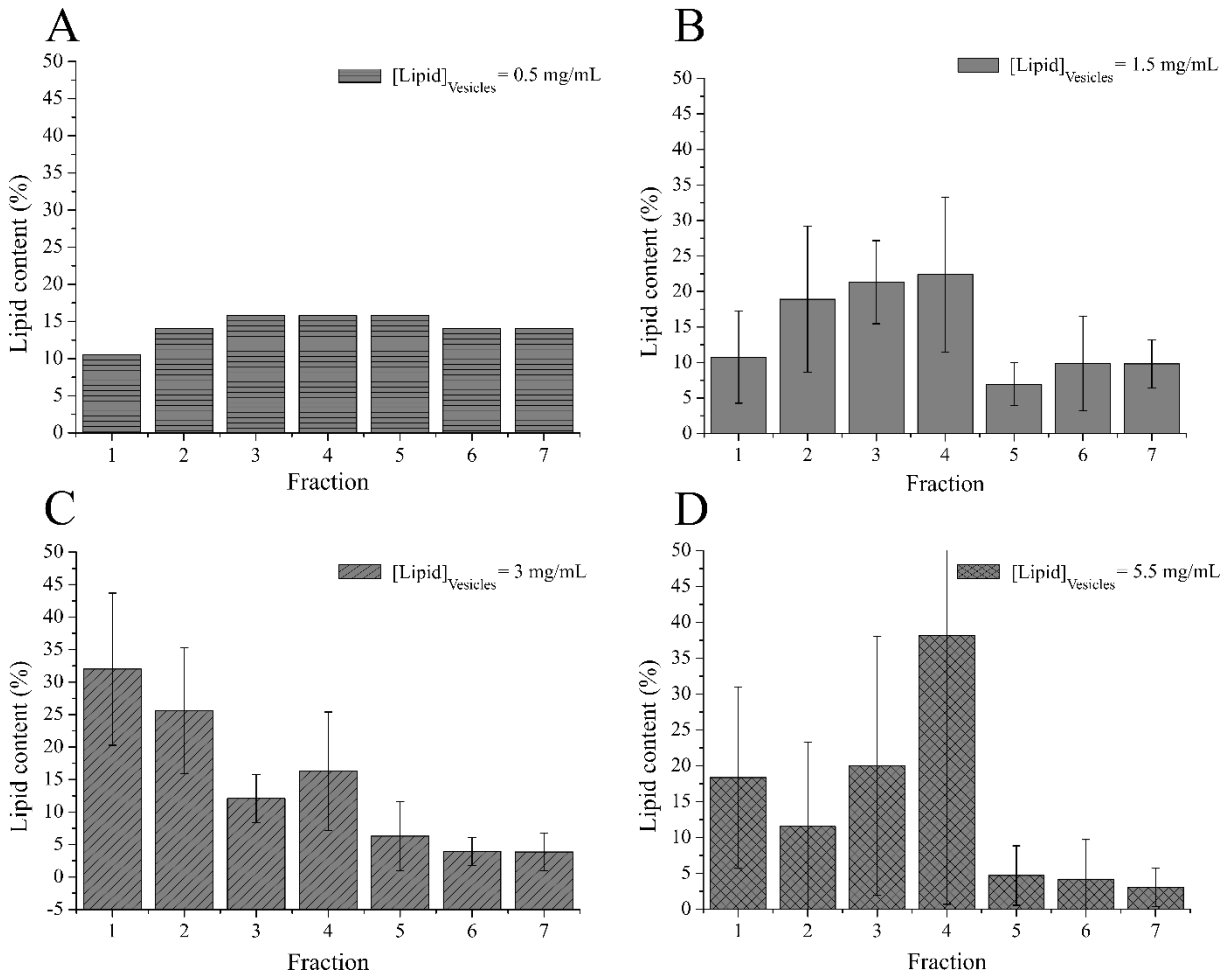

Figure 4-8. Distribution and comparison of the relative content of vesicles in the fractions after DGC when adding different concentrations of lipid to the reaction mixture. A) 0.5 mg/mL; B) 1.5 mg/mL; C) 3 mg/mL; D) 5.5 mg/mL. Lipid content for all cases was calculated as the absorption of Texas Red present in the fractions at 583 nm after DGC.

On the other hand, the amount of protein present on each fraction at different lipid concentrations in the reaction was also evaluated (see Figure 4-9). When the concentration of lipids in the reaction was of 0.5 mg/mL around ~79 % of the protein was in fractions 4-7 (Figure 4-9. A, N= 1). The distribution of protein content seemed quasi-homogeneous when adding 1.5 mg/mL (N= 5) or 5.5 mg/mL (N= 1) of lipids to the reaction (Figure 4-9. B-C). The scenario changed when supplementing the CFE reaction with 3 mg/mL of lipid, showing a decrease in the amount of protein in fractions 2-7 (N= 3) and suggesting that the protein fraction locates at the top fractions collected from DGC.

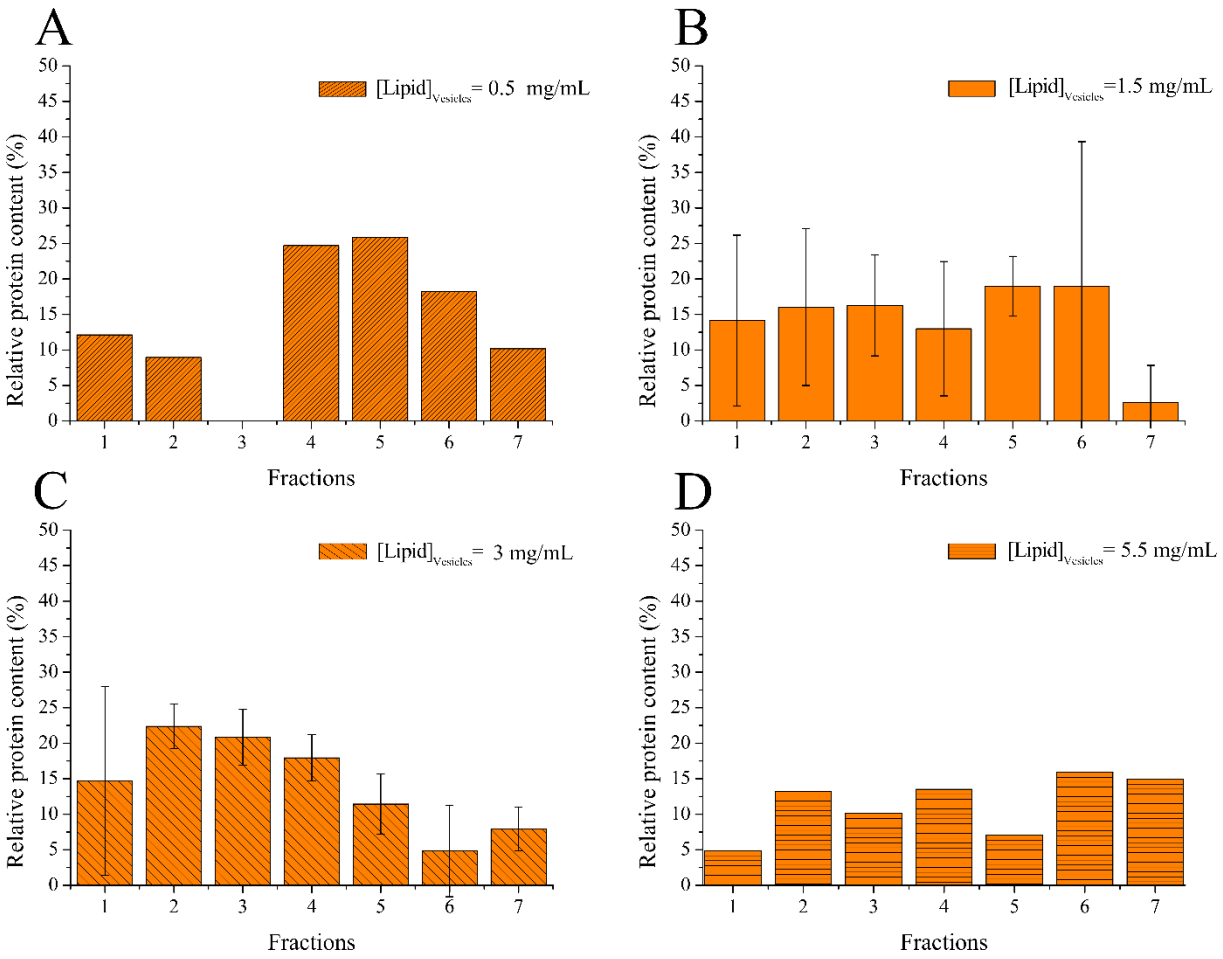

Figure 4-9. Distribution of the relative content of Cx43 in the different fractions obtained after DGC showing the effect of lipid concentration on the incorporation of Cx43 into vesicles. The composition of all vesicles preparations was L-α-PC: DOTAP: TxR (89.5:10:0.5) with final concentrations in the reaction mixture of A) 0.5 mg/mL; B) 1.5 mg/mL; C) 3 mg/mL; D) 5.5 mg/mL.

The distribution of the vesicles collected after DGC suggests that most of them are in fractions 1-4, therefore the amount of protein was also evaluated on these fractions since proteoliposomes are most likely to be present there. Figure 4-10 summarizes the effect of increasing the lipid concentration in the CFE and the impact on the protein and lipid content present in fractions 1-4. From Figure 4-10 is clear that the amount of vesicles in fractions 1-4 increases. In contrast, the amount of protein in fractions 1-4 shows a Gaussian trend showing the maximum amount of WT Cx43 (~76 %) when the CFE reaction mixture is supplemented with 3 mg/mL of lipids. In consequence, all the following experiments were carried out in presence of L-α-PC: DOTAP: TxR (89.5: 10; 0.5) liposomes of 100 nm in size at a concentration of 3 mg/mL since those conditions were optimal to synthesize and reconstitute Cx43 by means of cell-free expression.

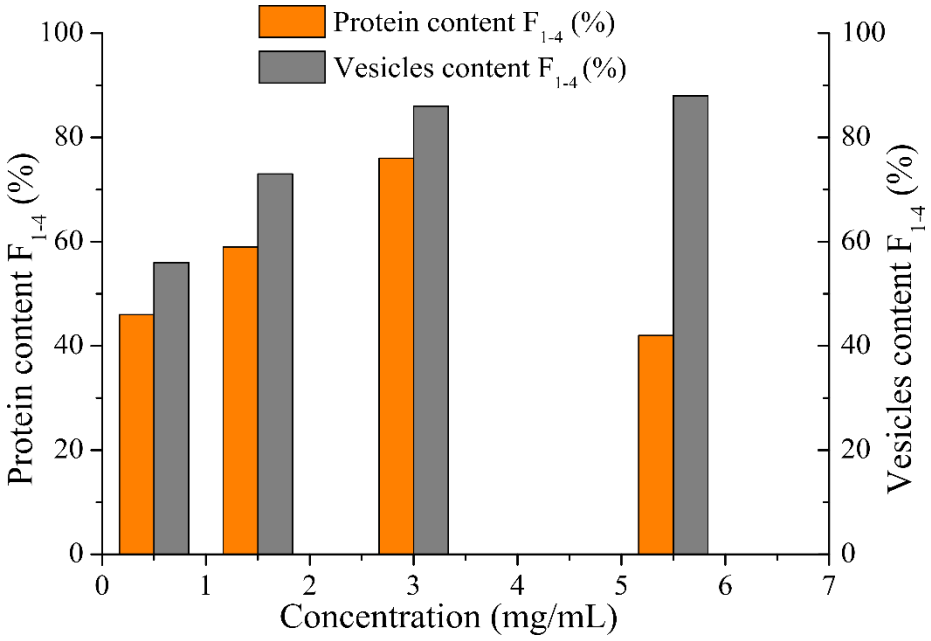

Figure 4-10. Summary of protein and lipid content located in fractions 1-4 with increasing lipid concentration in CFE reaction mixture. The displayed lipid concentrations in the CFE reaction were (0.5; 1.5; 3;5.5) mg/mL.

4.2.4 Direct insertion of C- & N-EGFP Cx43 into vesicles

After determining the optimal conditions to express WT Cx43 in presence of liposomes, the plasmids containing the sequences coding for C- & N-EGFP Cx43 were added to the reaction mixture. Figure 4-11 illustrates exemplary Western Blot membranes showing the overall distribution of C- or N-EGFP Cx43 among the fractions obtained after DGC and compared to

one sample expressing either C- or N-EGFP Cx43 in absence of vesicles as a reference of the expression (Figure 4-11 samples labeled: "(+) DNA, (-) Ves."). The presence of both the Cx43 and EGFP sequence was corroborated by using specific antibodies. Figure 4-11 shows a change in the molecular weight (MW) of Cx43 given by the presence of EGFP sequence as it is expected, changing from ~ 43 kDa to ~ 70 kDa. In Figure 4-11. A-D, the Western blot membranes reveal that the MW for C- & N-EGFP Cx43 was lower (between 55-70 kDa) than those predicted by the SnapGene software (72 and 78 kDa, respectively), though, it is a common phenomenon given by the interaction of SDS with membrane proteins [95]. Taken together, these results represent proof that C- & N-EGFP Cx43 can be successfully expressed in presence of vesicles composed of L-α-PC: DOTAP: TxR (89.5: 10: 0.5) at 3 mg/mL when supplementing the CFE reaction mixture.

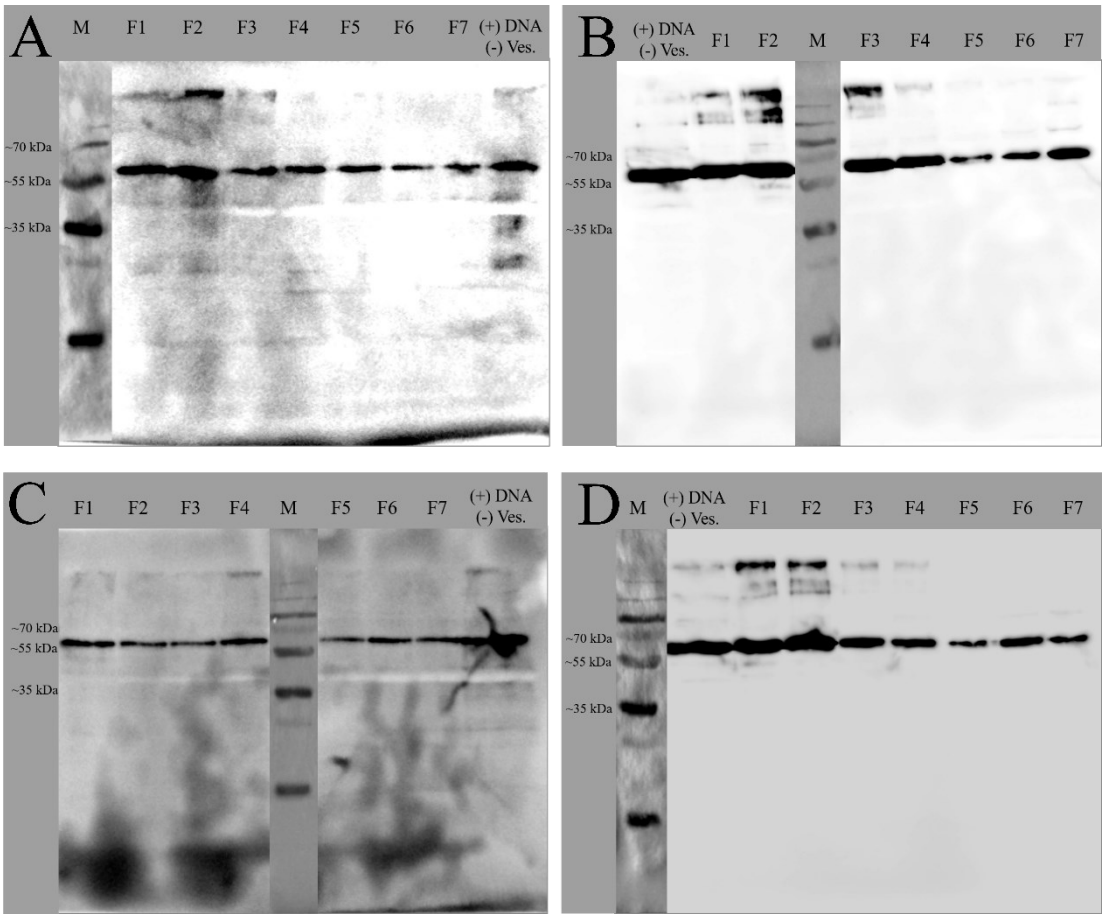

Figure 4-11. Expression of C- & N-EGFP Cx43 in presence of vesicles of L-α-PC: DOTAP: TxR (89.5: 10: 0.5) at 3 mg/mL in the reaction mixture. The top figures represent the expression of C-EGFP Cx43 when analyzed with A) Cx43 antibody or B) GFP antibody. Figures at the bottom represent the expression of N-EGFP Cx43 when analyzed with C) Cx43 antibody or D) GFP antibody.

Up to this point, it has been shown that expression of all three variants of Cx43 available in this project can be expressed as free proteins in solution (Figure 4-4) or in presence of liposomes in solution, by providing a hydrophobic environment in which Cx43 could directly insert as it gets synthesized [25,27,35]. Under the optimal conditions for expressing Cx43 in presence of vesicles, the amount of protein distributed in all fractions after DGC was evaluated. Figure 4-12 illustrates the distribution pattern of C-EGFP Cx43, N-EGFP Cx43, and WT Cx43 in all fractions. It becomes clear that C-EGFP and WT Cx43 follow a similar distribution, concentrating most of the protein in fractions 1-4. The amount of protein available in fractions 1-4 in the case of C-EGFP Cx43 accounts for ~80 % (N= 2), while for WT Cx43 ~76 % (N= 3) of the total amount of protein present in all fractions (Figure 4-12. A & .C). In contrast, N-EGFP Cx43 distributed variably among the fractions, showing that ~64% (N= 2) of the total amount of protein was available in fractions 1-4.

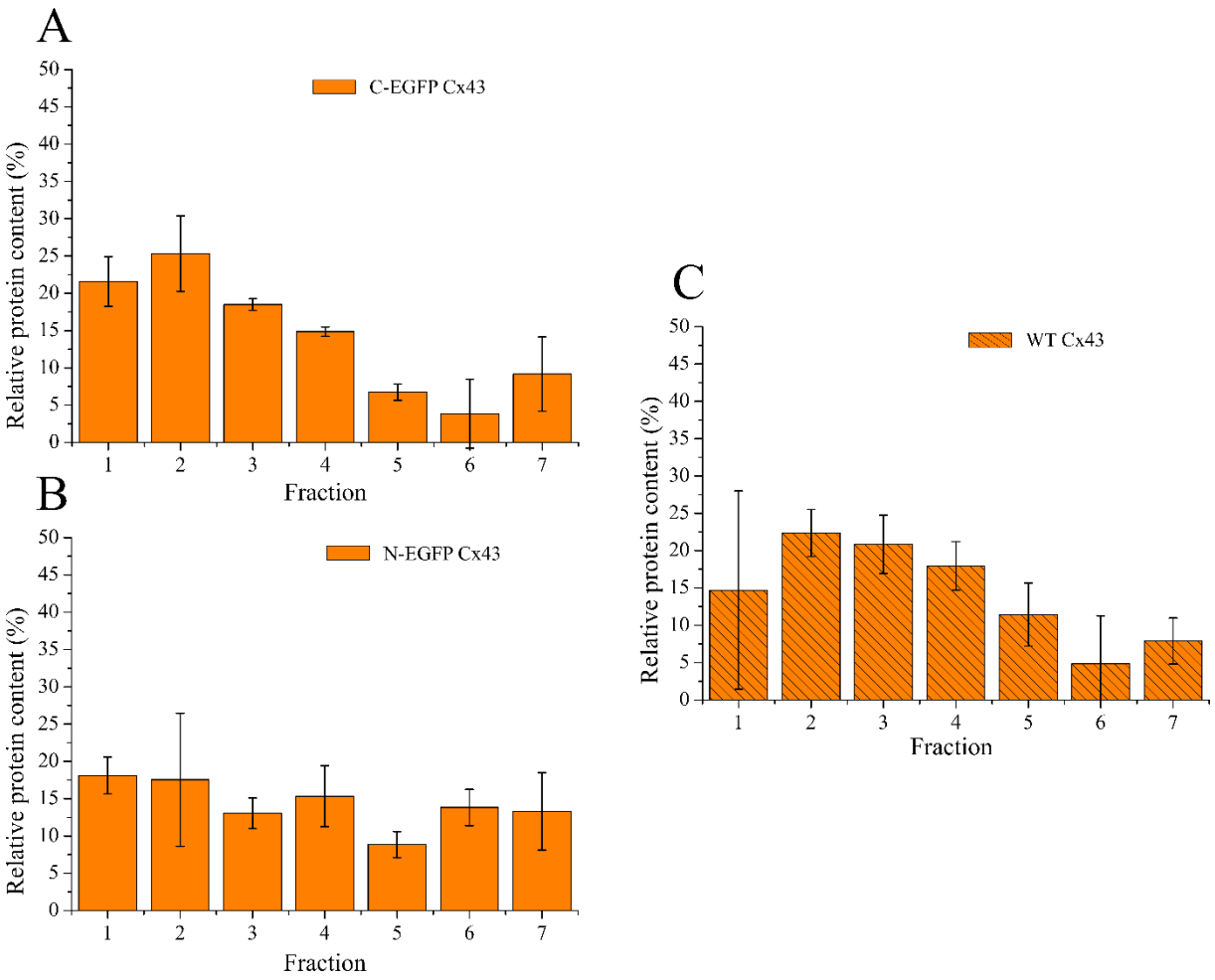

Figure 4-12. Comparison of the distribution of protein content in the different fractions obtained after DGC. Expression of the protein variants was achieved in presence of liposomes of L-α-PC: DOTAP: TxR (89.5: 10: 0.5) at 3 mg/mL in the reaction mixture for: A) C-EGFP Cx43 (N= 2); B) N-EGFP Cx43 (N= 2); C) WT Cx43 (N=3).

4.2.5 Localization of C- & N- EGFP Cx43 proteoliposomes via fluorescence spectroscopy

In section 4.2.4, it was determined that proteoliposomes are located preferentially in fractions 1-4. The experiments of this section aim to corroborate the localization of proteoliposomes *via* fluorescence spectroscopy for the Cx43 variants containing GFP. First, experiments to corroborate emission of C- & N-EGFP Cx43 in the green region were performed both in the presence (*e.g.,* "C-EGFP proteo.") and absence of vesicles (*e.g.,* "C-EGFP free"), and compared to control samples (see Figure 4-13). Three control samples were evaluated: i) synthesized WT Cx43 in absence of vesicles ("Cx43 WT free"), ii) a sample containing all components for protein expression except of a DNA template ("PURExpress (-DNA)"), and iii) a sample containing only diluted vesicles ("vesicles"). By comparing samples shown in Figure 4-13. A, it becomes clear that only those samples containing GFP show fluorescence; being the emission signal of C-EGFP Cx43 higher when synthesized in absence of vesicles. In contrast, Figure 4-13. B illustrates the relative emission signal for EGFP at 510 nm from which it is evident that samples containing free C- or N-EGFP show a higher emission than those synthesized in presence of liposomes. The relative fluorescence intensity for C- & N-EGFP Cx43 proteoliposomes was 0.38 ± 0.08 (N= 5) and 0.43 ± 0.05 (N= 3), whereas 0.57 ± 0.14 (N= 2) and 0.68 (N= 1) for C- & N- EGFP Cx43 expressed in absence of vesicles, respectively. Additionally, the control samples containing freely synthesized WT Cx43, PURExpress® components in absence of DNA template, and vesicles in aqueous solution reported a basal relative fluorescence intensity of approx. 0.11 ± 0.12 (N= 3); 0.07 ± 0.05 (N= 2) and 0.04 ± 0.03 (N= 4), respectively. Thus, this basal fluorescence is a product of the normalization step since all samples were normalized against the excitation peak of EGFP at λ= 495 nm (see section 3.4 for further details on the normalization step). All vesicles were composed of L-α-PC: DOTAP: TxR (89.5: 10: 0.5) with a lipid concentration in the reaction mixture of 3 mg/mL, and 100 nm in size.

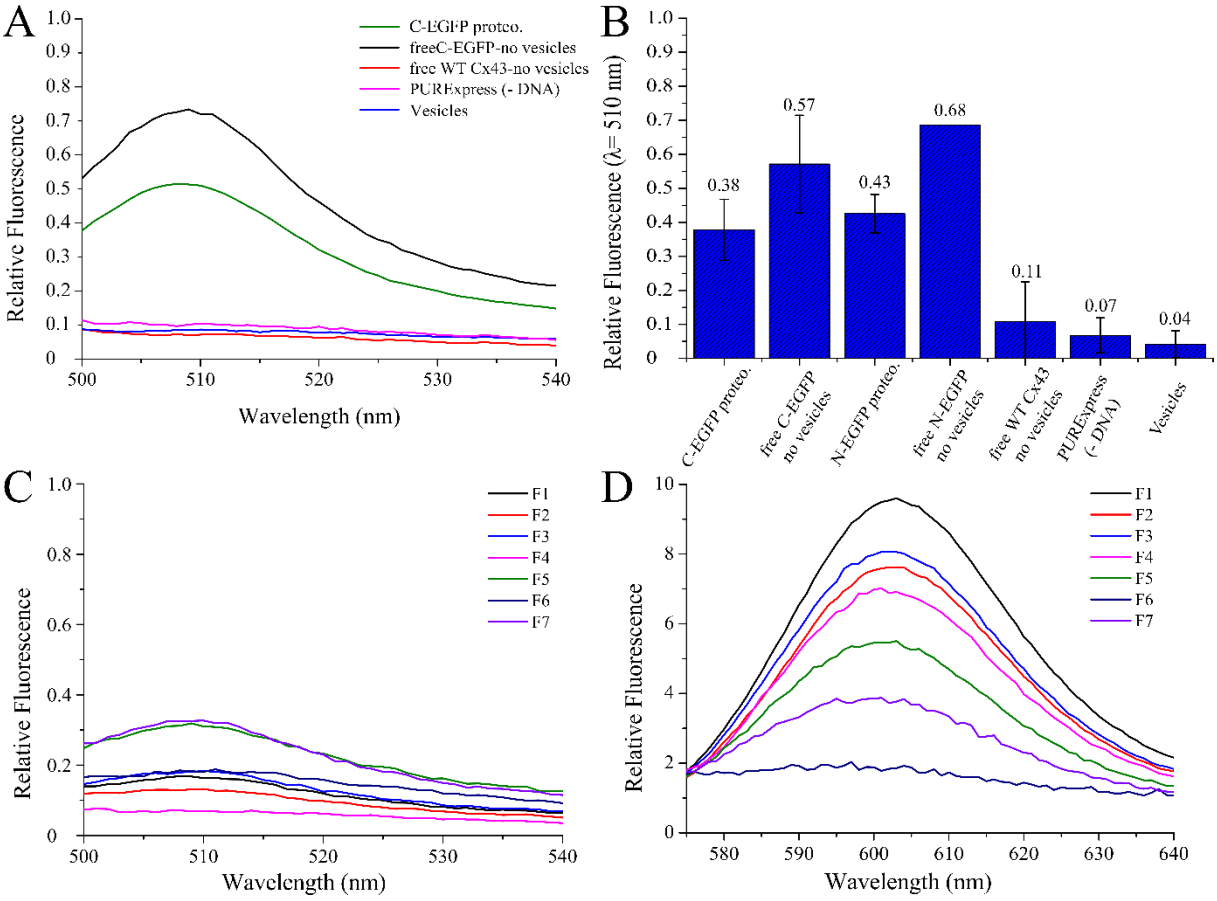

Figure 4-13. A) Emission spectra of GFP for samples containing C-EGFP free in solution or inserted in liposomes, WT Cx43 expressed in absence of liposomes, and two control samples containing PURExpress® components in absence of a DNA template and vesicles diluted in aqueous solution. B) Relative emission signal at 510 nm of samples containing C- or N-EGFP Cx43 proteoliposomes, C- & N-EGFP or WT Cx43 expressed in absence of liposomes, and two control samples as in A. C) Emission spectra of C-EGFP Cx43 proteoliposomes after DGC for samples excited at 495 nm (data normalized to maximum excitation peak). D) Emission spectra of proteoliposomes excited at 561 nm (data normalized to minimum emission value for all fractions).

To continue the investigation of proteoliposomes distribution after expression and purification by DGC, all collected fractions were evaluated in an emission range of 500-540 nm for EGFP, and 570-640 nm for Texas Red™. From Figure 4-13. C & .D, it is discernible that fractions 5 and 7 reported higher emission signals when compared to the rest. In the case of Texas Red™, the figure suggests that most vesicles locate in fractions 1-4. However, evaluation of the distribution of the protein or vesicles content among the different fractions with the emission spectra is not the most accurate method given that the signal from all fractions is normalized against the maximum peak for EGFP (or minimum emission value for Texas Red™, see more details about normalization in section 3.4) and does not give information of how much protein relative to the total was present in each fraction. Therefore, the emission signal for each fraction

was normalized against the total emission signal for all fractions either at 610 nm (for Texas Red™) or 510 nm (for EGFP) to evaluate the distribution of vesicles and protein among the fractions after DGC. From Figure 4-14. A, it is visible that up to 96 % (N= 3) of vesicles locate preferentially in fractions 1-4, showing a decrease on the amount of vesicles as progressing from fraction 1 to 7. When evaluating the amount of protein present on each fraction, C- & N-EGFP Cx43 showed a variable distribution among all fractions and reported up to ~62 % (N= 4) and ~50 % (N= 4) in fractions 1-4, respectively.

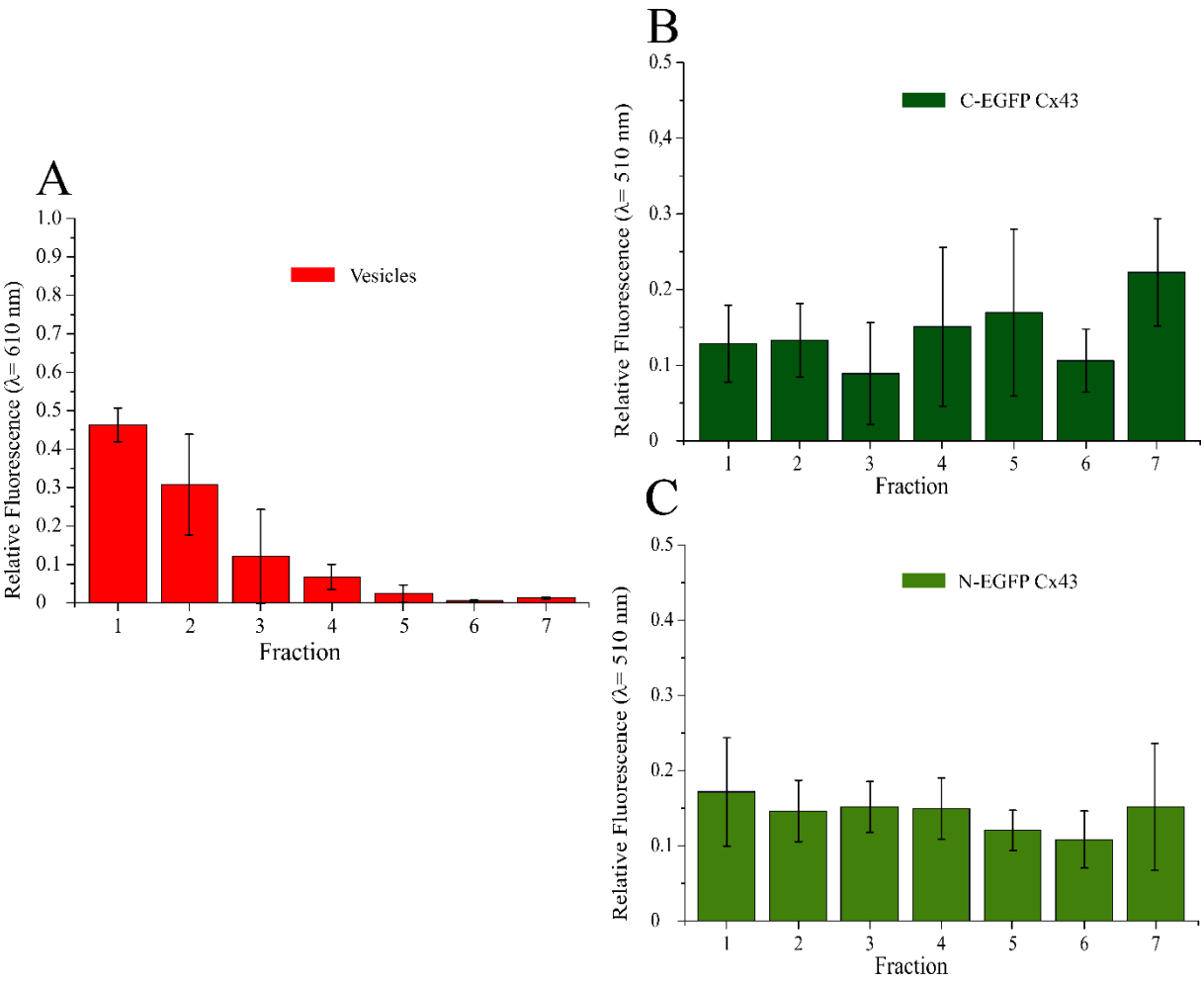

Figure 4-14. Localization of C- & N- EGFP Cx43 proteoliposomes. A) Relative fluorescence intensity of Texas Red at 610 nm for all fractions recovered after DGC. Relative fluorescence intensity of proteoliposomes containing B) C-EGFP Cx43 or C) N-EGFP Cx43 at 510 nm for all fractions recovered after DGC. All samples were normalized against the total signal recorded at 610 nm or 510 nm for all fractions to get a distribution profile for both the vesicles and protein fractions.

4.3 Characterization of Cx43 proteoliposomes

-Experiments with TEV digestion were carried out by Muriel Hartsch as part of her bachelor thesis-

4.3.1 Orientation of Cx43 incorporated in Larges Unilamellar Vesicles: TEV protease assays with N-EGFP Cx43

Among other properties, the plasmid coding for N-EGFP contains a *Tobacco Etch Virus* (TEV) sequence at the N-terminal domain between the EGFP and Cx43 sequences, which can be used to perform protease assays to determine the orientation of the Cx43 in proteoliposomes produced by CFE. In general, N-EGFP Cx43 proteoliposomes were prepared under the determined optimal conditions but changes were introduced in the purification step. More precisely, density gradient centrifugation (DGC) was still the method of choice, but it was used in combination with size exclusion chromatography (SEC). First, a control assay was carried out to determine the protease activity and test the cleavage conditions of TEV in the reaction. For that purpose, Ezrin (a soluble protein involved in the interactions between actin filaments and the plasma membrane) containing a Histag in its sequence, was kindly provided by Tim Heißenberg from the AK Steinem, and it was used as a control protein for the TEV reaction. In Figure 4-15. A, it is visible that in presence of TEV, Ezrin can no longer be recognized by the Histag antibody, proving that TEV is functional and able to recognize and cut at the specific sequence. Next, N-EGFP Cx43 in absence of liposomes (free in solution) was diluted by a factor of 10 or 50 and incubated either at room temperature or at 80 °C prior to the protease incubation step at 30 °C to enhance TEV cleavage. Figure 4-15. B illustrates the product of the TEV cleavage assay under the mentioned conditions, and it becomes clear that the presence of the protease in the reaction has no apparent effect on N-EGFP Cx43 given that no changes in the molecular weight are discernible at any of the conditions tested.

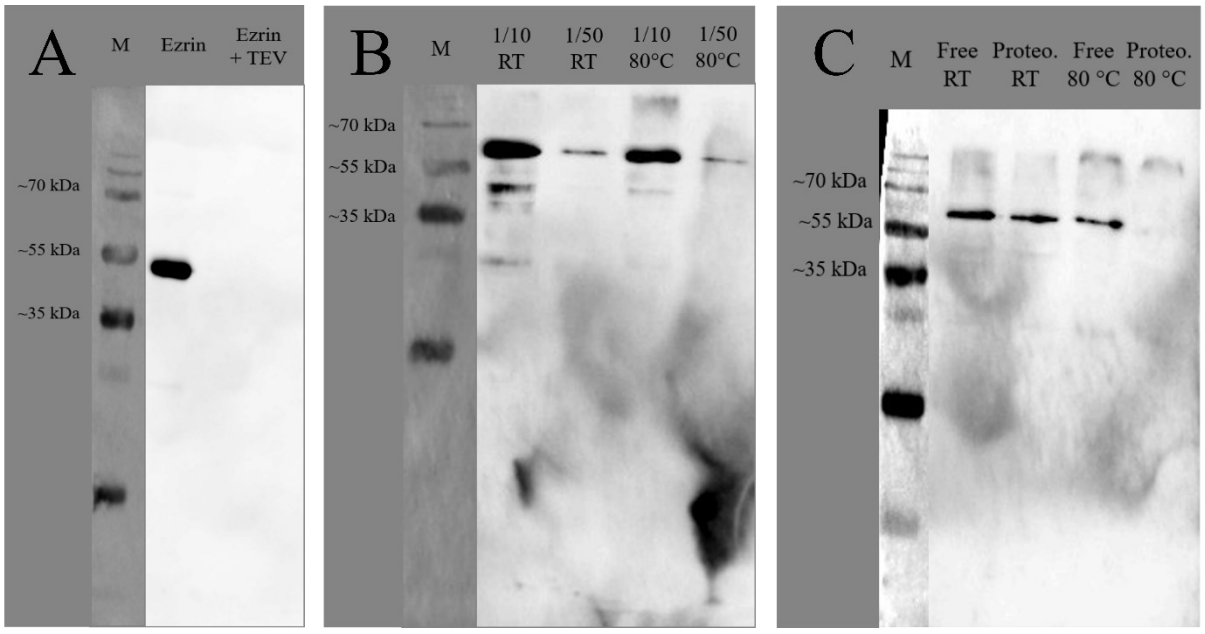

Figure 4-15. Digestion assays with free N-EGFP Cx43 in presence of TEV at different conditions to determine protein reactivity to TEV. Western Blot membranes illustrating A) Control assay with Ezrin in presence of TEV showing the activity of TEV by the cleavage of a Histag (Protein bands were recognized by a Histag antibody) B) Digestion trials with free N-EGFP Cx43 with TEV with dilution factors of 10 or 50, incubated at room temperature (RT) or 80 °C prior to the incubation at 30 °C for TEV cleavage. C) Digestion trial with free N-EGFP Cx43 ("Free") or proteoliposomes ("Proteo") incubated at RT or 80 °C prior to the digestion assay with TEV. Protein products in B and C were detected with the Cx43 antibody.

Alternatively, N-EGFP Cx43 was expressed in presence of LUVs followed by purification of the proteoliposomes by DGC in combination with SEC, or solely by means of SEC. The product of the purification steps was evaluated with SDS-PAGE, and it is shown in Figure 4-16. A. As shown previously in Figure 4-4. A and Figure 4-5. A, proteins and enzymes from the PURExpress® kit are still present after the purification step and are visible by SDS-PAGE. Nevertheless, an enriched protein band located between 55 and 70 kDa is identified as N-EGFP Cx43. For both purification approaches four fractions were recovered, fractions 1-4 when proteoliposomes were purified only by SEC, or fractions A-D when proteoliposomes were purified by DGC + SEC. From the latter purification approach, fractions B and C were directly used to perform a cleavage assay (Figure 4-16. B). Both fractions were incubated in the presence or absence of TEV but unfortunately, no changes in molecular weight were reported, suggesting that TEV could not reach the cleavage site or had no effect on the proteoliposomes enriched fractions.

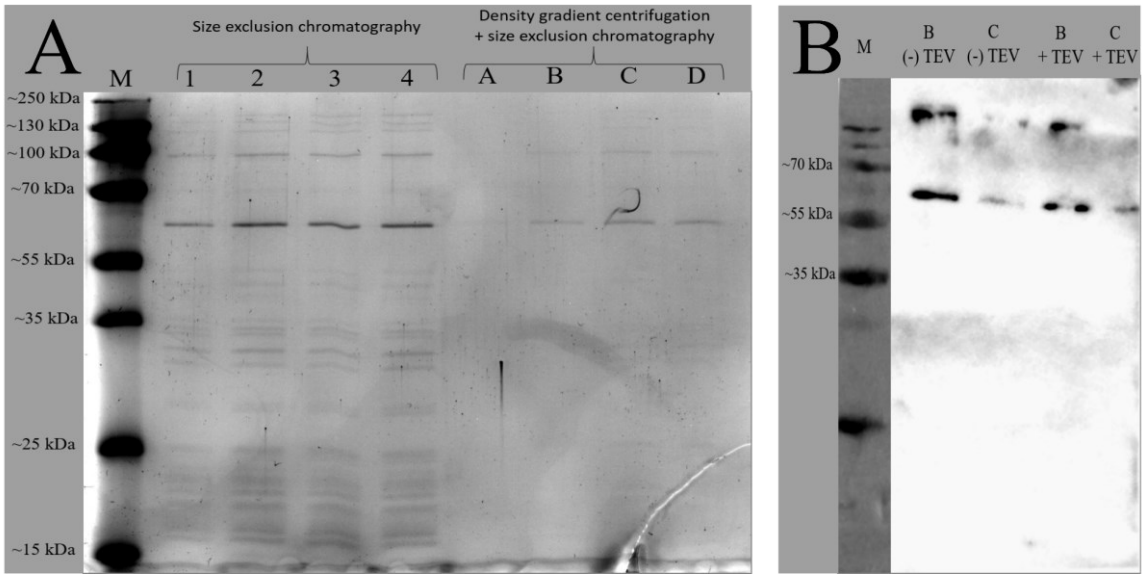

Figure 4-16. Digestion assays of N-EGFP Cx43 proteoliposomes purified directly by size exclusion chromatography (SEC) or prior by DGC. A) SDS-PAGE showing the product of purifying proteoliposomes only by SEC or DGC +SEC. B) Western blot membrane containing the product of N-EGFP Cx43 proteoliposomes purified by DGC + SEC in the presence or absence of TEV. Fractions B and C correspond to the same fractions on the right section of the SDS-PAGE. Protein product was detected with a Cx43 antibody.

4.3.2 Functional analysis of Cx43 proteoliposomes

-Part of the experiments on the Orbit 16 were carried out by Apinrix Menoha as part of his bachelor thesis-

An attempt to check the functionality and viability of Cx43 proteoliposomes by means of voltage-clamp was carried out. In more detail, an automated-BLM platform was used which allows for the screening of protein channels in 16 parallel micro-chambers that work simultaneously and independently from each other, thus increasing the probability of protein insertion in the bilayers. For these assays, WT Cx43 plasmid was used in combination with vesicles composed of L-α-PC: DOTAP: TxR (89.5: 10: 0.5) to reach a concentration of 3 mg/mL in the CFE reaction mixture. After DGC, fractions 2-3 were used to assure the presence of proteoliposomes and they were diluted 10 or 100 times in buffer B before the addition of the proteoliposomes to the BLM system.

Planar lipid bilayers were composed of L-α-PC: POPG (90: 10) to enhance vesicle fusion and therefore, protein insertion into the bilayer *via* charged mediated fusion. Preliminary results showed that after the addition of the proteoliposome fraction, the current of the system seemed to increase, sometimes also after the change in potential or buffer exchange. Nevertheless, the current differences found in the recordings did not show discrete changes as it might be expected from voltage-clamp experiments (data not shown). In most cases, changes in the level of current were visible but they normally showed a linear decreasing behavior with noise.

The addition of taurine to the experiments was intended to elucidate if the recorded electrical signal might have come from Cx43 or if it is an artifact. Approximately, in 40 % of the cases, taurine seemed to abolish the electrical signal completely or partially in the system. However, after buffer exchange, it was not always possible to recover electrical activity, and in some cases, recordings became noisier.

The composition of both the vesicles and the bilayers was slightly changed. Instead of using 10 % of negative and positive charges in both the vesicles and bilayer to mediate the fusion, 2 % or 0 % of these charges were used in both lipid environments. However, the same noisy effect with a decreasing trend was still visible. When repeating the experiments with empty vesicles as a control, in presence of the PURExpress® components or diluted in an aqueous solution, around 60 % of the evaluated cases still showed a highly noisy behavior. When checking the capacitance of the bilayers before and after adding vesicles to the experimental setup (with or without Cx43), an increase of approx. 28 % was found. In summary, it was not possible to record Cx43 channel activity under the proposed experimental design but two hypotheses derived from these experiments: i) high volumes of lipid material (or their composition) in the vesicles might destabilize the bilayers giving rise to the noise in the recordings, and/or ii) interaction of the components of the PURExpress® kit might interact and destabilize the bilayers and potentially mask electrical currents coming from Cx43 even after purification by DGC (see Figure 4-5.A).

4.4 Incorporation of Cx43 into vesicles of different size

4.4.1 Effect of vesicles sizes on the incorporation of Cx43 into liposomes

Moritani and colleagues found that increasing the average size of the liposomes in the CFE reaction mixture results in a decrease in the total amount of integrated protein [25]. In this project, the effect of different vesicle sizes on the incorporation of Cx43 was evaluated. For that, SUVs were prepared *via* sonication, LUVs *via* extrusion, and GUVs *via* electroformation to obtain different sizes for the liposomal fractions that would follow the supplementation of the CFE reaction mixture to express Cx43. For these experiments, the methodological procedure was adapted to the techniques used and slightly modified for comparison purposes. Up to now, the optimal lipid composition and concentration for the vesicles fraction determined in section 4.2.3 were used in the same manner to supplement the CFE with SUVs and LUVs (L-α-PC: DOTAP: TxR; in a ratio of 89.5: 10: 0.5 at 3 mg/mL). On the other hand, GUVs were composed of POPC: TxR (99.5: 0.5) and were used at 30 µg/mL in the CFE reaction mixture. After the purification step by DGC, three fractions instead of seven were collected to check if the recovery volume had an influence on the amount of protein found in the top fractions, *e.g.*, when adding LUVs to the CFE reaction. In literature, purification of Cx43 proteoliposomes has also been achieved by DGC and the number of collected fractions ranges from 2-4 to evaluate the presence of Cx43 [25–27] . Collection of three fractions after DGC, was also intended to compare the amount of Cx43 *via* Western Blot within the same nitrocellulose membrane, though, that was not possible to obtain.

Figure 4-17 shows the distribution profile of the vesicles and C-EGFP Cx43 among the three fractions collected after DGC as a function of vesicle sizes. The relative fluorescence intensity was evaluated for Texas Red™ (λ= 510 nm) and EGFP (λ= 510 nm) to evaluate the distribution of the vesicles and C-EGFP among the fractions. From Figure 4-17.A is visible that liposomes locate preferentially in fractions 1 and 2, showing a decrease in the amount of vesicle towards fraction 3. On average, 90 % (N= 1) of SUVs were found in fractions 1 and 2, in contrast to 95 % (N= 1) and 71 % (N= 1) of LUVs and GUVs, respectively. On the other hand, the amount of protein in each fraction varied depending on the size of the vesicles used. When expressing C-EGFP Cx43 in presence of LUVs the amount of protein in fractions 1-2 was 72 % (N= 1), whereas 55 % (N= 1) and 44 % (N= 1) in presence of SUVs or GUVs. Therefore, suggesting that the presence of C-EGFP Cx43 in fraction 3 accounts for free, non-inserted protein.

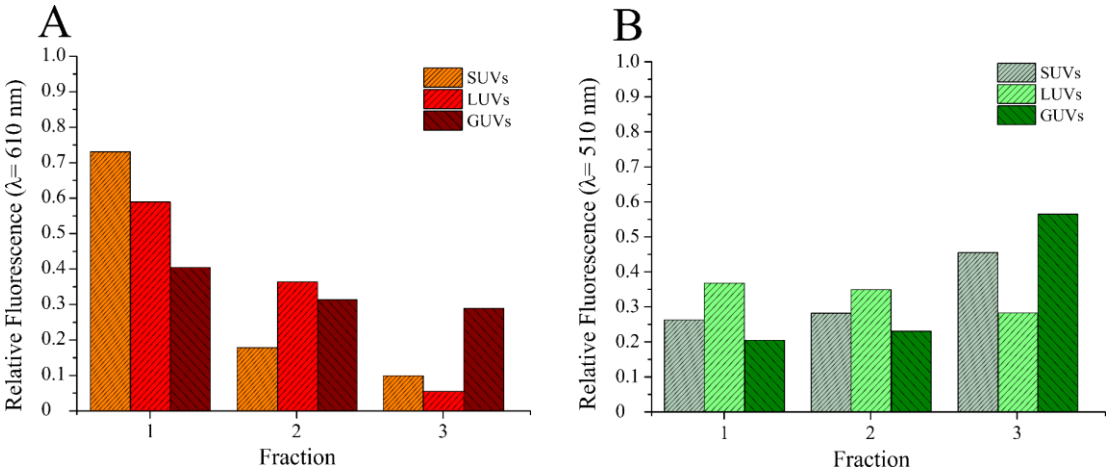

Figure 4-17. Effect of liposome sizes on the incorporation of C-EGFP Cx43. A) Distribution of the amount of vesicles among the fractions recovered from DGC. The amount of vesicles was estimated by the presence of Texas Red in the lipid composition and reported at 610 nm. B) Distribution of C-EGFP Cx43 among the fractions recovered from DGC. The total and relative amount of protein was evaluated at 510 nm for each fraction. Lipid composition for SUVs and LUVs was L-α-PC: DOTAP: TxR (89.5: 10: 0.5), while lipid composition for GUVs was POPC: TxR (99.5: 0.5) with a final concentration in the reaction of 3 mg/mL and 30 µg, respectively.

Given the increasing amount of free aggregated C-EGFP Cx43 in fraction 3 when protein expression took place in presence of SUVs or GUVs, the size of the vesicle populations was evaluated by dynamic light scattering (DLS) before and after supplementing the CFE reaction mixture with liposomes. A summary of the size populations encountered for each vesicle type is found in Table 4-1. SUVs do not show a change in size after being incorporated into the CFE reaction, showing an average diameter of 100 nm. In the case of LUVs, the average size was around 150 nm showing a unimodal distribution before CFE, while it showed a bimodal distribution with an average size of 159 nm for the first peak and 42 nm for the second one. The size of GUVs showed an heterogeneous distribution as it is expected when preparing them by electroformation [96]. Before addition of GUVs to the CFE reaction, the reported average sizes were (278; 0.96; 27) nm while they changed to (35; 121; 11) nm after adding them to the CFE reaction mixture. Now, DLS is not the appropriate method to evaluate the size of GUVs given their high heterogeneity in size, though it was used only for comparison purposes with the other vesicle populations evaluated. The size of GUVs before their addition to the CFE, reports a subpopulation of vesicles with an average size of 0.96 ± 0.03 which is clearly an artifact since the sample did not meet the quality controls to be used for DLS measurement. These results suggest that there might be a drastic change in the size of the GUVs after their addition to the CFE reaction mixture.

Table 4-1. Size distribution of liposomes before and after their addition to CFE reaction mixture. Data was obtained by DLS. The size of the vesicles is reported as the average. St. Dev., standard deviation of the samples. Complementary plots showing the size distribution of the vesicles can be found in Figure 8-3 in section 7.3 in the Appendix.

		Peak 1		Peak 2		Peak 3	
		Size (d. nm)	**St. Dev. (d. nm)**	**Size (d. nm)**	**St. Dev. (d. nm)**	**Size (d. nm)**	**St. Dev. (d. nm)**
SUVs	Before CFE	104	28	-	-	-	-
	After CFE	94	34	-	-	-	-
LUVs	Before CFE	150	40	-	-	-	-
	After CFE	159	37	42	5	-	-
GUVs	Before CFE	278	20	0.96	0.03	27	2
	After CFE	35	11	121	28	11	1

4.4.2 Monitoring the incorporation of Cx43 into artificial membranes

Direct expression and insertion of Cx43 into giant vesicles and its localization has been achieved using several strategies and for diverse purposes [25–27,35]. In section 4.4.1, GUVs were already used to evaluate the effect of vesicle sizes on the incorporation of Cx43 and the results suggested that only 44 % of the synthesized protein might be available to incorporate in the bilayer of the vesicles. Here, incorporation of EGFP-Cx43 into GUVs was monitored and evaluated by confocal laser scanning microscopy (CLSM). GUVs were produced by electroformation and added to the CFE reaction mixture to stabilize the synthesis of Cx43 prior to the imaging step. Before adding the vesicles to the reaction, their presence and integrity were evaluated by CLSM. Figure 4-18 shows exemplary micrographs of the vesicles freshly obtained after electroformation, therefore in absence of the PURExpress® components or DNA templates (Figure 4-18. A & .B). GUVs were still abundant in the imaging chambers after 24 h which was the approx. time to calculate the lipid concentration in the vesicles, perform CFE, purify the proteoliposomes, and prepare the chambers for imaging (see Figure 4-18. C &.D). It was common to find them as single vesicles or aggregates in solution. The diameter of the single vesicles was analyzed, reporting an average of (30 ± 11) µm obtained from 82 vesicles evaluated from 9 micrographs (N = 82; n= 9).

The effect of incubating GUVs in presence of the PURExpress® components but in absence of a DNA template was evaluated. Figure 4-19.A &.B illustrate exemplary micrographs for this control sample, where it is clear that the number of observed vesicles dramatically decreased upon addition of the vesicles to the CFE reaction mixture. These vesicles showed an average

diameter of (15 ± 4) µm (N= 5; n= 4), already suggesting that the CFE kit might influence the stability of the GUVs.

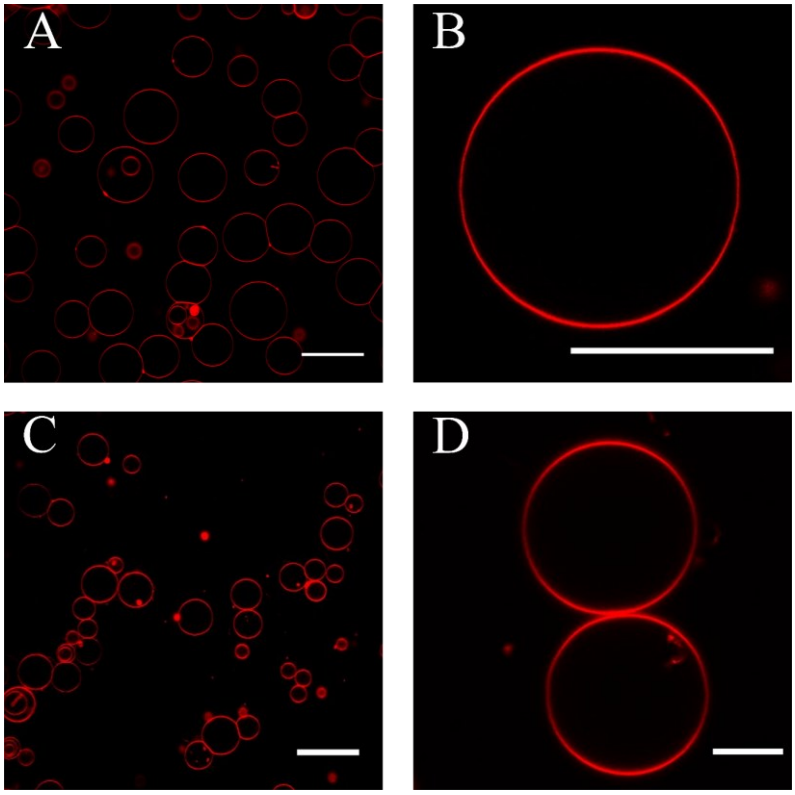

Figure 4-18. Giant vesicles were obtained by electroformation in absence of CFE kit components and DNA template. Micrographs showing the emission signal of Texas Red™ present in the lipid membranes. A) Enssemble of GUVs observed right after the electroformation step. B) Detail of a single GUV observed after electroformation. C) Emssemble of GUVs observed ~24 h after electroformation to check stability of the vesicles. D) GUVs in close contact observed ~24 h after electroformation. Composition of vesicles was POPC: TxR (99.5: 0.5) at 30 µg/mL in the measuring chamber. Scale bars: 50 µm.

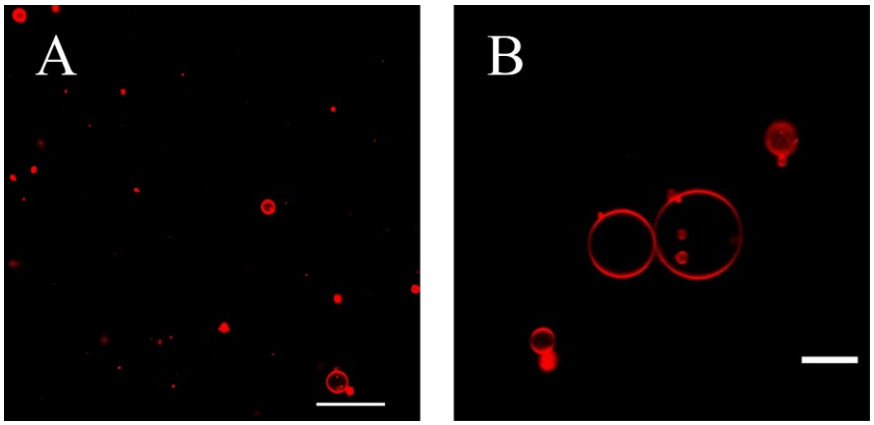

Figure 4-19. Giant vesicles after incubation with PURExpress® kit components but in absence of a DNA template as a negative control for CFE the reaction. A) Emission of Texas Red™ coming from the GUVs present in solution. B) Emission of Texas Red™ showing the localization of two GUVs forming an aggregate. Composition of vesicles was POPC: TxR (99.5: 0.5) at 30 µg/mL in the CFE reaction mixture. Scale bar for: A) 50 µm, B) 10 µm.

When adding GUVs composed of POPC: TxR (99.5: 0.5) to the CFE reaction mixture, it was difficult to find green fluorescence from the protein across the measuring chamber. When green emission signal was found, it did not correlate to the section where the vesicles were located. Therefore, Texas Red™ was taken out of the lipid composition to favor the search of possible EGFP-Cx43 proteoliposomes. Figure 4-20 shows an example of GUVs composed of pure POPC that were observed in bright field in absence of Texas Red™, PURExpress® kit components, or DNA templates. With this composition, GUVs reported an average diameter of (31 ± 21) µm.

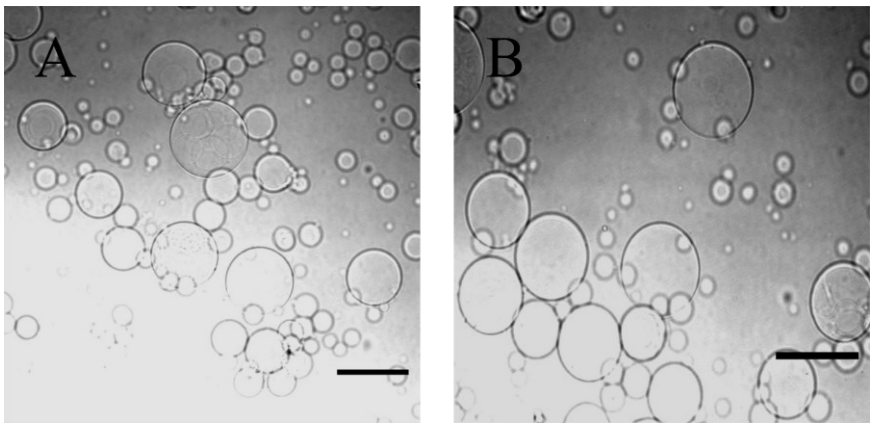

Figure 4-20. Giant vesicles prepared in absence of Texas Red™ were observed in bright field. GUVs were prepared for imaging in absence of CFE components or DNA templates as a control to localize vesicles in absence of the fluorophore. Composition of vesicles POPC (100 %) at 30 µg/mL in the CFE reaction mixture. Scale bars: 50 µm.

After supplementing the CFE reaction mixture with GUVs of pure POPC, the localization of proteo-GUVs was possible in presence of both C- & N-EGFP Cx43 (see Figure 4-21). The average diameter of the vesicles changed drastically, going from (31 ± 21) µm before the CFE step to (5.4 ± 1.8) µm (N= 27; n= 9) after expression of Cx43. It was also common to find proteo-GUVs forming aggregates instead of single vesicles. The incorporation of EGFP-Cx43 into GUVs was tested multiple times under the same conditions but the frequency of success was low. Nevertheless, these results are proof that Cx43 can incorporate in presence of preformed GUVs when synthesized by means of cell-free expression.

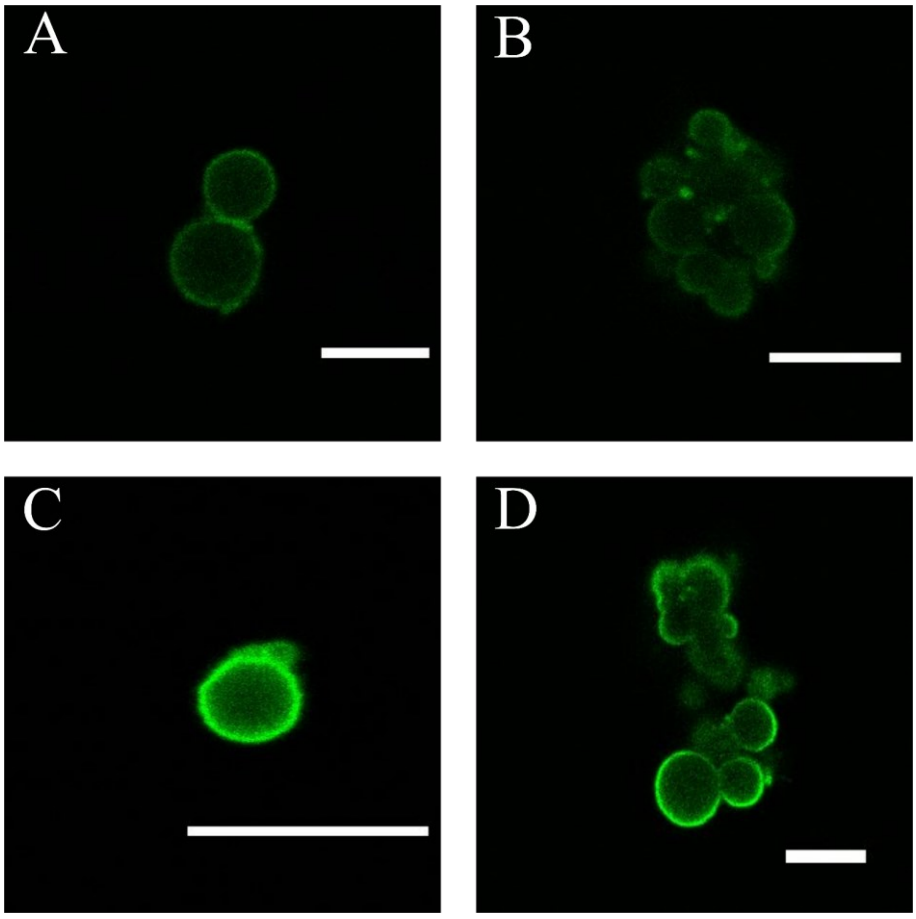

Figure 4-21. Incorporation of Cx43 into GUVs. Micrographs in showing the A) & B) Emission signal of GFP coming from the incorporation of C-EGFP Cx43 into GUVs, while in C) & D) Emission signal of GFP showing the incorporation of N-EGFP Cx43 into GUVs. Composition of vesicles POPC (100 %) at 30 µg/mL in the CFE reaction mixture. Scale bars: 10 µm.

In some cases, a green emission signal was observed at the bottom of the chamber not correlating with the vesicle fraction but with other structures as it is visible in Figure 4-22, both in the presence or absence of Texas Red™ in the lipid bilayers. Figure 4-22.A & .B are overlays of the protein and vesicle channel (green and red, respectively), while Figure 4-22. C-D & E-F represent the same region observed in bright field or in the green channel under the CLSM, to show the details of the emission signal from the EGFP product.

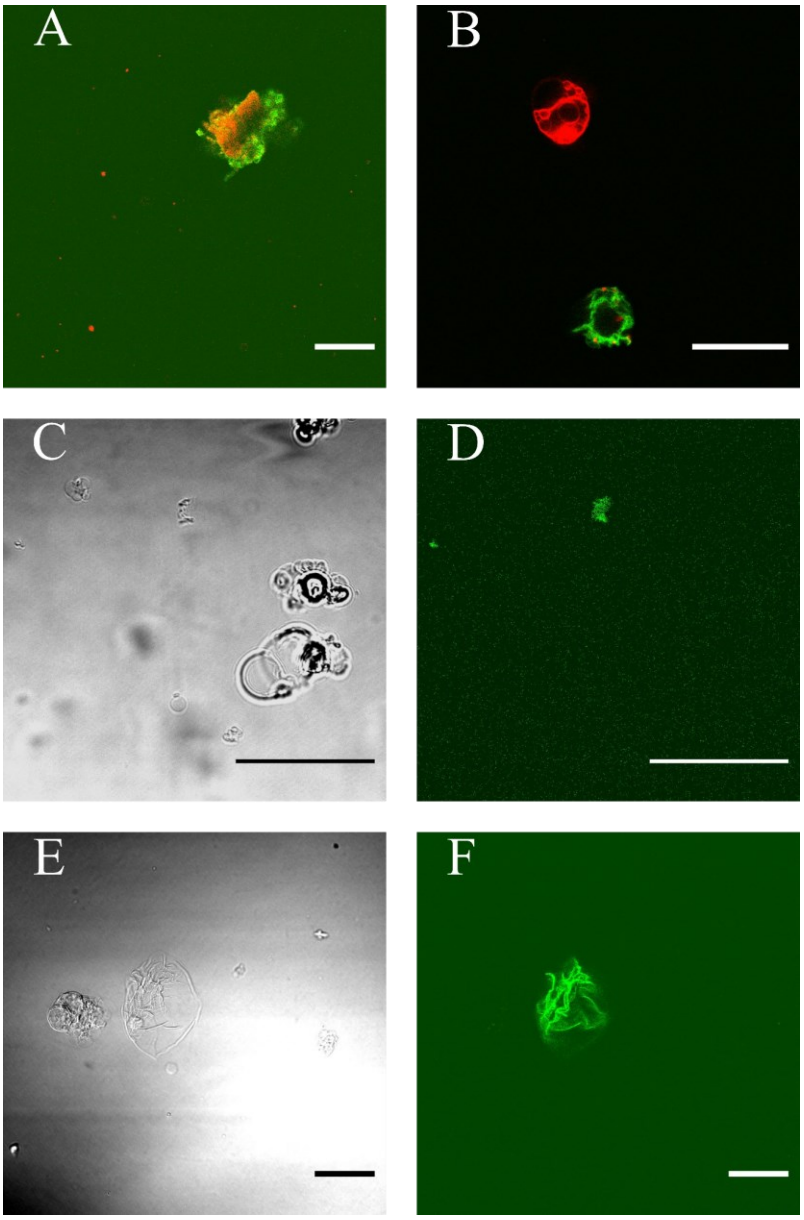

Figure 4-22. Examples of GFP emission signal after in vitro synthesis of N-EGFP Cx43 in presence of GUVs, showing that green fluorescence does not always localize to the liposomal area. Micrographs in A) & B) are overlays showing the colocalization of the emission signal for Texas Red™ and GFP. GUVs were composed of POPC: TxR (99.5: 0.5). Localization of vesicles or aggregates in bright field in micrographs C) & E), and the green channel in micrographs E) & F). GUVs were prepared with POPC (100 %) and added at 30 µg/mL to the CFE reaction mixture. Scale bars: 50 µm.

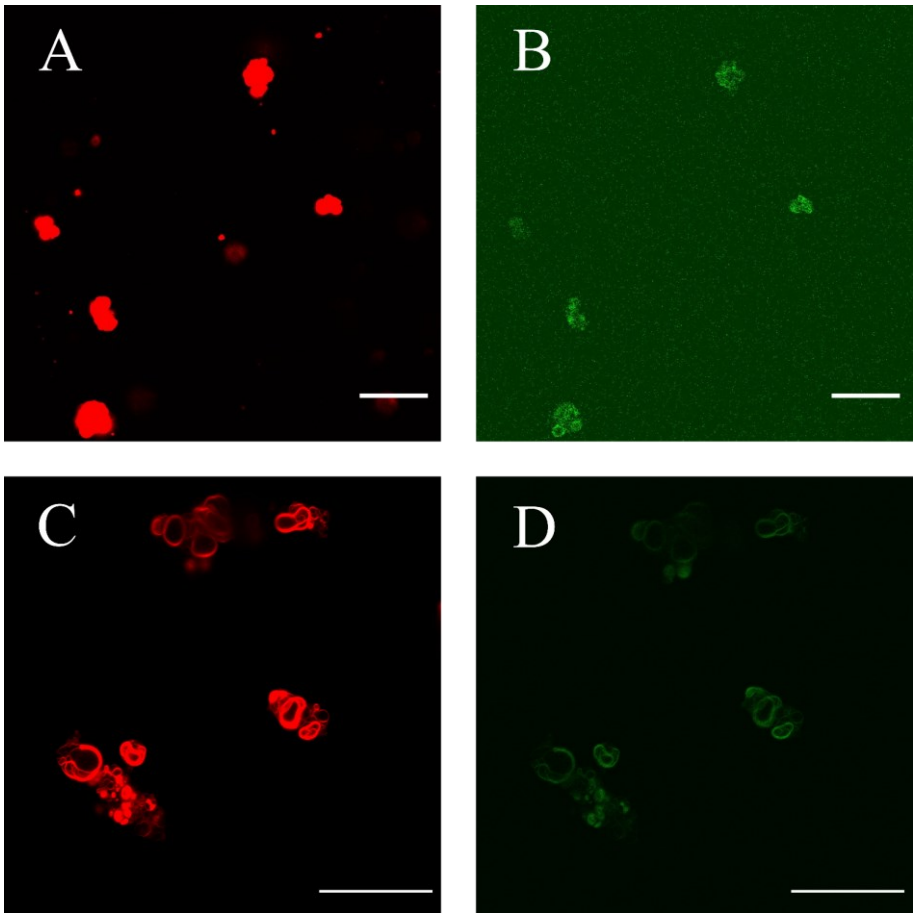

Figure 4-23. Incorporation of N-EGFP Cx43 into vesicles prepared by the natural swelling method. Micrographs showing in A) & C) Emission signal of Texas Red™ localized in the bilayer of the vesicles. In micrographs B) & D) Emission signal of EGFP coming from the N-EGFP Cx43 protein, colocalizing with the membrane channel. Lipid composition was POPC: TxR (99.5: 0.5). Scale bars: 50 µm.

In literature, the insertion of Cx43-GFP into giant vesicles have been achieved by either providing preformed GUVs into the cell-free reaction [25] or by hydrating the lipid film with a solution containing the components from the cell-free reaction to carry out the expression of Cx43 and production of GUVs by natural swelling in a simultaneous manner [26,27]. The first approach was adopted in this project, and it showed the successful incorporation of EGFP-Cx43 into GUVs (see Figure 4-21), though with a low reproducibility. Concerning the second approach, Kaneda and colleagues reported the direct and successful incorporation of GFP-Cx43 by using the cell-free expression solution to hydrate the lipid film used to obtain GUVs, in a swelling/hydration method [27]. Therefore, the natural swelling method in presence of the CFE reaction mixture was adopted in this project for comparison. Briefly, a lipid film composed of POPC: TxR (99.5: 0.5) was hydrated with the CFE mixture including the DNA template and

incubated at 37 °C for 3 h to promote the expression of Cx43. The product was directly added to the measuring chamber without prior purification to the check if vesicles were formed and if Cx43 inserted into their membranes. Figure 4-23 shows the emission of Texas Red located in the lipid fraction. This result indicates that production of vesicles by the swelling method took place. However, the vesicles obtained by this method are not clearly discernible in Figure 4-23. A since they are smaller than those obtained by electroformation. Additionally, Figure 4-23. C shows that the vesicles obtained are multilamellar instead on unilamellar. Nevertheless, the emission from N-EGFP Cx43 was observed in both cases, indicating that the protein inserts and colocalize in the membrane of the GUVs produced by natural swelling.

5. Discussion

The ability of connexin 43 (Cx43) to establish direct communication between two cellular compartments, was of special interest in this project. By using a bottom-up approach in the context of cell-free technology, Cx43 was reconstituted into artificial membranes as a first step in the direction of mimicking cell-to-cell communication. To achieve this, Cx43 was expressed in presence of vesicles of different compositions. After the successful expression of Cx43, the characterization of the proteoliposomes followed to get information about the orientation of the protein in the vesicles and its functionality. Moreover, the insertion of Cx43 into giant vesicles enabled direct observation of protein integration into artificial membranes by confocal laser scanning microscopy (CLSM). This project allowed the establishment and optimization of the cell-free technology in the research group as an alternative to the expression of proteins in cell-based systems. The arguments discussed here bring a better understanding of the cell-free technology, its limitations, and possible applications of the used model system.

5.1 Cell-free expression of Cx43

Connexin 43 has been directly integrated into artificial membranes in a cotranslational manner in presence of preformed vesicles using the PURExpress® system. These findings are in accordance with results reported by Moritani and colleagues, which is the first report that showed the expression of Cx43 with the commercial PURExpress® kit in presence of preformed vesicles [25]. In the same manner, Cx43 has been expressed *in vitro* in presence of microsomes [33] and exosome-mimic vesicles [26] or in presence of lipid emulsions which leads to the formation of vesicles and expression of the Cx43 simultaneously [27,35].

In absence of liposomes, the synthesized Cx43 has proven to aggregate given its hydrophobic nature [25–27,33]. Our experiments did not prove protein aggregation in absence of liposomes, but they showed the product of expression for WT-, C- & N- EGFP Cx43 in absence of vesicles and their recognition by the specific GFP and Cx43 antibodies. It is worth noting that even when aggregated, Cx43 was still being recognized by the antibodies at both C- and N- terminal

domains. The Cx43 antibody recognized the region of the amino acid 241-254 located at the C-terminal domain of the protein, and the GFP sequence was recognized either at the C- or N-terminal domain. These findings demonstrate the compatibility of the plasmids with the PURExpress® system and its potential use in further experiments to gain information about the Cx43 proteoliposomes system.

5.2 Composition and concentration of lipids in the vesicles can affect direct incorporation of Cx43

The addition of amphiphilic materials to the cell-free system has been used to facilitate the production of membrane proteins in a soluble form. Those materials mimic the hydrophobic membrane environment and stabilize membrane proteins by preventing aggregation [94]. Spontaneous integration of a protein into liposomes *in vitro* could in principle occur cotranslationally (protein integration occurs while the polypeptide is being synthesized on the ribosome) or post-translationally (protein integration occurs after the polypeptide release from the ribosome) [24]. In this project, we have demonstrated that WT Cx43 inserts preferentially into liposomes containing L-α-PC: DOTAP: TxR of 100 nm size. The density gradient centrifugation (DGC) analysis showed that vesicles locate preferentially in fractions 1-4. The amount of vesicles in these fractions ranges from ~60-90 % as the concentration of the lipids in the reaction tube was increased (refer to Figure 4-9 in section 4.2.3). Previously, Moritani and colleagues showed that the absence of vesicles in the CFE reaction resulted in the complete aggregation of Cx43 [25]. Thus, demonstrating that integration of Cx43 into vesicles occurs in a cotranslational manner by preventing protein aggregation and suggesting that vesicles act in a chaperone-like manner. They determined that over 70 % of Cx43 integrated into the vesicles as the concentration of the lipids increased from 1 mM (~20 % of Cx43 insertion) to 30 mM DOPC in the cell-free reaction [25]. Similarly, Falk and colleagues reported an increase of integrated Cx43 in presence of microsomes as the concentration of the latter ones increased in the cell-free reaction [33]. In this project, an increase in the amount of integrated Cx43 was observed when increasing the lipid concentration in the reaction from 0.5 mg/mL (0.64 mM) and up to 3 mg/mL (3.87 mM). The highest lipid concentration tested in this project was 5.5 mg/mL (7 mM), which reported a decrease in the amount of integrated protein dropping

from 76 % (at 3 mg/mL) to 42 %. The lipid concentrations used in this project fall within the range of evaluated concentrations in the work of Moritani and colleagues [25], suggesting that the decrease in the amount of inserted protein at a lipid concentration of 5.5 mg/mL (N= 1) could be an artifact since it is the product from a single measurement and could have been subjected to experimental error. Nevertheless, differences in the lipid compositions could also be the reason for such discrepancies. Moritani and colleagues used unilamellar vesicles of DOPC [25], while in this project vesicles with L-α-PC: DOTAP: TxR were used. Therefore, further examination of the effect of increasing the lipid concentration of the mentioned composition beyond 3 mg/mL in the CFE reaction is recommended.

Optimal conditions for the expression of Cx43 were determined. We found that vesicles composed of L-α-PC: DOTAP: TxR at a concentration of 3 mg/mL favored the insertion of Cx43 into artificial membranes up to 76 %. When using L-α-PC as a matrix lipid to produce vesicles with a net neutral or negative (with POPG) charge, the amount of inserted Cx43 in fractions 1-4 decreased. Moritani and colleagues have explained this by electrostatic repulsion between the negative charges in the liposomes and Cx43 which presumably has a overall negative charge at pH 7.5 [25]. Previously, Stockert and colleagues reported that Cx43 has an isoelectric point (pI) between 5.7 and 6.3 when expressed in HuH-7 and Trf1 cells [97]. Hence, under the buffer conditions used in this project Cx43 would also adopt an overall negative at pH 7.4 (or pH 8.0 for determine the orientation of Cx43 in the vesicles). However, the pI values for WT-, C- & N-EGFP Cx43 were calculated using the *ProtParam* tool from *Expasy* [98,99] and they revealed theoretical pI values of 8.58 for WT Cx43, 6.80 for C-EGFP Cx43, and 6.75 for N-EGFP Cx43. Assuming those values, WT Cx43 would exhibit a positive net charge in our system at pH 7.4. Yet, the amount of integrated WT Cx43 in vesicles with L-α-PC: POPG: TxR decreased from 59 % to 50 % in comparison to vesicles composed of L-α-PC: DOTAP: TxR at the same concentration (1.5 mg/mL in the cell-free reaction). On that topic, Kuruma and Ueda reported that liposomes with negatives charges could form aggregates when added to the expression reaction, since the PURE cell-free system contains abundant amounts of Mg^{2+} [13]. In consequence, one hypothesis could be that Mg^{2+} interacts with the negative charges of the vesicles, preventing the interaction of Cx43 with the liposomes as it is synthesized in the reaction. A model to explain this observation can be found in Figure 5-1.

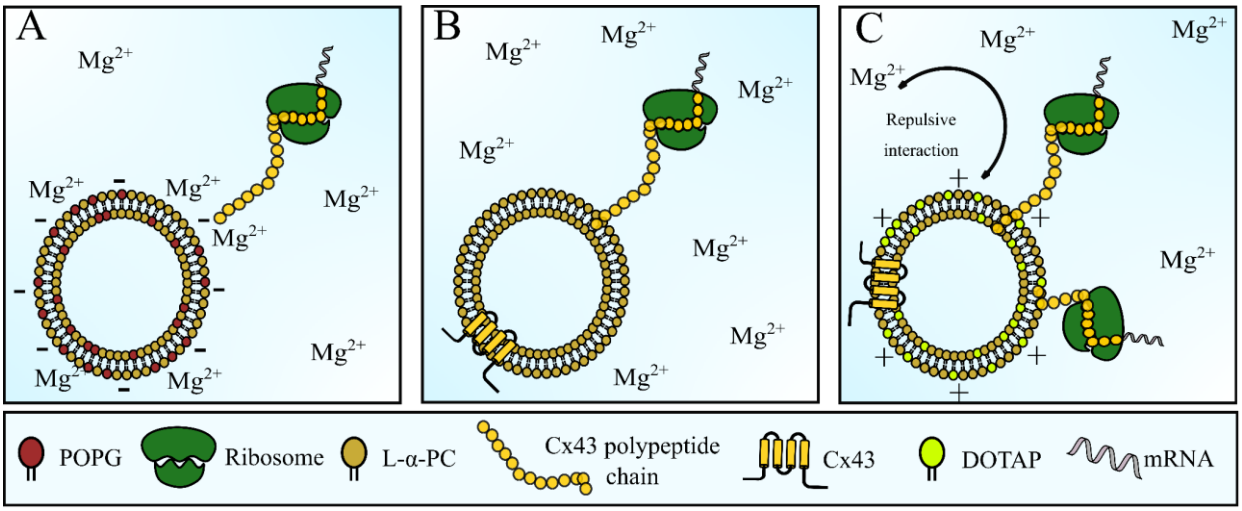

Figure 5-1. Hypothesis of the possible role of Mg^{2+} on the incorporation of Cx43 in bilayers of different charges. A) Liposomes composed of L-α-PC: POPG: TxR showing the possible masking effect of Mg^{2+} over the negative charges in the liposomes, thus, preventing insertion of Cx43 and reducing its reconstitution efficiency in those liposomes. B) Liposomes composed of L-α-PC: TxR showing the insertion of Cx43 as it is synthesized. C) Liposomes composed of L-α-PC: DOTAP: TxR showing an ease interaction of Cx43 with the liposomes as Mg^{2+} is repealed by electrostatic interactions.

On the other hand, changing the composition of the matrix lipid in the vesicles to DOPC: TxR at 3 mg/mL (~3.82 mM) registered a 43 % insertion of Cx43, which is in agreement with findings in literature when using the same lipid composition and concentration [25]. When changing the composition of the vesicle to DPhPC: Chol: TxR at 3 mg/mL (~3.55 mM), the percentage of insertion for Cx43 was 84 %, showing the highest amount of insertion for all three lipid compositions tested. This observation could be explained by the analysis in the lipid composition of gap junction preparations isolated from different cell types, which have revealed a substantial enrichment of the relative cholesterol to phospholipid ratio, suggesting that cholesterol plays an important in the assembly and function of gap junctions [28,100,101]. Moreover, several connexin isoforms (including Cx43) have been shown to preferentially associate in caveolin-containing rafts which are specialized invaginations in the plasma membrane rich in cholesterol [100]. This result suggests that addition of cholesterol to liposomes might be advantageous to further increase the reconstitution efficiency of Cx43 in artificial membranes. Nevertheless, it is recommended to repeat experiments with this lipid composition to test the hypothesis and findings from this project. It is worth mentioning that the analysis of reconstitution efficiency of Cx43 in vesicles containing DPhPC: Chol: TxR was the product of

a single determination given that obtaining Western Blot membranes for this composition was challenging.

Using vesicles with L-α-PC: DOTAP: TxR seemed the optimal lipid composition to insert Cx43 into membranes. Nevertheless, adding vesicles of DOPC or DPhPC: Chol showed the versatility of the system and its potential use in experiments for further applications. Some membrane proteins require specific lipid composition for unassisted integration into the artificial membranes as is the case for bacteriorhodopsin [22] or the mitochondrial ADP/ATP Carrier [24], while others do not discriminate about the lipid composition of the artificial membranes to insert [25]. Our findings suggest and corroborate that Cx43 does not discriminate about the lipid composition of the vesicles, but rather its insertion is favored by the presence of lipid mixtures that resemble those in natural membranes as reported previously [26,33].

5.3 Localization of Cx43 proteoliposomes in the purified fractions

In this project, the localization of the purified fractions for C- or N- EGFP Cx43 proteoliposomes was achieved by two approaches, *via* Western Blot or fluorescence spectroscopy. The expression of both Cx43 variants was also successful in the presence of vesicles of L-α-PC: DOTAP: TxR (at 3 mg/mL, 100 nm size). Western Blot analysis revealed that the percentage of insertion for Cx43 was 76 %, 80 % and 64 % for WT-, C- & N-EGFP Cx43, respectively. On the other hand, localization of the purified proteoliposomes *via* fluorescence spectroscopy showed that up to 62 % of C-EGFP Cx43 was inserted into the artificial membranes, while 50 % of the total amount of N-EGFP Cx43 was incorporated into the vesicles. Interestingly, the amount of inserted C-EGFP Cx43 in artificial membranes was higher than for N-EGFP Cx43 despite of the method used. Both analytical methods are sensitive enough to recognize the presence of EGFP-Cx43. Nevertheless, fluorescence spectroscopy seems to be more precise to quantify the amount of protein and vesicles present in each fraction after DGC since it directly measures the emission signal of the fluorescent probes after the excitation at a specific wavelength. The evaluation of the amount of inserted protein by Western Blot can be subjected to interference due to the high affinity of nitrocellulose membranes. Even so, Western Blot has been the method of choice to evaluate the amount of synthesized protein when those are not coupled with fluorescent tags [25,27,33].

The differences in the amount of inserted C- & N-EGFP Cx43 into the membranes of the vesicles, could be explained by their hydrophobicity. It has been reported that membrane proteins with a large hydrophilic domains cannot be properly insert into the membrane of vesicles [13,94]. Thus, the presence of the EGFP sequence in the Cx43 variants is expected to change the hydrophobicity of the protein [102,103]. To check this, the GRAVY values of all Cx43 variants were calculated using the *ProtParam* tool from *Expasy* [98,99], which is a measure of the hydrophobicity (or hydrophilicity) of a protein based on its amino acid sequence [98,99,104]. The GRAVY values are obtained from the sum of hydropathy scores of all amino acids divided by the number of residues in the protein sequence, which typically ranges from -2 to +2 [104]. These are descriptive relative values useful to predict and compare properties of proteins, but it does not determine the folding process that a membrane proteins follows to insert into lipid bilayer since that process is governed by the nature of the hydrophobic amino acid residues [102,104] . The GRAVY values for protein variants evaluated in this project were -0.266 for WT Cx43, -0.346 for C-EGFP Cx43, and -0.386 for N-EGFP Cx43. This indicates that the hydrophobicity of Cx43 was indeed affected by the presence of EGFP in the protein sequence, making C- and N-EGFP Cx43 less hydrophobic than the WT version since positively rated proteins are an indication of their hydrophobic character [102,104]. The change in the hydrophobicity of N-EGFP Cx43 might be the reason why this variant displays a lower reconstitution efficiency into membranes when compared to C-EGFP and WT Cx43. In cell-free systems, the mechanism of insertion of membrane proteins into vesicles has not been clearly elucidated. Yet, it has been proposed that in presence of liposomes the insertion of polypeptide chains initially takes place, followed by the formation of the secondary and tertiary structures within the lipid membrane [105]. Hence, when the hydrophobic nature of a membrane protein changes, its reconstitution efficiency into lipid bilayers might be affected as our findings suggest.

5.4 Characterization of Cx43 proteoliposomes

5.4.1 Orientation of Cx43 in the vesicles

The configuration that a membrane protein adopts when inserted into artificial membranes is of great importance for further applications. By exploiting the feature of N-EGFP Cx43 of having a *Tobacco Etch Virus* (TEV) sequence, the orientation that the protein adopted when inserted in the membrane of the vesicles could be analyzed. This sequence was in the plasmid at the N-terminal domain between the Cx43 and EGFP sequences. A successful cleavage of the protein would have resulted in two fragments, one corresponding to Cx43 with an approximate molecular mass of 43 kDa and the other of ~26 kDa corresponding to the EGFP fragment. Unfortunately, no cleavage of N-EGFP Cx43 could be observed when incubated with TEV regardless of the conditions used. On the other hand, a control assay with Ezrin revealed that the TEV enzyme was active, and that conditions tested were optimal for proteolytic cleavage. These findings suggest that the TEV site was probably not accessible in the protein. To resolve this issue, the addition of several glycine residues between the Cx43 and TEV sequence could be advantageous for the cleavage assays as reported by Sarpong & Bose [106]. In literature, the orientation of Cx43 has been investigated by a protease protection assay in combination with immunoprecipitation [25,33]. These assays revealed that cotranslational expression of Cx43 in presence of microsomes [33] or liposomes [25] exposed the C- & N-terminal domains as well as the extracellular loops to the outside of the liposomes. This outside-out configuration of Cx43 is in accordance with the native orientation that it adopts in microsomes from the endoplasmic reticulum in living cells when being transported to the plasma membranes [33].

5.4.2 Functional analysis of Cx43

The experiments presented in this manuscript provide evidence that Cx43 can be successfully inserted into artificial membranes of different compositions in a cell-free manner. In the experimental design, Cx43 proteoliposomes were planned to act as carriers to deliver the protein into the planar bilayer system by charged-mediated fusion. Unfortunately, the functional analysis of the purified Cx43 proteoliposomes was not successful. As explained before, the presence of negative charges in the system (POPG) might have influenced the outcome since

the abundant amounts of Mg^{2+} in the PURE cell-free system could trigger aggregation of anionic liposomes [13].Nevertheless, in the experiments presented in this project, the negative charges were part of the planar lipid bilayer which was prepared independently from the proteoliposomes. Additionally, proteoliposomes were purified by density gradient centrifugation prior to the single-channel experiments to ensure the presence of the proteoliposomes and avoid interference. Under our expression conditions, Cx43 was produced in a dephosphorylated state, thus, as an open pore [25,35,107] which could have led to the incorporation of Mg^{2+} or other charged small molecules into the vesicles, and might have resulted in the noisy interference observed.

The pioneering study of Falk and colleagues demonstrated the functionality of Cx43 expressed in a cell-free manner in presence of microsomes. In that study, the single-channel activity of Cx43, Cx32, and Cx26 was elucidated by the planar lipid membrane method [34]. Other studies have used the cell-free technology to express and incorporate protein channels into nanodiscs [108,109], liposomes [108], or microsomes [110] to deliver them into the planar bilayers or by direct bilayer incorporation into droplet-in-oil mixtures [111] for single-channel analysis. Thus, the experimental design presented here seemed appropriate to test the functionality of Cx43 embedded in the membranes of the vesicles. Interestingly in other studies, the function of Cx43 expressed *in vitro* had been carried out using different methods, like dye transfer [26,27] or quenching assays [25], probably because they are easier to perform. Future experiments to check Cx43 function when expressed using the cell-free technology might benefit from the usage of a eukaryotic system which can ensure post-translational modifications of the protein as well as using nanodiscs instead of liposomes to deliver the protein into the planar system.

5.5 Incorporation of Cx43 into giant unilamellar vesicles

Incorporation of EGFP-Cx43 into giant vesicles was possible. Nevertheless, the reproducibility of the experiments to monitor protein insertion in the membrane of the vesicles was difficult to accomplish. Our findings suggest that the integrity of giant unilamellar vesicles (GUVs) might have been affected by an osmotic imbalance between the sucrose solution contained in the GUVs and the osmolarity from the PURExpress® system, from which there is no report from the manufacturer. The size of the GUVs changed upon incubation with the cell-free reaction

mixture, which led to the localization of vesicles forming aggregates even in the absence of the DNA template. Another reason for the disruption and aggregation of these vesicles could be the interaction of the vesicles with the components of the PURExpress® system (*e.g.,* ribosomes or other big enzymes) since purification of the proteoliposomes did not occur in these experiments.

We found that the amount of Cx43 in vesicles decreases with an increment in the size of the vesicles which is in agreement with the results of Moritani and colleagues [25]. They suggest that adding smaller vesicles to the cell-free reaction enhances the insertion of the protein since they have a larger total surface area because of the larger curvature, which increases the probability of interactions between the protein and vesicles [25]. In literature, the incorporation of Cx43-GFP into vesicles and its analysis by confocal microscopy has also been reported [25–27,35]. The preparation of giant vesicles has been consequently accomplished by natural swelling, either prior to the expression step [25,26] or simultaneously in presence of the CFE reaction to carry out the production of protein and vesicles at the same time [27,35]. Localization of Cx43-GFP in GUVs membranes had been shown as complementary information to corroborate the insertion of the protein, but no further characterization of the Cx43-functionalized GUVs or usage of those structures are shown. In this project, the simultaneous production of Cx43 and GUVs by natural swelling was also tested, which showed the insertion of Cx43 into multilamellar membranes.

In this project, we have shown the possibilities of expressing Cx43 *in vitro* and directly inserting it into artificial membranes of different compositions. Cell-free systems provide a flexible platform for the synthesis of Cx43 for further applications. The knowledge gathered from this project can be used and further optimized to obtain GUVs functionalized with Cx43 in a reproducible manner that allows the establishment of an artificial transport system through the gap junction channels. As the amount of Cx43 inserted into LUVs is higher in L-α-PC: DOTAP: TxR membranes and consistent, these proteoliposomes could be used in combination with droplet-in-oil methods to produce GUVs [112–115] containing Cx43 exposing the extracellular loops to the outside of the vesicles, so gap junctions could be potentially established. Assuming that posttranslational modifications are present in proteoliposomes containing Cx43, it could be possible to study the transport of small molecules by changing the pH of the solution in microfluidic trap chambers [116] to gain information about the function of both the connexons and gap junction channels.

6. Conclusion

Implementation of the cell-free technology has enabled the reconstitution of complex functions from purified components to build minimal cells [1]. In that context, the current project aimed to reconstitute connexin 43 (Cx43) into artificial membranes as a potential system to mimic cell-to-cell communication. In synthetic biology, cellular communication has been studied by establishing a chemical communication system through diffusible inducer molecules between bacterial and artificial cells [117–119]. On the other hand, the ability of Cx43 to form gap junctions has also been exploited to exchange molecules between artificial and cultured cells expressing Cx43 [26,27].

In this project, we expressed Cx43 *in vitro* and directly inserted it into artificial membranes of different compositions. The insertion of Cx43 was favored by the presence of lipid mixtures that resemble the composition of natural membranes, as it was the case when liposomes were composed of L-α-PC: DOTAP: TxR or when cholesterol was present. The amount of inserted Cx43 into membranes of DOPC: TxR was lower (~43 %; N= 1) in comparison to membranes containing L-α-PC: DOTAP: TxR (~76 %; N= 3) or DPhPC: Chol: TxR (~84 %; N= 1). Being able to regulate the insertion of Cx43 into artificial membranes could be advantageous for functional studies, either to study the transport properties of Cx43 as a single channel (*e.g.,* by electrophysiological measurements) or as an ensemble, forming gap junctions (*e.g.,* dye-transfer assays).

The analysis of WT, C- & N-EGFP Cx43 proteoliposomes revealed that these structures could be purified by density gradient centrifugation (DGC) and used for further applications. The presence of the EGFP tag along the sequence of Cx43 modified the hydrophobicity of the C- & N-EGFP Cx43. The percentage of insertion of Cx43 into artificial membranes changed from 76 % for WT Cx43 to 80 % or 64 % for C- & N-EGFP Cx43, respectively. This information is essential since the presence EGFP could modify the functional behavior of Cx43 as it has been reported previously [92]. Carnarius and colleagues demonstrated that the presence of an GFP sequence at the C-terminal domain of Cx43, changed the conductance as well as the open probability of the pore [92].

Incorporating C- & N- EGFP Cx43 into GUVs was successfully achieved, but reproducibility of these results could be further improved. To avoid an osmotic imbalance between the inner and outer solution of the vesicles, the preparation of GUVs could be optimized using the natural swelling procedure since the composition of the inner and outer solution would be exact. Thus, preventing the establishment of gradients and osmotic imbalance. Another possibility to incorporate Cx43 into GUVs could be to encapsulate the cell-free components in double emulsions (water-in-oil-in-water droplets) [120,121] since the method provides a homogeneous distribution of the vesicle size and more control over the expression conditions of Cx43.

With this model system in hand, a possible next step could be the addition of enzymes to the cell-free reaction that would allow posttranslational modifications of Cx43. Hence, the control over the gating properties of Cx43 in artificial systems could be assessed, *e.g.,* by changing the pH of the solution. Optimizing the conditions to insert Cx43 into GUVs could lead to the analysis of the direct interaction between minimal cells through the gap junction system. These artificial intercellular connections (gap junctions) could be studied by using microfluidic trapping chambers [116] to allow the encounter of two populations of proteoliposomes encapsulating different dyes. This project has opened the way for the usage of cell-free technology in bottom-up approaches to study membrane proteins and their applications in the research group. Even though, optimization of the conditions for protein expression is still required, we have found a reliable approach to obtain Cx43 proteoliposomes by providing LUVs in the cell-free reaction mixture.

7. Bibliography

1. Jia, H., Heymann, M., Bernhard, F., Schwille, P. & Kai, L. Cell-free protein synthesis in micro compartments: building a minimal cell from biobricks. *New Biotechnology* **39**, 199–205 (2017).
2. Katzen, F., Peterson, T. C. & Kudlicki, W. Membrane protein expression: no cells required. *Trends in Biotechnology* **27**, 455–460 (2009).
3. Andrianantoandro, E., Basu, S., Karig, D. K. & Weiss, R. Synthetic biology: new engineering rules for an emerging discipline. *Molecular Systems Biology* **2**, 2006.0028 (2006).
4. Forster, A. C. & Church, G. M. Synthetic biology projects in vitro. *Genome Res.* **17**, 1–6 (2007).
5. Luisi, P. L., Ferri, F. & Stano, P. Approaches to semi-synthetic minimal cells: a review. *Naturwissenschaften* **93**, 1–13 (2006).
6. Noireaux, V., Maeda, Y. T. & Libchaber, A. Development of an artificial cell, from self-organization to computation and self-reproduction. *PNAS* **108**, 3473–3480 (2011).
7. Perez, J. G., Stark, J. C. & Jewett, M. C. Cell-Free Synthetic Biology: Engineering Beyond the Cell. *Cold Spring Harb Perspect Biol* **8**, a023853 (2016).
8. Tinafar, A., Jaenes, K. & Pardee, K. Synthetic Biology Goes Cell-Free. *BMC Biology* **17**, 64 (2019).
9. Yue, K., Zhu, Y. & Kai, L. Cell-Free Protein Synthesis: Chassis toward the Minimal Cell. *Cells* **8**, 315 (2019).
10. Katzen, F., Chang, G. & Kudlicki, W. The past, present and future of cell-free protein synthesis. *Trends Biotechnol.* **23**, 150–156 (2005).

11. Shimizu, Y. *et al.* Cell-free translation reconstituted with purified components. *Nature Biotechnology* **19**, 751–755 (2001).
12. Shimizu, Y., Kanamori, T. & Ueda, T. Protein synthesis by pure translation systems. *Methods* **36**, 299–304 (2005).
13. Kuruma, Y. & Ueda, T. The PURE system for the cell-free synthesis of membrane proteins. *Nat Protoc* **10**, 1328–1344 (2015).
14. Kuruma, Y., Nishiyama, K., Shimizu, Y., Müller, M. & Ueda, T. Development of a Minimal Cell-Free Translation System for the Synthesis of Presecretory and Integral Membrane Proteins. *Biotechnology Progress* **21**, 1243–1251 (2005).
15. Schwarz, D., Dötsch, V. & Bernhard, F. Production of membrane proteins using cell-free expression systems. *PROTEOMICS* **8**, 3933–3946 (2008).
16. Rigaud, J.-L. & Lévy, D. Reconstitution of Membrane Proteins into Liposomes. in *Methods in Enzymology* vol. 372 65–86 (Academic Press, 2003).
17. Sachse, R., Dondapati, S. K., Fenz, S. F., Schmidt, T. & Kubick, S. Membrane protein synthesis in cell-free systems: From bio-mimetic systems to bio-membranes. *FEBS Letters* **588**, 2774–2781 (2014).
18. Klammt, C. *et al.* Cell-free expression as an emerging technique for the large scale production of integral membrane protein. *FEBS Journal* **273**, 4141–4153 (2006).
19. Klammt, C. *et al.* Evaluation of detergents for the soluble expression of α-helical and β-barrel-type integral membrane proteins by a preparative scale individual cell-free expression system. *The FEBS Journal* **272**, 6024–6038 (2005).
20. Nomura, S. M. *et al.* Direct preparation of giant proteo-liposomes by in vitro membrane protein synthesis. *Journal of Biotechnology* **133**, 190–195 (2008).

21. Hovijitra, N. T., Wuu, J. J., Peaker, B. & Swartz, J. R. Cell-free synthesis of functional aquaporin Z in synthetic liposomes. *Biotechnology and Bioengineering* **104**, 40–49 (2009).

22. Kalmbach, R. *et al.* Functional Cell-free Synthesis of a Seven Helix Membrane Protein: In situ Insertion of Bacteriorhodopsin into Liposomes. *J. Mol. Biol.* **371**, 639–648 (2007).

23. Matthies, D. *et al.* Cell-Free Expression and Assembly of ATP Synthase. *J. Mol. Biol.* **413**, 593–603 (2011).

24. Long, A. R., O'Brien, C. C. & Alder, N. N. The Cell-Free Integration of a Polytopic Mitochondrial Membrane Protein into Liposomes Occurs Cotranslationally and in a Lipid-Dependent Manner. *PLoS ONE* **7**, e46332 (2012).

25. Moritani, Y., Nomura, S. M., Morita, I. & Akiyoshi, K. Direct integration of cell-free-synthesized connexin-43 into liposomes and hemichannel formation: Direct integration of connexin-43 into liposomes. *FEBS Journal* **277**, 3343–3352 (2010).

26. Lu, M. *et al.* Cell-free synthesis of connexin 43-integrated exosome-mimetic nanoparticles for siRNA delivery. *Acta Biomater.* S1742706119304866 (2019) doi:10.1016/j.actbio.2019.07.006.

27. Kaneda, M. *et al.* Direct formation of proteo-liposomes by in vitro synthesis and cellular cytosolic delivery with connexin-expressing liposomes. *Biomaterials* **30**, 3971–3977 (2009).

28. Sosinsky, G. E. & Nicholson, B. J. Structural organization of gap junction channels. *Biochimica et Biophysica Acta (BBA) - Biomembranes* **1711**, 99–125 (2005).

29. Loewenstein, W. R. Junctional intercellular communication: the cell-to-cell membrane channel. *Physiol. Rev.* **61**, 829–913 (1981).

30. Goodenough, D. A. & Paul, D. L. Gap Junctions. *Cold Spring Harb Perspect Biol* **1**, a002576 (2009).

31. Ribeiro-Rodrigues, T. M., Martins-Marques, T., Morel, S., Kwak, B. R. & Girão, H. Role of connexin 43 in different forms of intercellular communication – gap junctions, extracellular vesicles and tunnelling nanotubes. *J. Cell Sci.* **130**, 3619–3630 (2017).

32. Duffy, H. S. *et al.* pH-Dependent Intramolecular Binding and Structure Involving Cx43 Cytoplasmic Domains. *J. Biol. Chem.* **277**, 36706–36714 (2002).

33. Falk, M. M., Kumar, N. M. & Gilula, N. B. Membrane insertion of gap junction connexins: polytopic channel forming membrane proteins. *Journal of Cell Biology* **127**, 343–355 (1994).

34. Falk, M. M., Buehler, L. K., Kumar, N. M. & Gilula, N. B. Cell-free synthesis and assembly of connexins into functional gap junction membrane channels. *EMBO J.* **16**, 2703–2716 (1997).

35. Liu, Y.-J., Hansen, G. P. R., Venancio-Marques, A. & Baigl, D. Cell-Free Preparation of Functional and Triggerable Giant Proteoliposomes. *ChemBioChem* **14**, 2243–2247 (2013).

36. Bruzzone, R., White, T. W. & Goodenough, D. A. The cellular internet: On-line with connexins. *BioEssays* **18**, 709–718 (1996).

37. Hodgman, C. E. & Jewett, M. C. Cell-free synthetic biology: Thinking outside the cell. *Metabolic Engineering* **14**, 261–269 (2012).

38. Lampe, P. D. & Lau, A. F. Regulation of Gap Junctions by Phosphorylation of Connexins. *Arch. Biochem. Biophys.* **384**, 205–215 (2000).

39. Bertero, A., Brown, S. & Vallier, L. Methods of Cloning - ScienceDirect. in *Basic Science Methods for clinical Researchers* 19–39 (Academic Press, 2017).

40. Celie, P. H., Parret, A. H. & Perrakis, A. Recombinant cloning strategies for protein expression. *Current Opinion in Structural Biology* **38**, 145–154 (2016).

41. Caetano-Anollés, D. Polymerase Chain Reaction. in *Brenner's Encyclopedia of Genetics (Second Edition)* (eds. Maloy, S. & Hughes, K.) 392–395 (Academic Press, 2013). doi:10.1016/B978-0-12-374984-0.01186-4.

42. Gibson, D. G. Chapter fifteen - Enzymatic Assembly of Overlapping DNA Fragments. in *Methods in Enzymology* (ed. Voigt, C.) vol. 498 349–361 (Academic Press, 2011).

43. Aslanidis, C. & de Jong, P. J. Ligation-independent cloning of PCR products (LIC-PCR). *Nucleic Acids Research* **18**, 6069–6074 (1990).

44. Thermo Fisher Scientific. GeneArt Gibson Assebly HiFi Cloning Kits: USer Guide. (2020).

45. Invitrogen. S.O.C Medium- Information for User. (2002).

46. Birnboim, H. C. & Doly, J. A rapid alkaline extraction procedure for screening recombinant plasmid DNA. *Nucleic Acids Research* **7**, 1513–1523 (1979).

47. Barrow, D. A. & Lentz, B. R. Large vesicle contamination in small, unilamellar vesicles. *Biochimica et Biophysica Acta (BBA) - Biomembranes* **597**, 92–99 (1980).

48. Olson, F., Hunt, C. A., Szoka, F. C., Vail, W. J. & Papahadjopoulos, D. Preparation of liposomes of defined size distribution by extrusion through polycarbonate membranes. *Biochimica et Biophysica Acta (BBA) - Biomembranes* **557**, 9–23 (1979).

49. Angelova, M. I. & Dimitrov, D. S. Liposome electroformation. *Faraday discussions of the Chemical Society* **81**, 303–311 (1986).

50. Lefrançois, P., Goudeau, B. & Arbault, S. Electroformation of phospholipid giant unilamellar vesicles in physiological phosphate buffer. *Integrative Biology* **10**, 429–434 (2018).

51. Reeves, J. P. & Dowben, R. M. Formation and properties of thin-walled phospholipid vesicles. *Journal of Cellular Physiology* **73**, 49–60 (1969).

52. Bell, R. D. & Doisy, E. A. RAPID COLORIMETRIC METHODS FOR THE DETERMINATION OF PHOSPHORUS IN URINE AND BLOOD. *Journal of Biological Chemistry* **44**, 55–67 (1920).

53. Fiske, C. H. & Subbarow, Y. THE COLORIMETRIC DETERMINATION OF PHOSPHORUS. *Journal of Biological Chemistry* **66**, 375–400 (1925).

54. Harris, W. D. & Popat, P. Determination of the phosphorus content of lipids. *J Am Oil Chem Soc* **31**, 124–127 (1954).

55. Murphy, J. & Riley, J. P. A modified single solution method for the determination of phosphate in natural waters. *Analytica Chimica Acta* **27**, 31–36 (1962).

56. John, M. Colorimetric determination of phosphorus in soil and plant materials with ascorbic acid. *Soil Science* **109**, 214–220 (1968).

57. Nourian, Z. Towards the assembly of a minimal oscillator: Genetic networks in liposomes. (Technische Universiteit Delf, 2015).

58. New England Biolabs Inc. Protein expression & Analysis: PURExpress In Vitro Protein Synthesis- Instruction Manual. (2017).

59. Brakke, M. K. Density Gradient Centrifugation: A New Separation Technique [1]. *J. Am. Chem. Soc.* **73**, 1847–1848 (1951).

60. Brakke, M. K. Zonal separations by density-gradient centrifugation. *Archives of Biochemistry and Biophysics* **45**, 275–290 (1953).

61. Laemmli, U. K. Cleavage of Structural Proteins during the Assembly of the Head of Bacteriophage T4. *Nature* **227**, 680–686 (1970).

62. Schägger, H. & von Jagow, G. Tricine-sodium dodecyl sulfate-polyacrylamide gel electrophoresis for the separation of proteins in the range from 1 to 100 kDa. *Analytical Biochemistry* **166**, 368–379 (1987).

63. Schägger, H. Tricine–SDS-PAGE. *Nat. Protoc.* **1**, 16–22 (2006).

64. Brunelle, J. L. & Green, R. Chapter Thirteen - Coomassie Blue Staining. in *Methods in Enzymology* (ed. Lorsch, J.) vol. 541 161–167 (Academic Press, 2014).

65. Mahmood, T. & Yang, P.-C. Western Blot: Technique, Theory, and Trouble Shooting. *N Am J Med Sci* **4**, 429–434 (2012).

66. Hnasko, T. S. & Hnasko, R. M. The Western Blot. in *ELISA: Methods and Protocols* (ed. Hnasko, R.) 87–96 (Springer, 2015). doi:10.1007/978-1-4939-2742-5_9.

67. Kurien, B. & Scofield, R. Western blotting. *Methods* **38**, 283–293 (2006).

68. Ruf, H., Georgalis, Y. & Grell, E. [21] Dynamic laser light scattering to determine size distributions of vesicles. in *Methods in Enzymology* vol. 172 364–390 (Academic Press, 1989).

69. Stetefeld, J., McKenna, S. & Patel, T. Dynamic light scattering: a practical guide and applications in biomedical sciences. *Biophys Rev* 409–427 (2016) doi:DOI 10.1007/s12551-016-0218-6.

70. Pecora, R. *Dynamic Light Scattering: Applications of Photon Correlation Spectroscopy*. (Springer Science & Business Media, 2013).

71. Pecora, R. Dynamic Light Scattering Measurement of Nanometer Particles in Liquids. *Journal of Nanoparticle Research* **2**, 123–131 (2000).

72. Yadav, L. D. S. *Organic Spectroscopy*. (Springer-Science+ Business Media, B.V., 2005).

73. Gauglitz, G. Ultraviolet and Visible Spectroscopy. in *Handbook of Analytical Techniques* 419–463 (John Wiley & Sons, Ltd, 2001). doi:10.1002/9783527618323.ch16.

74. Förster, H. UV/VIS Spectroscopy. in *Molecular Sieves- Characterization I* vol. 4 337–426 (Springer-Verlag, 2004).

75. Tissue, B. Ultraviolet and Visible Absorption Spectroscopy. in *Characterization of Materials* vol. 1 2438 (John Wiley & Sons, Inc., 2012).

76. McGOWN, L. B. & Nithipatikom, K. MOLECULAR FLUORESCENCE AND PHOSPHORESCENCE. *Applied Spectroscopy Reviews* **35**, 353–393 (2000).

77. Lakowicz, J. R. *Principles of fluorescence spectroscopy*. (Springer, 2006).

78. Lichtman, J. W. & Conchello, J.-A. Fluorescence microscopy. *Nature methods* **2**, 910–919 (2005).

79. Naredi-Rainer, N., Prescher, J., Hartschuh, S. & Lamb, D. Confocal Microscopy. in *Fluorescence Microscopy: From principles to biological applications* (Wiley-VCH Verlag GmbH & Co. KGaA, 2017). doi:10.1002/9783527687732.

80. Földes-Papp, Z., Demel, U. & Tilz, G. Laser scanning confocal fluorescence microscopy: an overview. *Int. J. Immunopharmacol.* **3**, 1715–1729 (2003).

81. Labarca, P. & Latorre, R. Insertion of ion channels into planar lipid bilayers by vesicle fusion. in *Methods in Enzymology* vol. 207 447–463 (Elsevier, 1992).

82. White, S. The physical nature of planar bilayer membranes. in *Ion channel reconstitution* (Springer Science & Business Media New York, 1986).

83. Molecular Devices, LLC. *The Axon guide, electrophysiology and biophysics laboratory techniques*. (Sunnyvale, California: Molecular devices, 1993).

84. Kongsuphol, P., Fang, K. B. & Ding, Z. Lipid bilayer technologies in ion channel recordings and their potential in drug screening assay. *Sensors and Actuators B: Chemical* **185**, 530–542 (2013).

85. Mueller, P., Rudin, D. O., Tien, H. T. & Wescott, W. C. Methods for the formation of single bimolecular lipid membranes in aqueous solutions. *J. Phys. Chem.* **67**, 534–535 (1963).

86. Montal, M. Formation of bimolecular membranes from lipid monolayers. in *Methods in Enzymology* vol. 32 545–554 (Elsevier, 1974).

87. Montal, M. & Mueller, P. Formation of Bimolecular Membranes from Lipid Monolayers and a Study of Their Electrical Properties. *Proc. Natl. Acad. Sci. U.S.A.* **69**, 3561–3566 (1972).

88. Hanke, W. & Miller, C. Reconstitution of Ion Channel. *Critical Reviews in Biochemistry* **19**, 1–44 (1985).

89. Schindler, H. Formation of planar bilayers from artificial or native membrane vesicles. *FEBS Letters* **122**, 77–79 (1980).

90. Schindler, H. & Rosenbusch, J. P. Matrix protein from Escherichia coli outer membranes forms voltage-controlled channels in lipid bilayers. *PNAS* **75**, 3751–3755 (1978).

91. Baaken, G., Sondermann, M., Schlemmer, C., Rühe, J. & Behrends, J. C. Planar microelectrode-cavity array for high-resolution and parallel electrical recording of membrane ionic currents. *Lab Chip* **8**, 938 (2008).

92. Carnarius, C. *et al.* Green Fluorescent Protein Changes the Conductance of Connexin 43 (Cx43) Hemichannels Reconstituted in Planar Lipid Bilayers. *J. Biol. Chem.* **287**, 2877–2886 (2012).

93. Klammt, C. *et al.* High level cell-free expression and specific labeling of integral membrane proteins. *European Journal of Biochemistry* **271**, 568–580 (2004).

94. Niwa, T. *et al.* Comprehensive study of liposome-assisted synthesis of membrane proteins using a reconstituted cell-free translation system. *Sci Rep* **5**, 18025 (2015).

95. Rath, A., Glibowicka, M., Nadeau, V. G., Chen, G. & Deber, C. M. Detergent binding explains anomalous SDS-PAGE migration of membrane proteins. *Proc. Natl. Acad. Sci. U.S.A.* **106**, 1760–1765 (2009).

96. Angelova, M. & Dimitrov, D. S. A mechanism of liposome electroformation. in *Trends in Colloid and Interface Science II* (ed. Degiorgio, V.) vol. 76 59–67 (Steinkopff, 1988).

97. Stockert, R. J. *et al.* Deficient assembly and function of gap junctions in Trf1, a trafficking mutant of the human liver–derived cell line HuH-7. *Hepatology* **30**, 740–747 (1999).

98. Gasteiger, E. *et al.* Protein Identification and Analysis Tools on the ExPASy Server. in *The Proteomics Protocols Handbook* (ed. Walker, J. M.) 571–607 (Humana Press, 2005). doi:10.1385/1-59259-890-0:571.

99. Gasteiger, E. ExPASy: the proteomics server for in-depth protein knowledge and analysis. *Nucleic Acids Res.* **31**, 3784–3788 (2003).

100. Cascio, M. Connexins and their environment: effects of lipids composition on ion channels. *Biochimica et Biophysica Acta (BBA) - Biomembranes* **1711**, 142–153 (2005).

101. Henderson, D., Eibl, H. & Weber, K. Structure and biochemistry of mouse hepatic gap junctions. *Journal of Molecular Biology* **132**, 193–218 (1979).

102. Ki, M.-R. & Pack, S. P. Fusion tags to enhance heterologous protein expression. *Appl Microbiol Biotechnol* **104**, 2411–2425 (2020).

103. Xie, H., Guo, X.-M. & Chen, H. Making the Most of Fusion Tags Technology in Structural Characterization of Membrane Proteins. *Mol Biotechnol* **42**, 135–145 (2009).

104. Kyte, J. & Doolittle, R. F. A simple method for displaying the hydropathic character of a protein. *Journal of Molecular Biology* **157**, 105–132 (1982).

105. Baumann, A. *et al.* In-Situ Observation of Membrane Protein Folding during Cell-Free Expression. *PLOS ONE* **11**, e0151051 (2016).

106. Sarpong, K. & Bose, R. Efficient sortase-mediated N-terminal labeling of TEV protease cleaved recombinant proteins. *Analytical Biochemistry* **521**, 55–58 (2017).

107. Kim, D. Y., Kam, Y., Koo, S. K. & Joe, C. O. Gating Connexin 43 Channels Reconstituted in Lipid Vesicles by Mitogen-activated Protein Kinase Phosphorylation *. *Journal of Biological Chemistry* **274**, 5581–5587 (1999).

108. Dondapati, S. K., Wüstenhagen, D. A. & Kubick, S. Functional Analysis of Membrane Proteins Produced by Cell-Free Translation. in *Protein Engineering: Methods and Protocols* (eds. Bornscheuer, U. T. & Höhne, M.) 171–186 (Springer, 2018). doi:10.1007/978-1-4939-7366-8_10.

109. Winterstein, L.-M. *et al.* Reconstitution and functional characterization of ion channels from nanodiscs in lipid bilayers | Journal of General Physiology | Rockefeller University Press. https://rupress.org/jgp/article/150/4/637/43669/Reconstitution-and-functional-characterization-of (2018).

110. Rosenberg, R. L. & East, J. E. Cell-free expression of functional Shaker potassium channels. *Nature* **360**, 166–169 (1992).

111. S. Friddin, M. *et al.* Single-channel electrophysiology of cell-free expressed ion channels by direct incorporation in lipid bilayers. *Analyst* **138**, 7294–7298 (2013).

112. Weiss, M. *et al.* Sequential bottom-up assembly of mechanically stabilized synthetic cells by microfluidics. *Nature Materials* **17**, 89–96 (2018).

113. Göpfrich, K., Platzman, I. & Spatz, J. P. Mastering Complexity: Towards Bottom-up Construction of Multifunctional Eukaryotic Synthetic Cells. *Trends Biotechnol.* **36**, 938–951 (2018).

114. Haller, B. *et al.* Charge-controlled microfluidic formation of lipid-based single- and multicompartment systems. *Lab Chip* **18**, 2665–2674 (2018).

115. Göpfrich, K. *et al.* One-Pot Assembly of Complex Giant Unilamellar Vesicle-Based Synthetic Cells. *ACS Synth. Biol.* **8**, 937–947 (2019).

116. Robinson, T. Microfluidic Handling and Analysis of Giant Vesicles for Use as Artificial Cells: A Review. *Adv. Biosys.* 1800318 (2019) doi:10.1002/adbi.201800318.

117. Gardner, P. M., Winzer, K. & Davis, B. G. Sugar synthesis in a protocellular model leads to a cell signalling response in bacteria. *Nature Chem* **1**, 377–383 (2009).

118. Lentini, R. *et al.* Integrating artificial with natural cells to translate chemical messages that direct E. coli behaviour. *Nat Commun* **5**, 4012 (2014).

119. Weitz, M. *et al.* Communication and Computation by Bacteria Compartmentalized within Microemulsion Droplets. *J. Am. Chem. Soc.* **136**, 72–75 (2014).

120. Gonzales, D. T., Yandrapalli, N., Robinson, T., Zechner, C. & Tang, T.-Y. D. Cell-Free Gene Expression Dynamics in Synthetic Cell Populations. *ACS Synth. Biol.* acssynbio.1c00376 (2022) doi:10.1021/acssynbio.1c00376.

121. Robinson, A. O., Venero, O. M. & Adamala, K. P. Toward synthetic life: Biomimetic synthetic cell communication. *Current Opinion in Chemical Biology* **64**, 165–173 (2021).

8. Appendix

8.1 Primer sequences used for the construction of Cx43 plasmids containing EGFP

Table 8-1. Sequence of primers used for LIC-PCR for customization of the N-EFGP Cx43 plasmid.

Primer name	Sequence
Forward (LIC) primer	TACTTCCAATCCAATGCAAATAATGAATTCGAAACGATGGGTGACTGGAG
Reverse (LIC) primer	CTCCCACTACCAATGCCATATATTCTAGAATCTCCAGGTCATCAGGCCGA

Table 8-2. Sequence of primers used for Gibson Assembly for the production of C-EGFP Cx43 plasmid.

Primer name	Sequence
Forward (Gibson) primer	TCGGCCTGATGACCTGGAGATTCTAGAATATATACTCGAGGTGAGCAAGGGCGAGGAGCTGTTCACCG
Reverse (Gibson) primer	GTTTAGAGGCCCCAAGGGGTTATGCTAGTTATTGCTCAGCCTTGTACAGCTCGTCCATGCCGAGAGTGATCCCG

GeneArt Gibson Assembly HiFi Cloning Kit by Invitrogen

To calculate the equimolar concentration of DNA insert and vector for the Gibson Assembly in 3.2.1.2, the formula in Equation 8-1 was used.

Equation 8-1

$$pmoles \approx \frac{(weigth\ in\ ng) \cdot 1000}{(fragment\ length\ in\ bp) \cdot 660}$$

8.2 Amino acid sequences of Cx43 protein variants

Table 8-3. Amino acid sequence for Cx43 variants: WT, C- & N-EGFP Cx43.

Protein variant	Amino acid sequence of the translated product
WT Cx43	MGNNEFETMGDWSALGKLLDKVQAYSTAGGKVWLSVLFIFRILLLGTA VESAWGDEQSAFRCNTQQPGCENVCYDKSFPISHVRFWVLQIIFVSVPTL LYLAHVFYVMRKEEKLNKKEEELKVAQTDGVNVEMHLKQIEIKKFKY GIEEHGKVKMRGGLLRTYIISILFKSVFEVAFLLIQWYIYGFSLSAVYTCK RDPCPHQVDCFLSRPTEKTIFIIFMLVVSLVSLALNIIELFYVFFKGVKDR VKGRSDPYHATTGPLSPSKDCGSPKYAYFNGCSSPTAPLSPMSPPGYKL VTGDRNNSSCRNYNKQASEQNWANYSAEQNRMGQAGSTISNSHAQPF DFPDDSQNAKKVAAGHELQPLAIVDQRPSSRASSRASSRPRPDDLEILEY ILEHHHHHH*
C-EGFP Cx43	MGNNEFETMGDWSALGKLLDKVQAYSTAGGKVWLSVLFIFRILLLGTA VESAWGDEQSAFRCNTQQPGCENVCYDKSFPISHVRFWVLQIIFVSVPTL LYLAHVFYVMRKEEKLNKKEEELKVAQTDGVNVEMHLKQIEIKKFKY GIEEHGKVKMRGGLLRTYIISILFKSVFEVAFLLIQWYIYGFSLSAVYTCK RDPCPHQVDCFLSRPTEKTIFIIFMLVVSLVSLALNIIELFYVFFKGVKDR VKGRSDPYHATTGPLSPSKDCGSPKYAYFNGCSSPTAPLSPMSPPGYKL VTGDRNNSSCRNYNKQASEQNWANYSAEQNRMGQAGSTISNSHAQPF DFPDDSQNAKKVAAGHELQPLAIVDQRPSSRASSRASSRPRPDDLEILEY ILEVSKGEELFTGVVPILVELDGDVNGHKFSVRGEGEGDATNGKLTLKFI CTTGKLPVPWPTLVTTLTYGVQCFSRYPDHMKQHDFFKSAMPEGYVQE RTISFKDDGTYKTRAEVKFEGDTLVNRIELKGIDFKEDGNILGHKLEYNF NSHNVYITADKQKNGIKANFKIRHNVEDGSVQLADHYQQNTPIGDGPV LLPDNHYLSTQSKLSKDPNEKRDHMVLLEFVTAAGITLGMDELYKAEQ *
N-EGFP Cx43	MGSSHHHHHHGSSVSKGEELFTGVVPILVELDGDVNGHKFSVRGEGEG DATNGKLTLKFICTTGKLPVPWPTLVTTLTYGVQCFSRYPDHMKQHDFF KSAMPEGYVQERTISFKDDGTYKTRAEVKFEGDTLVNRIELKGIDFKED GNILGHKLEYNFNSHNVYITADKQKNGIKANFKIRHNVEDGSVQLADH YQQNTPIGDGPVLLPDNHYLSTQSKLSKDPNEKRDHMVLLEFVTAAGIT LGMDELYKGIEENLYFQSNYFQSNANNEFETMGDWSALGKLLDKVQA YSTAGGKVWLSVLFIFRILLLGTAVESAWGDEQSAFRCNTQQPGCENVC YDKSFPISHVRFWVLQIIFVSVPTLLYLAHVFYVMRKEEKLNKKEEELK VAQTDGVNVEMHLKQIEIKKFKYGIEEHGKVKMRGGLLRTYIISILFKSV FEVAFLLIQWYIYGFSLSAVYTCKRDPCPHQVDCFLSRPTEKTIFIIFMLV VSLVSLALNIIELFYVFFKGVKDRVKGRSDPYHATTGPLSPSKDCGSPKY AYFNGCSSPTAPLSPMSPPGYKLVTGDRNNSSCRNYNKQASEQNWANY SAEQNRMGQAGSTISNSHAQPFDFPDDSQNAKKVAAGHELQPLAIVDQ RPSSRASSRASSRPRPDDLEILEYMALVVGDWKWITDPNSSAVDKLAAA LEHHHHHH*

8.3 Supplemental figures to the Results section

Figures shown in this section are complementary to those shown in the Results part, section 4.

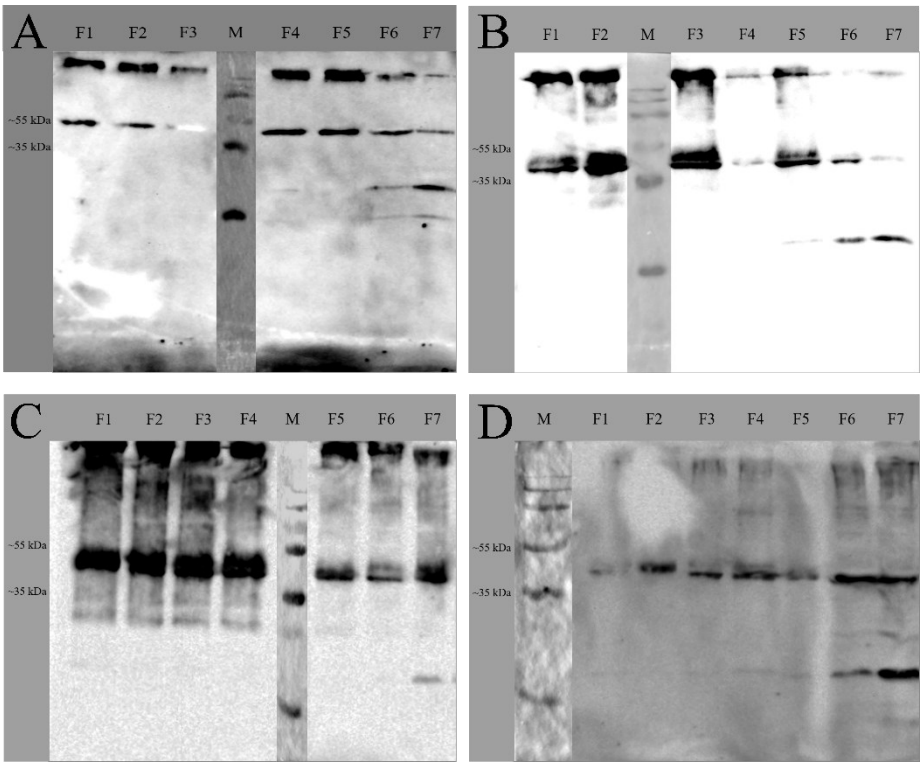

Figure 8-1. Western Blot images showing the effect of increasing the lipid concentration in the vesicles for the CFE reaction after DGC purification. A) 0.5 mg/mL; B) 1.5 mg/mL; C) 3 mg/mL; D) 5.5 mg/mL.

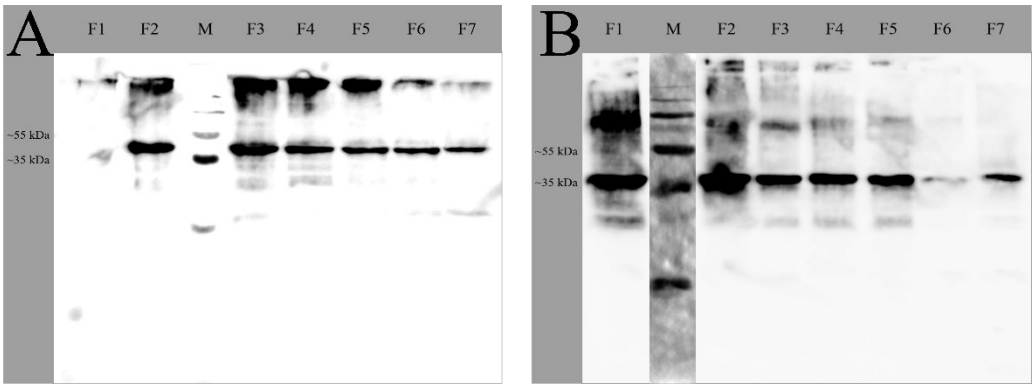

Figure 8-2. Comparison between two Western Blot membranes from proteoliposomes prepared with L-α-PC: DOTAP: Tx (89.5:10:0.5) at 3 mg/mL showing different protein intensity patterns in all collected fractions from DGC.

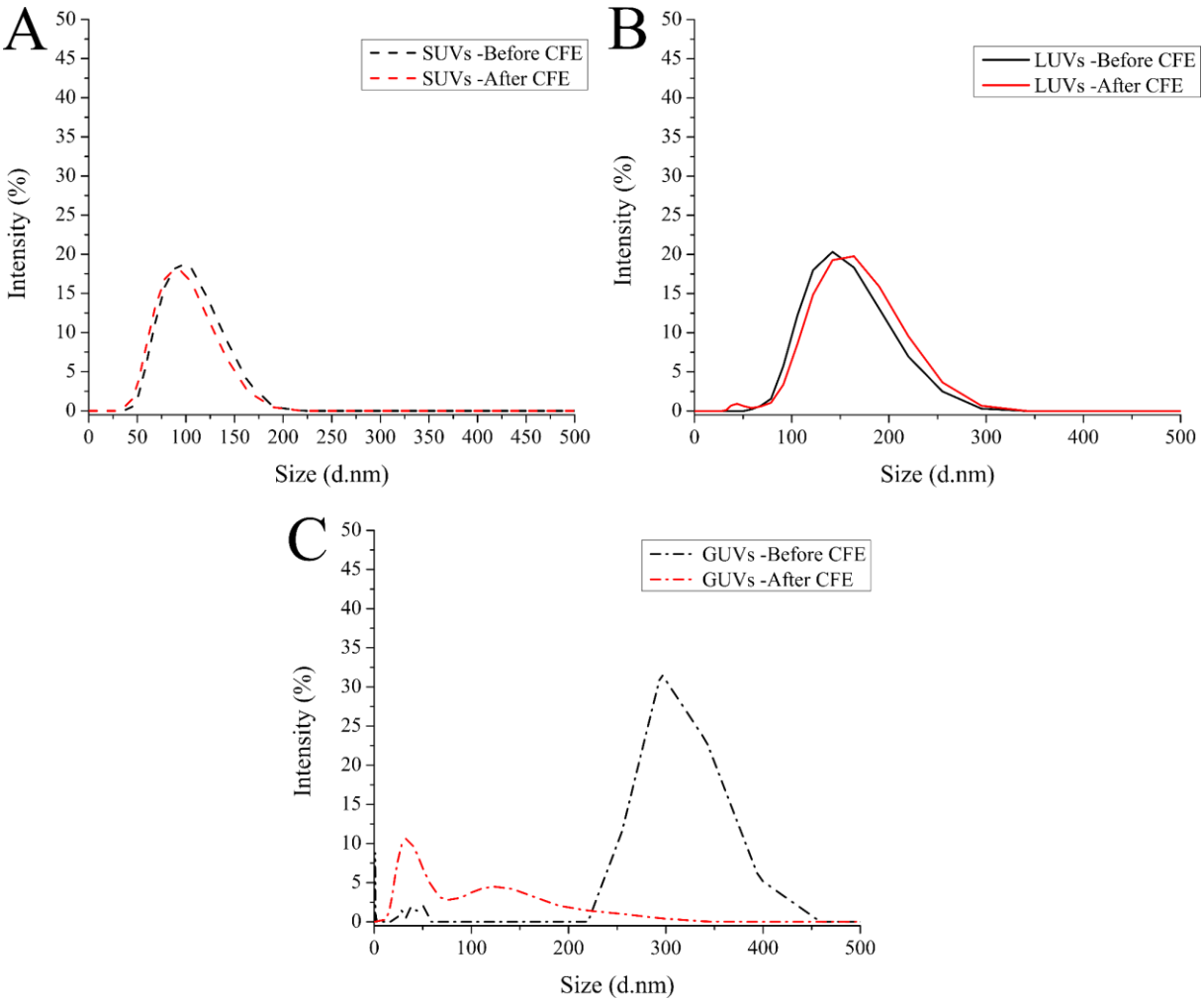

Figure 8-3. Size distribution of vesicles before and after addition to the CFE reaction by DLS. A) SUVs; B9 LUVs; C) GUVs. The distribution for SUVs and LUVs is monodisperse while for GUVs is polydisperse. DLS is not the appropriate method to evaluate GUVs but it is shown here for comparison purposes.

8.4 List of symbols and abbreviations

3D	three dimensional
APS	ammonium persulfate
aa	amino acid
c	concentration
CFE	cell-free expression
CLSM	confocal laser scanning microscopy
cm	centimeter
Cx43	connexin 43
d	diameter
DLS	dynamic light scattering
DOPC	1,2-dioleoyl-sn-glycero-3-phosphocholine
DOTAP	1,2-dioleoyloxy-3-trimethylammonium-propane
DPhPC	1,2-diphytanoyl-sn-glycero-3-phosphocholine
E. coli	*Escherichia coli*
e.g.	*exempli gratia*
GUV	giant unilamellar vesicle
His6	Hexa-histidine
HRP	horse radish peroxidase
Hz	Hertz
ITO	indium tin oxide
kB	Boltzmann constant
kDa	kilodalton
kg	kilogram
L	liter
LB-medium	lysogeny broth medium
LIC	Ligation independent cloning
LUV	large unilamellar vesicle
L-α-PC	L-α-phosphatidylcholine
M	molar
µm	micrometer
mg	milligram
min	minutes
mL	milliliter
mOsm	milliosmolar
MW	molecular weight
η	medium viscosity
nm	nanometer
OD260	optical thickness at 260 nm
pI	isoelectric point
POPC	1-palmitoyl-2-oleoyl-sn-glycero-3-phosphocholine
POPG	1-palmitoyl-2-oleoyl-sn-glycero-3-phospho-(1´-rac-glycerol)
PURE	Protein synthesis Using Recombinant Elements

R	hydrodynamic radius
ROI	region of interest
rpm	rounds per minute
RT	room temperature
s	seconds
S.O.C	super optimal broth with catabolite repression
SDS-PAGE	sodium dodecyl sulfate polyacrylamide gel electrophoresis
siRNA	small interfering RNA
St. Dev.	standard deviation
SUV	small unilamellar vesicle
TEMED	tetramethylethylenediamine
TM	transmembrane domain
TxR	Texas Red®
UV-Vis	ultraviolet-visible
V	volt
v/v	volume per volume
w/v	weight per volume
ε	extinction coefficient
λ	wavelength

8.5 List of chemicals and consumables

Acetic acid	Thermo Fischer Scientific GmbH, Dreiech, Germany
Acrylamide (AA)- mix	Sigma-Aldrich, Taufkirchen, Germany
Agar-agar	Merck KGaA, Darmstadt, Germany
Kanamycin sulfate	Carl Roth, Karlsruhe, Germany
Anti-Cx43 monoclonal mouse	Santa Cruz Biotechnology Inc., Heidelberg, Germany
Anti-GFP monoclonal mouse	Santa Cruz Biotechnology Inc., Heidelberg, Germany
Penta-His antibody	Qiagen, Hilden, Germany
HRP Goat anti-mouse Ig	*BD Pharmigen, San Diego, USA*
APS	Sigma-Aldrich, Taufkirchen, Germany
Texas Red™-DHPE	Sigma-Aldrich, Taufkirchen, Germany
Bromophenol blue	VWR International, Darmstadt, Germany
Chloroform	VWR International, Darmstadt, Germany
Coomassie Brilliant blue G-250	Carl Roth, Karlsruhe, Germany
Eppendorf tubes	Eppendorf, Hamburg, Germany
Eppendorf pipettes	Eppendorf, Hamburg, Germany
Ethanol p.a.	VWR International, Darmstadt, Germany
Glycine	Merck Chemicals, Darmstadt, Germany
HEPES	Carl Roth, Karlsruhe, Germany
Isopropyl alcohol	Merck Chemicals, Darmstadt, Germany
KCl	Merck Chemicals, Darmstadt, Germany

Methanol	Carl Roth, Karlsruhe, Germany
Mucasol®	Merck Chemicals, Darmstadt, Germany
NaCl	VWR International, Darmstadt, Germany
NaN_3	Merck Chemicals, Darmstadt, Germany
Nitrocellulose membrane	Bio-Rad Laboratories Inc., Hercules, USA
Parafilm®	American National Can, Chicago, USA
Petri dishes	Sarstedt, Nürnbrecht, Germany
Pipette tips	Sarstedt, Nürnbrecht, Germany
Ponceau S	Sigma-Aldrich, Taufkirchen, Germany
POPC	Avanti Polar Lipids, Alabaster, USA
POPG	Avanti Polar Lipids, Alabaster, USA
Cholesterol	Avanti Polar Lipids, Alabaster, USA
DOPC	Avanti Polar Lipids, Alabaster, USA
DOTAP	Avanti Polar Lipids, Alabaster, USA
L-α-PC	Sigma-Aldrich, Taufkirchen, Germany
NucleoBond® Xtra Midi EF-kit	Macherey-Nagel, Düren, Germany
SDS	Merck Chemicals, Darmstadt, Germany
TEMED	Sigma-Aldrich, Taufkirchen, Germany
TEV protease	Sigma-Aldrich, Taufkirchen, Germany
Tris	Carl Roth, Karlsruhe, Germany
Tryptone	Carl Roth, Karlsruhe, Germany
Tween-20	Carl Roth, Karlsruhe, Germany
Ultrapure water	Milipore, Billerica, USA
Yeast extract	Carl Roth, Karlsruhe, Germany
Albumin	Carl Roth, Karlsruhe, Germany
QIAprep® Spin miniprep kit	Qiagen, Hilden, Germany
Amerscham ECL Prime	Cytiva Europe GmbH, Fraiburg, Germany
Agarose	Carl Roth, Karlsruhe, Germany
Gel Red	VWR International, Darmstadt, Germany
GeneArt™ Gibson Assembly HiFi kit by Invitrogen™	Thermo Fischer Scientific GmbH, Dreiech, Germany
Phusion® High-Fidelity polymerase	New England Biolabs, Frankfurt, Germany
Bpu1101I, XhoI, SspI	Thermo Fischer Scientific GmbH, Dreiech, Germany
T4 DNA polymerase	Thermo Fischer Scientific GmbH, Dreiech, Germany
ITO-slides	Präzisions Glas & Optik GmbH, Iserlohn, Germany
PURExpress® *In Vitro* protein synthesis kit	New England Biolabs, Frankfurt, Germany

8.6 List of devices and software

Devices

Fluorescence spectroscopy

FluroMax® 4	*Horiba Scientific, Bensheim, Germany*

UV-Vis spectroscopy

Jasco V-650	*Jasco Corp., Tokyo, Japan*
NanoDrop™ 2000c	*Thermo Fisher Scientific, Waltham, USA*

CLSM

FluoView 1200	Olympus, Tokyo, Japan
LSM 710 Examiner	Carl Zeiss Microscopy GmbH, Oberkochen, Germany

Other devices

Mini-PROTEAN® Tetra Cell, PAGE	Bio-Rad Laboratories Inc., Hercules, USA
Trans-Blot® device	*Bio-Rad Laboratories Inc., Hercules, USA*
Azure 3000	Azure Biosystems, Dublin, USA
Eppendorf Mastercycler	Eppendorf, Hamburg, Germany
Power Pac 200 & 1000	Bio-Rad Laboratories Inc., Hercules, USA
Allegra™ X-22R Centrifuge	Beckman Coulter, Krefeld, Germany
Sigma 3-30 KS centrifuge	Sigma-Aldrich, Taufkirchen, Germany
Osmomat 030	Gonotec, Berlin, Germany
Herasafe 2030i (Flow-box)	Thermo Fischer Scientific GmbH, Dreiech, Germany
Heraeus Fresco 17 centrifuge	Thermo Fischer Scientific GmbH, Dreiech, Germany
Thermomixer compact	Eppendorf, Hamburg, Germany
Ultrasonic bath Sonorex RK 255H	Bandelin, Berlin, Germany
Liposofat®	Avestin, Ontario, Canada
pH meter: Calimatic 766	Knick, Berlin, Germany
MiliQ Gradient A10	Milipore, Eschborn, Germany
Incubator TH 30	Edmund Bühler GmbH, Bodelshausen, Germany
Tip sonifier Sonoplus HD 2070	Bandelin, Berlin, Germany

Software

ImageJ 1.52t	https://imagej.nih.gov/ij/
OriginPro 8.5G	OriginLab Corporation, Northampton, USA
SnapGene® viewer 2.5.4	GSL Biotech LLC, San Diego, USA
ChemDraw 20.1.1.125	PerkinElmer Informatic Inc., Waltham, USA
Inkscape 1.0	https://inkscape.org/

9. List of Figures

10. List of Tables

Acknowledgments

I would like to extend my gratitude to Prof. Dr. Claudia Steinem for the opportunity of joining her group, the constructive advice, and for all the learning lessons throughout the years.

To the members of my thesis advisory committee, Prof. Dr. Michael Meinecke and Prof. Dr. Sebastian Kruss, thank you for the warm support, insightful advice discussions.

Thanks to Prof. Dr. Burkhard Geil, Prof. Dr. Timo Betz, and Prof. Dr. Bert de Groot for kindly agreeing to be part of my examination board.

A special thanks to Dr. Tabea Oswald, who kindly helped me with all the processes and paperwork before and after arriving in Germany. Many thanks for being so supportive, for listening to my research concerns, and for always looking at the positive side.

I am grateful for the opportunity of becoming the mentor of Sven Hermeling, Apinrix Menoha, and Muriel Hartsch. Their motivation and openness to learning challenged me and helped me develop mentoring skills. It is rewarding to see you all grow and develop in science.

A sincere thanks to Jutta and Michaela for all the scientific assistance Jutta, thanks for all the interesting conversations at lunch, for always asking about my family, and for sharing practical advice. Micha, it was fun and rewarding to teach the practical courses with you. We made a great “Denglish” teaching team.

A million thanks to Melanie and Marianne for all the organizational help. Thanks for being so kind and for always welcoming us into the office with a smile.

Thanks to Sarmini, Merve, Larissa, Janina, Domi, Tim, Niko, Manuel, and Philipp for the helpful corrections to the manuscript.

I am grateful to have found good colleagues and supportive friends in Sarmini, Merve, and Larissa. Thank you girls for all the good moments.

Thanks to Ingo and the AK Steinem for adopting me these years and letting me bring a little Latin American diversity to the group. I had so much fun learning about the German culture and language through jokes and funny discussions. Thanks for always putting a smile on my face.

I am immensely grateful for the love and support that I received from my family, friends, and Philipp Beesten in the last months. Many thanks for believing in me, you were part of the fuel that always kept me going.

For all of you who were part “my team” during the doctoral time: Thanks a million!